3 Systematics and Paragenesis of Uranium Minerals

Robert Finch
Argonne National Laboratory
9700 South Cass Ave.
Argonne, Illinois 60439

Takashi Murakami
Mineralogical Institute
University of Japan
Bunkyo-ku, Tokyo 113, Japan

INTRODUCTION

Approximately five percent of all known minerals contain U as an essential structural constituent (Mandarino 1999). Uranium minerals display a remarkable structural and chemical diversity. The chemical diversity, especially at the Earth's surface, results from different chemical conditions under which U minerals are formed. U minerals are therefore excellent indicators of geochemical environments, which are closely related to geochemical element cycles. For example, detrital uraninite and the absence of uranyl minerals at the Earth's surface during the Precambrian are evidence for an anoxic atmosphere before about 2 Ga (Holland 1984, 1994; Fareeduddin 1990; Rasmussen and Buick 1999).

The oxidation and dissolution of U minerals contributes U to geochemical fluids, both hydrothermal and meteoric. Under reducing conditions, U transport is likely to be measured in fractions of a centimeter, although F and Cl complexes can stabilize U(IV) in solution (Keppler and Wyllie 1990). Where conditions are sufficiently oxidizing to stabilize the uranyl ion, UO_2^{2+}, and its complexes, U can migrate many kilometers from its source in altered rocks, until changes in solution chemistry lead to precipitation of U minerals. Where oxidized U contacts more reducing conditions, U can be reduced to form uraninite, coffinite, or brannerite. The precipitation of U(VI) minerals can occur in a wide variety of environments, resulting in an impressive variety of uranyl minerals. Because uraninite dissolution can be rapid in oxidizing, aqueous environments, the oxidative dissolution of uraninite caused by weathering commonly leads to the development of a complex array of uranyl minerals in close association with uraninite. Understanding the conditions of U mineral formation and alteration is an important part of understanding the geochemical behavior of U.

Renewed interest in the paragenesis and structures of uranyl minerals has arisen lately due, in part, to their roles as alteration products of uraninite under oxidizing conditions (Frondel 1958; Garrels and Christ 1959; Finch and Ewing 1992b). But uranyl compounds are also important corrosion products of the UO_2 in spent nuclear fuel (Finch and Ewing 1991; Forsyth and Werme 1992; Johnson and Werme 1994; Wronkiewicz et al. 1992, 1996; Buck et al. 1998; Finn et al. 1998; Finch et al. 1999b) and they may control groundwater concentrations of U in contaminated soils (Buck et al. 1996; Morris et al. 1996). Studies of the natural occurrences of uranyl minerals can be used to test the extrapolation of results from short-term experiments to periods relevant to high-level nuclear-waste disposal (Ewing 1993) and to assess models that predict the long-term behavior of spent nuclear fuel buried in a geologic repository (Bruno et al. 1995).

0275-0279/99/0038-0003$10.00

URANIUM MINERALS SYSTEMATICS

The most complete descriptions of U minerals to date were provided by Frondel (1958); however, during the intervening 40 years there has been a dramatic increase in our understanding of U mineralogy and crystal chemistry, and many new species have been described. Smith (1984) provided an extensive review of U mineralogy, including summaries of structures, occurrences and mineral descriptions for U minerals described since Frondel (1958). In this volume, detailed descriptions of U-mineral structures are provided by Burns (this volume). Here, we focus on U-mineral paragenesis and chemistries. Some detailed descriptions are provided for U minerals reported since Smith's (1984) paper. Minerals containing reduced U are discussed first, followed by uranyl minerals, in which U occurs as U^{6+}. Minerals are further divided chemically according to the major anionic component (e.g. silicate, phosphate, etc.), with some chemical groups listed together because of structural similarities. Tables list minerals in alphabetical order within each chemical group. The name, formula, and references are provided, together with comments pertaining to recent work reported for these minerals.

Minerals containing reduced U

Most U in nature occurs in accessory minerals in which it may be a major (Table 1) or minor component (Table 2), but only a few of these minerals are found with U concentrations sufficient to be economically important. By far the most important U mineral, both in terms of abundance and economic value, is the nominally simple oxide, uraninite. The U silicate, coffinite, is of secondary economic importance, with most major coffinite-bearing deposits restricted to low-temperature deposits, such as the sandstone-hosted deposits in the west central USA (Finch 1996; Plant et al., Chapter 6, this volume). However, coffinite is increasingly recognized as an important alteration product of uraninite under reducing conditions and has been identified in many diverse U deposits (Janeczek 1991, 1992c; Fayek and Kyser 1997; Fayek et al. 1997). The U titanate brannerite is perhaps the next most abundant U(IV) mineral, occurring in quantities sufficient to be economically mined in a few localities. Most of the remaining minerals listed in Tables 1 and 2 do not form economic ore deposits; they are, nevertheless, important hosts for U in the rocks in which they reside, and the alteration of these minerals by both hydrothermal and meteoric waters is the source of dissolved U in surface waters, groundwaters and hydrothermal fluids, from which many U deposits are derived (Plant et al. this volume).

Uraninite. Uraninite is a common accessory mineral in pegmatites and peraluminous granites, and is probably the most important source of dissolved U in groundwaters emanating from weathered granite terrains (Frondel 1958; Förster 1999 and references therein; Plant et al. this volume). Uraninite is isometric (fluorite structure type, *Fm*3*m*) with nominal composition UO_{2+x} (Z = 4); however, pure UO_2 is not known in nature, being always at least partly oxidized (x < 0.25-0.3) and containing additional elements. In addition to radiogenic Pb (and other radiogenic daughter products) produced by decay of ^{238}U and ^{235}U, uraninite commonly contains Th, REE, Ca, and other elements. The commonly extreme non-stoichiometry exhibited by uraninite is apparent from the structural formula: $(U^{4+}_{1-x-y-z}U^{6+}_{x}REE^{3+}_{y}M^{2+}_{z}\square_{v})O_{2+x-0.5y-z-2v}$ (Janeczek and Ewing 1992b). Synthetic UO_2 is brick red, becoming black upon slight oxidation. Uraninite is commonly black with an iron-black metallic luster, although various dark shades of brown and green have also been reported for more weathered material (Frondel 1958). The unit-cell parameter, a_o for synthetic $UO_{2.03}$ is 5.4682 Å, decreasing as U^{4+} oxidizes to U^{6+} up to $UO_{2.25}$, for which a_o equals 5.440 Å (Smith et al. 1982). The unit-cell parameter for synthetic UO_{2+x} decreases linearly with increasing values of x, whereas unit cell parameters reported for uraninite are highly variable, depending in a complex way on composition (Brooker and Nuffield 1952;

Table 1. Minerals in which reduced U is an essential component

Name	*Formula*	*Comments*
Uraninite*	$(U^{4+}_{1-x-y-z}U^{6+}_{x}REE^{3+}_{y}M^{2+}_{z})O_{2+x-y/2}$	Fluorite structure type; s.s. with ThO_2; Frondel (1958); Janeczek & Ewing (1992b); Kotzer & Kyser (1993); Pourcelot et al. (1998); Förster (1999)
Coffinite	$USiO_4{\cdot}nH_2O$	Zircon structure type; minor P; REE; As?; Frondel (1958); Speer (1982); Smits (1989); Janeczek (1991
Brannerite*	$(U,Ca,Y,Ce)(Ti,Fe)_2O_6$	metamict; brannerite-thoruzite structure type; Frondel (1958); Szymanski & Scott (1982); Smith (1984); Singh et al. (1990); Gaines et al. (1997)
Orthobrannerite	$(U^{6+},U^{4+})(Ti,Fe)_2O_6(OH)$	metamict; Singh et al. (1990); Gaines et al. (1997). Compare synth. $UTiO_5$ (Marshall & Hoekstra 1965; Miyake et al. 1994), $UMoO_5$ (D'yachenko et al 1996), and UVO_5 (Dickens et al. 1992).
Ianthinite*	$U^{4+}(U^{6+}O_2)O_4(OH)_6(H_2O)_9$	β-U_3O_8 structure derivative; Finch & Ewing (1994); Burns et al. (1997b)
Ishikawaite*	$(U,Ca,Y,Ce)(Nb,Ta)O_4$	Samarskite group; Wolframite structure type; Gaines et al. (1997); Hanson et al. (1999)
Lermontovite	$U(PO_4)(OH)(H_2O)$ (?)	ill defined; compare vyacheslavite; Smith (1984); Gaines et al. (1997)
Moluranite	$H_4U(UO_2)_3(MoO_4)_7(H_2O)_{18}$	amorphous; Gaines et al. (1997)
Mourite	$UMo_5O_{12}(OH)_{10}$ (?)	IR suggests molecular H_2O; Gaines et al. (1997)
Ningyoite	$(U,Ca,Ce,Fe)_2(PO_4)_2{\cdot}1\text{-}2H_2O$	Rhabdophane grp.; compare synthetic $U(HPO_4)_2(H_2O)_4$ [G&92]; Gaines et al. (1997)
Petschekite	$UFe^{2+}(Nb,Ta)_2O_8$	hypothetical formula for unaltered material; Smith (1984); Gaines et al. (1997)
Sedovite	$U(MoO_4)_2$	Gaines et al. (1997)
Uranomicrolite	$(U,Ca,Ce)_2(Ta,Nb)_2O_6(OH,F)$	Pyrochlore grp.; microlite subgroup (Ta > Nb); Frondel (1958); Lumpkin & Ewing (1992a)
Uranopolycrase	$(U,Y)(Ti,Nb)_2O_6$	Columbite structure type; Aurisicchio et al. (1993); Gaines et al. (1997)
Uranopyrochlore	$(U,Ca,Ce)_2(Nb,Ta)_2O_6(OH,F)$	Pyrochlore grp.; pyrochlore subgroup (Nb > Ta); Frondel (1958); Lumpkin & Ewing (1995)
Vyacheslavite	$U(PO_4)(OH)(H_2O)_{2.5}$	Rhabdophane grp.; compare lermontovite; Belova et al. (1984)
Wyartite*	$CaU^{5+}(UO_2)O(OH)_4(CO_3)(H_2O)_7$	mixed U^{5+}-U^{6+}; Clark (1960); Burns & Finch (1999)
Wyartite II*	$CaU^{5+}(UO_2)O(OH)_4(CO_3)(H_2O)_3$	mixed U^{5+}-U^{6+}; dehydration product of wyartite; Clark (1960); unpublished data
Unnamed*	$U(HAsO_4)_2(H_2O)_4$	possible synthetic analogue: PDF 38-644; Chernorukov et al. (1985); Ondrus et al. (1997c)

New or supplemental data or not listed in Dana's New Mineralogy (Gaines et al. 1997).
*Minerals containing both U^{4+} and U^{6+} are also listed in tables according to the predominant oxyanion.

Table 2. Miscellaneous minerals that commonly contain substantial U^{4+} as a minor component

Name	*Formula*	*Comments; Ref.*
Betafite*	$(Ca,Na,U)_2(Ti,Nb,Ta)_2O_6(OH)$	Pyrochlore grp.; betafite subgroup; Lumpkin & Ewing (1996); Gaines et al. (1997)
Brabantite*	$Ca(Th,U)(PO_4)_2$	Monazite group; Gaines et al. (1997); Förster (1998a,b)
Brockite	$(Ca,Th,REE)(PO_4)\cdot H_2O$	Rhabdophane group; Gaines et al. (1997)
Cheralite	$(Ca,Ce,Th)(P,Si)O_4$	Monazite group; Gaines et al. (1997)
Davidite	$(Ce,La)(Y,U,Fe^{2+})(Ti,Fe^{3+})_{20}(O,OH)_{38}$	Crichtonite group; Frondel (1958); Gaines et al. (1997)
Ekanite	$Ca_2(Th,U)Si_8O_{20}$	cf. iraqite; steacyite; thornasite; umbozerite; unnamed ("thorsite"); Gaines et al. (1997)
Euxenite-(Y)	$(Y,Ca,Ce,U,Th)(Nb,Ta,Ti)_2O_6$	metamict; polycrase structure type; Gaines et al. (1997)
Grayite	$(Th,Ca,Pb)PO_4\cdot H_2O$	Rhabdophane grp.; ill defined; questionable; Gaines et al. (1997)
Huttonite	$(Th,U)SiO_4$	Monazite structure type; Speer (1982); Boatner & Sales (1988); Gaines et al. (1997)
Iraqite-(La)	$K(Ca,Na)_4(La,Ce,Th)_2(Si,Al)_{16}O_{40}$	cf. steacyite; ekanite; thornasite; umbozerite; unnamed ("thorsite"); Gaines et al. (1997)
Kobeite-(Y)	$(Y,U)(Ti,Nb)_2(O,OH)_6$	Columbite structure derivative; (= polycrase?); 8; Gaines et al. (1997)
Mckelveyite-(Y)	$Ba_3Na(Ca,U)Y(CO_3)_6(H_2O)_3$	Gaines et al. (1997)
Monazite-(REE)*	$(La\text{-}Sm)PO_4$	Monazite grp.; REE = La; Ce; Nd; Sm; 7; 9; Gaines et al. (1997)
Plumbobetafite*	$(Pb,U,Ca)(Ti,Nb)_2O_6(OH,F)$	Pyrochlore grp.; betafite subgroup; Lumpkin & Ewing (1996); Gaines et al. (1997)
Plumbomicrolite*	$(Pb,U,Ca)_2Ta_2O_6(OH)$	Pyrochlore grp.; microlite subgroup; Lumpkin & Ewing (1992a); Gaines et al. (1997)
Plumbopyrochlore*	$(Pb,U,Ca)_{2-x}Nb_2O_6(OH)$	Pyrochlore grp.; pyrochlore subgroup; Lumpkin & Ewing (1995); Gaines et al. (1997)
Samarskite-(Y)*	$(Y,REE,U,Fe^{3+},Fe^{2+})(Nb,Ta)O_4$	Samarskite group; Wolframite structure type; Warner & Ewing (1993); Hanson et al. (1999)
Steacyite	$K_x(Ca,Na)_2ThSi_8O_{20}$ ($x = 0.6 - 0.8$)	cf. ekanite; iraqite; thornasite; umbozerite; unnamed; Gaines et al. (1997)
Thorianite	$(Th,U)O_2$	Fluorite structure type; s.s. with UO_2 & CeO_2; Gaines et al. (1997)
Thorite	$(Th,U)SiO_4$	Zircon structure type; Frondel (1958); Smits (1989); Speer (1982); Lumpkin & Ewing (1992b)
Thornasite	$(Na,K)ThSi_{11}(O,F,OH)_{25}(H_2O)_8$	cf. ekanite; iraqite; steacyite; umbozerite; unnamed ("thorsite"); Gaines et al. (1997)
Thorogummite	$(Th,U)(SiO_4)_{1-x}(OH)_{4x}$	Zircon structure type; Gaines et al. (1997)
Thorutite	$(Th,U,Ca)Ti_2(O,OH)_6$	Brannerite structure type; Gaines et al. (1997)
Tristramite	$(Ca,U^{4+},Fe^{2+})(PO_4,SO_4)(H_2O)_2$	Rhabdophane group; Atkins et al. (1983)
Umbozerite	$Na_3Sr_4ThSi_8(O,OH)_{24}$	amorphous; cf. ekanite; iraqite; thornasite; steacyite; unnamed ("thorsite"); Gaines et al. (1997)
Yttrobetafite-(Y)	$(Y,U,Ce)(Ti,Nb,Ta)_2O_6(OH)$	Pyrochlore grp.; betafite subgroup; Gaines et al. (1997)
Yttrocolumbite-(Y)	$(Y,U,Fe^{2+})(Nb,Ta)O_4$ or $(Y,U,Fe^{2+})(Nb,Ta)_2O_6$	ill defined; compare yttrotantalite; Gaines et al. (1997)
Yttrocrasite-(Y)	$(Y,Th,Ca,U)(Ti,Fe^{3+})_2(O,OH)_6$	Pyrochlore structure type; compare thorutite; Gaines et al. (1997)
Yttropyrochlore-(Y)	$(Y,Na,Ca,U)_{1-2}(Nb,Ta,Ti)_2(O,OH)_7$	Pyrochlore grp.; ill defined; Gaines et al. (1997)
Yttrotantalite-(Y)	$(Y,U,Fe^{2+})(Ta,Nb)O_4$ or $(Y,U,Fe^{2+})(Ta,Nb)_2O_6$	Samarskite group (?); Gaines et al. (1997)
Unnamed*	$Ca_{3.5}(Th,U)_{1.5}Si_3O_{12}(OH)$	Apatite structure type; Jamveit et al. (1997)
Unnamed*	$Th_2(Ca,Ba)[Si_9O_{22}](OH)_2(H_2O)_n$	"thorsite" cf. Ekanite; iraqite; steacyite; thornasite; umbozerite; Lazebnik et al (1994)

* New or supplemental data or not listed in Dana's New Mineralogy (Gaines et al. 1997).

Berman 1957; Frondel 1958). There is no simple correlation between the oxidation state of U in uraninite and unit-cell size (Janeczek and Ewing 1992a).

The impurity content of uraninite depends strongly upon the environment of deposition, as well as the conditions under which dissolved U may have been transported. Three types of uraninite can be roughly defined in terms of their geneses (McMillan 1978; Plant et al. this volume): (1) igneous, magmatic, and metamorphic, including pegmatitic uraninite; (2) hydrothermal (e.g. vein type and unconformity-related deposits); (3) low temperature (sedimentary-hosted deposits). The chemistry of unaltered uraninite can be a reasonably reliable indicator of its origin (Frondel 1958). Magmatic uraninite commonly contains Th and REE, whereas these elements are largely absent from hydrothermal and low-temperature sedimentary uraninite (Frondel 1958). These compositional differences reflect differences in the aqueous chemistries of U, Th and REE; U may be readily oxidized and transported as the UO_2^{2+} ion and its complexes, whereas Th and REE tend to be less mobile (Langmuir 1978). These different solution behaviors fractionate U from Th and REE in many aqueous environments, especially where redox conditions favor UO_2^{2+} formation.

Impurities can provide insight into the genesis of uraninite and uraninite-fluid interactions, and may also affect uraninite stability. The most important impurities in uraninite are Pb, Th, Ca, Y and lanthanides.

Radiogenic Pb can reach quite high levels in ancient uraninite, with reports of 15-20 wt % PbO in some analyses, although 7-10 wt % is more common (Berman 1957; Frondel 1958; Janeczek and Ewing 1995). In many uraninite specimens, especially those of sedimentary and hydrothermal origin, Pb is the most abundant cation after U. Lead is incompatible in the UO_2 structure, however, and the structural role of Pb in uraninite has long perplexed researchers. Berman (1957) suggested that Pb exsolves as PbO (massicot) at the unit-cell scale, such that it is not detectable by XRD; however, high-resolution transmission electron microscopy (HRTEM) has not supported this hypothesis (Janeczek et al. 1993). It appears that Pb may replace some U and occupy interstitial sites within the uraninite structure (Janeczek and Ewing 1992b). X-ray powder diffraction data indicate that unit-cell volumes of Pb-rich uraninite are larger than those of Pb-poor uraninite (Janeczek and Ewing 1992c, 1995), suggesting that Pb accumulation can induce significant strain. Because Pb is incompatible in the uraninite structure, it is eventually lost from uraninite. Lead is relatively immobile in most groundwaters (Mann and Deutscher 1980), and under reducing conditions, Pb released from uraninite commonly forms galena, provided the activity of S is sufficient (Janeczek and Ewing 1995).

The decay of U to Pb also influences the average oxidation state of uraninite. This is because U in uraninite is predominantly U^{4+}, leading to Pb^{4+} as the ionic species produced by decay (ignoring potential redox steps for intermediate daughters). But Pb^{4+} is a strong oxidizer and is unstable in the presence of U^{4+}; thus U^{4+} oxidizes to U^{6+} (or two U^{4+} may each oxidize to U^{5+}) and Pb^{4+} is reduced to Pb^{2+}. This process has been called "auto-oxidation" (Frondel 1958) and may lead to relatively high U^{6+}/U^{4+} ratios in uraninite. The valence of Pb^{2+} in uraninite has been verified by X-ray photon spectroscopy (XPS) (Sunder et al. 1994, 1996). These same authors report U^{6+}/U^{4+} ratios of approximately 0.02 to as high as ~0.75 in uraninite from the Cigar Lake U deposit in northern Saskatchewan, despite reducing to anoxic conditions at the depth of the ore deposit (>400 m). Radioactive decay of U in "old" uraninite can therefore destabilize uraninite by two mechanisms: (1) auto-oxidation, which leads to U^{6+}/U^{4+} ratios at which the uraninite structure becomes unstable; and (2) accumulation of Pb^{2+} to levels that cannot be accommodated by the uraninite structure. These two processes occur simultaneously

leading to Pb loss and, commonly, recrystallization of uraninite under reducing conditions (Janeczek and Ewing 1992b, Kotzer and Kyser 1993, Janeczek and Ewing 1995). The effects of Pb on the stability of uraninite and other U minerals are discussed further in another section.

After radiogenic Pb, the most important impurity elements in most uraninite occurrences are probably Th, Ca, and REE (Janeczek and Ewing 1992b). Synthetic UO_2 and ThO_2 are isostructural, and form a complete solid solution, with the lattice parameter varying linearly with Th content (Frondel 1958). Thorium contents of magmatic uraninite, however, rarely reach levels above approximately 10 or 12 wt % ThO_2 (Frondel 1958; Grandstaff 1976; Förster 1999). Most Th in Ca-poor peraluminous granites resides in monazite-group minerals (Friederich and Cuney 1989), suggesting a greater affinity of Th for phosphate minerals than U. Reduced U shows a strong tendency to crystallize as uraninite (Förster 1998a). Although Podor et al. (1995) demonstrated that U + Ca can substitute without limit for La in synthetic monazite-(La), even U-rich granites with low molar Th/U ratios tend to crystallize monazite-group minerals with low U contents and Th well in excess of U (Förster 1998a,b). In contrast to uraninite, thorianite is relatively rare. Crystallizing in some Th-rich pegmatites, thorianite is most commonly found as detrital grains, sometimes forming economic Th deposits (Frondel 1958).

Calcium contents reported in magmatic uraninite tend to be rather low, up to perhaps 0.5 wt % CaO (~12 mol %) (Frondel 1956; Förster 1999). The ionic radius of Ca^{2+} (1.12 Å) makes it reasonably compatible with the uraninite structure, provided a charge-balance mechanism is available. High-temperature studies of UO_2-CaO solid solutions suggest that approximately 47 mol % CaO may be incorporated into the UO_2 structure above approximately 1500 to 1800°C (Alberman et al. 1951; Pialoux and Touzelin 1998). The high-temperature solid solution is disordered, whereas below approximately 1250°C an ordered solid solution, cubic $U_{1-x}Ca_xO_{2-x}$, exists between $x \cong 0.25$ and $x \cong 0.15$-0.05 (x decreasing with temperature) (Pialoux and Touzelin 1998). Maximum reported Ca contents in natural magmatic uraninite are close to the lower end of this solid-solution range. The degree to which these results apply to natural uraninite is uncertain; however, Ca^{2+} may help charge balance U^{5+} or U^{6+} in uraninite, a factor not addressed in the studies by Alberman et al. (1951) and Pialoux and Touzelin (1998). Comparatively high concentrations of Ca reported for hydrothermal and low-temperature uraninite (Frondel 1958; Janeczek and Ewing 1992b may reflect Ca^{2+} incorporated for charge-balance during uraninite formation, possibly compensating U^{6+} (Janeczek and Ewing 1992b; Finch and Ewing 1992b); however, high Ca contents are most commonly reported for fine-grained uraninite and may include mineral inclusions such as calcite (Janeczek and Ewing 1995; Janeczek this volume). Calcium may also be an important charge-balancing species replacing Pb^{2+} during uraninite alteration, especially under conditions where U^{6+} (or U^{5+}) are not completely reduced. A Ca-Pb exchange reaction may be something like

$$(U^{4+}_{1-2y}U^{6+}_{y}Pb^{2+}_{y})O_{2\,(cr)} + yCa^{2+} + yHS^{-} \Rightarrow (U^{4+}_{1-2y}U^{6+}_{y}Ca_{y})O_{2\,(cr)} + yPbS_{\,(cr)} + yH^{+}$$

Support for the potential importance of this reaction is found in commonly negative correlations between Pb and Ca in uraninite altered under anoxic or reducing conditions (Berman 1957; Frondel 1958; Janeczek and Ewing 1992c and references therein; Fayek et al. 1997). The above reaction may be most important where volume- and grain-boundary-enhanced diffusion dominate, because dissolution and reprecipitation under reducing conditions should favor reduction of U^{6+}.

Yttrium and lanthanides (REE) tend to be relatively minor substituents in uraninite, with typical concentrations being a few tens of ppm to a few tenths of a weight percent

REE_2O_3. Although concentrations of 10-15 wt % REE_2O_3 have been reported for some pegmatitic uraninites (Berman 1957; Frondel 1958), such high values may reflect spurious mineral inclusions, such as monazite. Most recent analyses by microprobe techniques indicate that REE_2O_3 concentrations in uraninite rarely exceed 2-4 wt % (Janeczek and Ewing 1992b; Foord et al. 1997; Förster 1999). Concentrations of REE in uraninite can vary widely, depending on local environment (Pagel et al 1987; Foord et al. 1997; Förster 1999), and, as for Th, concentrations of P in mineralizing fluids probably play a crucial role in determining the degree to which REE are incorporated into uraninite. Relative REE trends in uraninite are variable, with some uraninite displaying light REE (LREE) enrichments relative to Y and heavy REE (HREE). Others display relative enrichments in HREE, whereas yet others show no REE fractionation or even middle REE enrichment (Pagel et al. 1987). Positive Ce anomalies are rare (though not unknown), whereas negative Eu anomalies are rather common (Pagel et al. 1987); both observations are consistent with expected redox influences on Ce and Eu under reducing conditions where uraninite is stable. Substitution of REE^{3+} for U^{4+} in synthetic UO_2 increases the lattice parameter (Stalbauer et al. 1974), but the influence of minor REE substitution on the lattice parameter of natural uraninite has not been examined.

Other elemental impurities reported in uraninite include Si, P, Al, Fe, Mg, Na and K (Berman 1957; Frondel 1958; Finch and Ewing 1992b; Pearcy et al. 1994; Janeczek at al. 1996; Foord et al. 1997). The exact roles of these elements in uraninite remain uncertain, but most are not compatible with the uraninite structure. Unaltered magmatic uraninite commonly contains few if any of these elements (Berman 1957; Frondel 1958; Förster 1999), although Foord et al. (1997) report more than 2 wt % K_2O and up to 0.5 wt % Na_2O in pegmatitic uraninite (exposed to alkali metasomatism). The highest concentrations of impurities are most commonly reported for exceptionally fine-grained uraninite ("pitchblende"). Silicon and P may be relatively high in partly altered uraninite due to replacement of uraninite by coffinite (Janeczek 1991; Janeczek and Ewing 1992a,c). It is not always clear how much Si and P are due to inclusions of coffinite in uraninite, but reports of relatively high Si contents in uraninite are not uncommon, even where coffinite is not identified (Finch and Ewing 1992b; Pearcy et al. 1994; Foord et al. 1997). Uraninite precipitated from low-temperature groundwaters (T < 100°C) in sedimentary-hosted U deposits can be very fine grained, and analyses reported for such fine-grained uraninite commonly include elements from mineral inclusions along grain and sub-grain boundaries (Janeczek et al. 1996; Janezcek and Ewing 1995). Detailed TEM examinations of fine-grained uraninite commonly reveal sub-micron-scale Si-rich inclusions along grain boundaries. The most common mineral inclusion is probably coffinite (Janeczek and Ewing 1991, 1992c; Fayek et al. 1997), but other minerals, especially clay minerals such as kaolinite (Pearcy et al. 1994) and chlorite (Janeczek and Ewing 1995) may be intimately intergrown with fine-grained uraninite. It is increasingly apparent that elements such as Al, Si and P do not substitute in the uraninite structure to any significant degree, so that uraninite analyses that include these elements probable indicate spurious mineral inclusions.

Uranium(IV) silicates

Coffinite. After uraninite, coffinite is the most important ore mineral for U. Coffinite is a tetragonal orthosilicate isostructural with zircon, $ZrSiO_4$, hafnon, $HfSiO_4$, thorite, $ThSiO_4$, and synthetic $PuSiO_4$ and $NpSiO_4$ (Speer 1982). Uranium occupies triangular-dodecahedral sites coordinated by isolated Si tetrahedra (see Burns this volume). Chemical analyses of coffinite commonly indicate H_2O, and the formula was first reported as $U(SiO_4)_{1-x}(OH)_{4x}$ in allusion to thorogummite (Stieff et al. 1956); however, compositional and IR data indicate that H_2O is molecular and the correct formula is $USiO_4 \cdot nH_2O$ (Speer

1982; Lumpkin and Chakoumakos 1988; Smits 1989; Janeczek 1991) (Table 1). Uranium-Th silicates form two complete series of anhydrous and hydrated compounds, for which the general formulas are $(U,Th)SiO_4$ and $(Th,U)SiO_4{\cdot}nH_2O$ ($n < 4$). These two formulas encompass three mineral species (Smits 1989): coffinite, the hydrated and anhydrous end member with U > Th; thorite, the anhydrous Th end member with Th > U; and thorogummite, the hydrated Th end member with Th > U (Tables 1 and 2). All three minerals are tetragonal and thorogummite may be redundant as a separate species. Coffinite samples tend to be so fine grained and impure that accurate analyses can be exceedingly difficult to obtain. Metamictization and aqueous alteration may also be significant, especially for thorite and thorogummite (Lumpkin and Chakoumakos 1988). Coffinite may be less amenable to substitutions than uraninite, and many impurities reported in coffinite analyses may be present as mineral inclusions. There are, however, some chemical substitutions that are well documented.

Phosphorous and REE are among the most common impurity elements in most reported coffinite analyses. Coffinite may contain substantial amounts of REE and P, suggesting some solid solution with xenotime, YPO_4 (Hansley and Fitzpatrick 1989; Janeczek and Ewing 1996), with which coffinite is isostructural. Calcium-rich coffinite from Bangombé, Gabon, has P well in excess of REE, which was explained by fine-scale (< 1 μm) inclusions of amorphous material with a composition similar to that of ningyoite (Belova et al. 1980); however, Janeczek and Ewing (1996) found no evidence for such inclusions and proposed a limited solid solution between coffinite and ningyoite, according to the substitutions,

$$2\ Ca^{2+} + 0.8\ P^{5+} + 0.2\ {}^{IV}\square = U^{4+} + Si^{4+} \text{ and } 2\ Ca^{2+} + P^{5+} + (OH)^- = U^{4+} + Si^{4+},$$

where ${}^{IV}\square$ represents tetrahedral-site vacancies in the coffinite structure. It is unclear whether the extra Ca^{2+} cation is proposed to occupy interstitial sites in coffinite or what the structural role of $(OH)^-$ might be (Janeczek and Ewing 1996 only refer to "hydroxylation"). Perhaps the second substitution should be written, $Ca^{2+} + P^{5+} + (OH)^- = U^{4+} + Si^{4+} + O^{2-}$, although it has already been noted that hydroxyl substitution in coffinite is relatively minor (Speer 1982; Janeczek 1991). Of course, because of structural differences, a complete solid solution between coffinite and ningyoite is impossible, whereas substantial solid solution between coffinite and xenotime seems likely.

Coffinite is the major U-bearing mineral in many sandstone-hosted U deposits that extend from western South Dakota to eastern Arizona in the United States (Finch 1996). In these mostly low-temperature U deposits, coffinite most commonly occurs intimately intermixed with organic material, such as lignite. Coffinite is also a common alteration product of uraninite in Si-rich, reducing environments (Janeczek 1991; Janeczek and Ewing 1992a). Coffinite occurs in placer deposits in the Dominion Reef of the Witwatersrand, South Africa, where it replaces detrital uraninite grains (Smits 1989). Janeczek (1991) describes the crystal chemistry and paragenesis of coffinite from Jáchymov, Czech Republic. Plant et al. (this volume) provide more detail on the origin of coffinite-bearing U deposits.

U(IV) niobates, tantalates and titanates

A large number of complex Ta, Nb and Ti oxides are known that contain U in various amounts (Table 2). For the most part these minerals occur as accessory minerals in granitic rocks and granite pegmatites. Several are important Ta and Nb ore minerals and may be mined for REEs. A few contain U as an essential constituent (Table 1), and the U is usually oxidized to some degree (Smith 1984). Nearly all contain some U and Th in solid solution, and are therefore important actinide hosts in many granitic rocks, as well as being important

sources for dissolved U in hydrothermal and meteoric waters with which they interact. Many of these minerals have long defied detailed understanding because, due to their abilities to incorporate radioactive elements, they are commonly metamict; specimens may also be strongly altered. Metamict minerals offer a special challenge to mineralogists trying to glean structural information about their crystalline precursors. Attempts to elucidate compositional and structural details of metamict minerals may involve annealing (heating) mineral specimens in order to recrystallize the original structure. Although annealing is commonly successful, it is not always known whether the recrystallized compounds represent the original minerals. Redox conditions during annealing may change oxidation states of some elements (e.g. Fe or U), and, because of possible post-formation alteration, it not always clear what oxidation state some elements were in at the time of crystallization (Sugitani et al. 1984; Warner and Ewing 1993). Such experimental difficulties are exacerbated by the nearly ubiquitous alteration of these minerals (Ewing 1975; Lumpkin and Ewing 1992a, 1995, 1996; Warner and Ewing 1993), so that annealed samples may include spurious compounds formed from aqueous alteration products.

These minerals share a common structural feature: Nb, Ta, and Ti occupy octahedral sites, and the octahedra share corners or edges (or both) to form the structural framework; these are designated as B sites in the structural formulas. Additional cations occupy the so-called A sites, which are (ideally) either six-coordinated (octahedral) or eight coordinated (distorted cube), depending on the size of the A-site cation. U and Th occupy the A sites in these minerals. Eight structurally related groups are listed in Table 3, which gives the name of each mineral or mineral group as a function of the dominant B-site cation. Minerals in these groups may have prefixes that identify the dominant A-site cation (e.g. uranopyrochlore). There are also Sb^{5+} analogues for several of these minerals, including sibiconite, bindhemite, triphuyite, and others (Gaines et al. 1997), but they are not discussed in detail here. Recent data for the pyrochlore-group mineral roméite are reported by Brugger et al. (1997).

Structurally, these minerals may be divided into two groups. The structures of the ixiolite, samarskite (wolframite), and columbite groups consist of approximately hexagonally close packed O atoms. The A and B sites are both octahedrally coordinated. Octahedra share edges to form chains along [001] and layers parallel to (100) (notation after Warner and Ewing 1993). The A and B octahedral layers alternate along [100]. All three groups have structures that are derivatives of the α-PbO_2 structure (Graham and Thornber 1974; Warner and Ewing 1993) (Fig. 1). The structure of brannerite is distinct from the above groups; however, it is related, with both A and B sites being octahedrally coordinated (Szymanski and Scott 1982; Burns this volume). The second group is closely similar to the first, with octahedrally coordinated B cations; however, the A sites occupy distorted cubic sites (ideally 8-coordinated, but distortions are known). The larger A site in this second group accommodates cations such as Ca^{2+} and Na^+, in addition to actinides and REE. Fergusonite and aeschynite are structurally similar, differing primarily in how their alternate (100) layers stack (Warner and Ewing 1993). The structures of pyrochlore and zirconolite share some basic features with those of fergusonite and aeschynite: octahedral chains and large A sites; however, the pyrochlore structure is a derivative of the CaF_2 structure (Chakoumakos 1984) and zirconolite is a derivative of the pyrochlore structure (Mazzi and Munno 1983; Bayliss et al. 1989). The most important U-bearing Ta-Nb-Ti oxides are discussed further below.

Brannerite AB_2O_6. After uraninite and coffinite, brannerite is the most important ore mineral for U. Nominally $U^{4+}Ti_2O_6$, the U in brannerite is nearly always partly oxidized. Brannerite is typically metamict and requires annealing to produce an XRD pattern. As noted, the structure of brannerite is related to, but distinct from other AB_2O_6

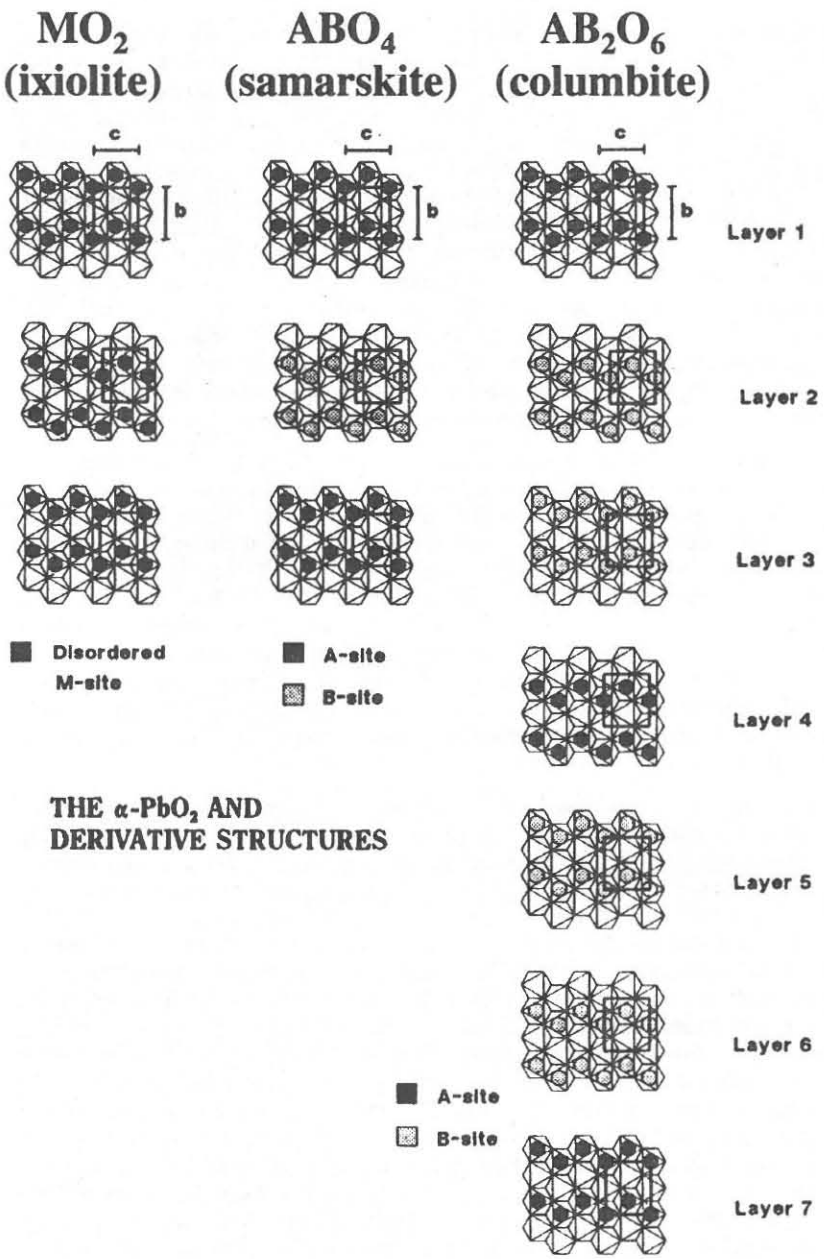

Figure 1. Depiction of the α-PbO and derivative structures (above) and the mixed coordinate structures (next page) in Nb-Ta-Ti oxides. Both A and B sites in the α-PbO and derivative structures are octahedral, whereas the mixed coordination structures have sheets of eight-coordinated A sites alternating with sheets of zigzag chains of octahedra (B sites). The *a* cell dimension is tripled in the AB_2O_6 structure types (columbite and polycrase) relative to the ABO_4 and MO_2 structure types due to cation ordering. Both AB_2O_6 structure types and the α-PbO-type MO_2 structure are orthorhombic, but distortions caused by ordering result in the ABO_4 structure types being monoclinic (modified slightly from Warner and Ewing 1993).

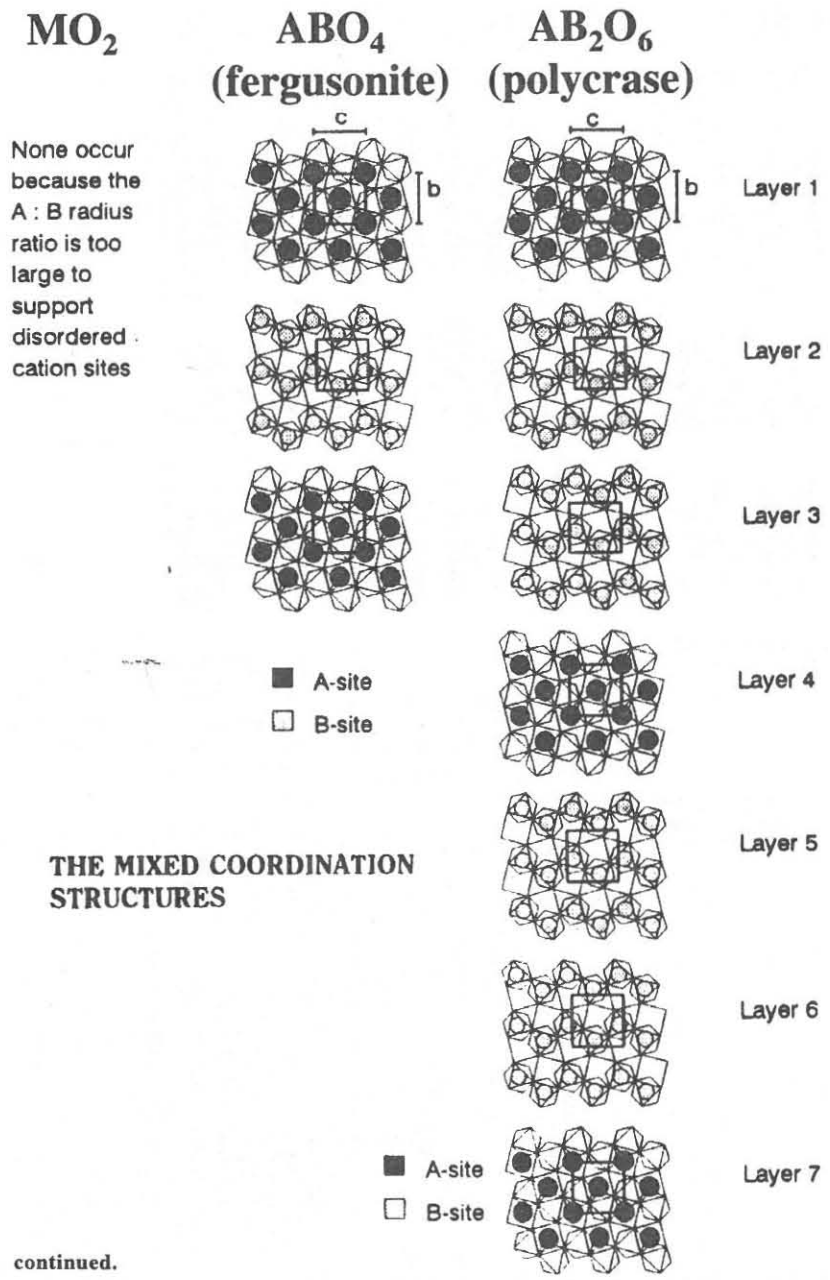

Figure 1, continued.

oxides, with layers of edge-sharing Ti octahedra and layers of distorted U octahedra (see Burns this volume). The structure of orthobrannerite remains unknown and crystals are essentially metamict. It is not simply a polymorph of brannerite, as it reportedly contains substantial U^{6+} (Table 1). Singh et al. (1990) report that a metamict brannerite heated to 900°C in air revealed $U^{6+}TiO_5$ and rutile in addition to brannerite. When heated to 1000°C,

Table 3. Structural comparisons among some Nb, Ta, Ti oxides

Representative mineral	*Formula*	*A-site**	*Dominant B-site cation*			*Structure type*
			Ta	Nb	Ti	
Ixiolite	MO_2	octahedral	ixiolite	ashanite	zirkelite	α-PbO_2
Wolframite	ABO_4	octahedral	X	samarskite	X	α-PbO_2 derivative
Columbite	AB_2O_6	octahedral	tantalite	columbite	X	α-PbO_2 derivative
Brannerite	AB_2O_6	octahedral	X	X	brannerite	$ThTi_2O_6$
Fergusonite	ABO_4	distorted cube	formanite	fergusonite	X	interlayered α-PbO_2 derivative
Polycrase	AB_2O_6	distorted cube	rynersonite	vigezzite	polycrase, aeschynite	interlayered α-PbO_2 derivative
Pyrochlore	$A_{1-2}B_2O_6(O,OH,F)$	distorted cube	microlite	pyrochlore	betafite	distorted CaF_2 derivative
Zirconolite	$AA'B_2O_7$	distorted cube	X	(unamed)[#]	zirconolite	pyrochlore derivative

* U substitution occurs at the A site. [#] See Williams & Gieré (1998).

the $UTiO_5$ and rutile disappeared and only brannerite was detected in the XRD powder pattern. Singh et al. (1990) proposed that $UTiO_5$ and rutile are formed during metamictization and alteration of brannerite, caused by oxidation of U^{4+} in brannerite according to the reaction, $2UTi_2O_6 + O_2 \Rightarrow 2UTiO_5 + 2TiO_2$. Smith (1984) suggested that orthobrannerite is related to synthetic $UTiO_5$, which tends to be substoichiometric ($UTiO_{5-x}$, x 0.15) and contains U^{5+} (Miyake et al. 1994). Though readily synthesized (Bobo 1964; Marshall and Hoekstra 1965), the structure of $UTiO_5$ is apparently unknown. However, it is almost certainly related to $U^{6+}Mo^{4+}O_5$ (D'yachenko et al 1996) and $U^{6+}V^{4+}O_5$ (Chevalier and Gasperin 1970; Dickens et al. 1992), both of which are orthorhombic and possess the uranophane-type sheet anion topology (cf. Miller et al. 1996; Burns et al. 1996, Burns this volume). These two synthetic compounds lack UO_2^{2+} ions (Bobo 1964; D'yachenko et al 1996), and if orthobrannerite turns out to be isostructural with $UMoO_5$ or UVO_5, it would be the only mineral known to contain U^{6+} without forming UO_2^{2+} ions.

Brannerite is a common accessory mineral in numerous uraninite and coffinite U deposits and has been identified at both unconformity-type and hydrothermal-vein U deposits (Finch 1996). In some deposits, brannerite may form following adsorption of U onto Ti oxides (McCready and Parnell 1997, 1998). The paragenesis of brannerite is distinct from that of most Ta, Nb, and Ti oxides, which form primarily in magmatic systems. This may explain why there are no known Ta- or Nb-analogues of brannerite (Table 3), although coupled cation substitutions such as $REE^{3+} + Ta^{5+} = U^{4+} + Ti^{4+}$ might be expected. Thorutite is the Th-analogue of brannerite (Smith 1984); it too is commonly metamict.

Columbite group AB_2O_6**.** The columbite group of minerals comprises a large number of structurally related orthorhombic AB_2O_6 compounds (B = Ta, Nb). The columbite subgroup is Nb-dominant, and the tantalite subgroup Ta-dominant; there are no known minerals in which Ti is dominant (Table 3), although there seems no reason not to expect one, provided charge balance can be maintained. Most commonly occurring as accessory minerals in granite pegmatites (Gaines et al. 1997), columbite-group minerals contain U (and Th) in various amounts and are commonly metamict (Table 3), but none has been described with U as an essential constituent. The relatively small octahedral A site is commonly occupied by Mg^{2+} (magnesiocolumbite) and transition-metal cations, such as Fe^{2+} (ferrocolumbite) and Mn^{2+} (manganocolumbite), and U and Th substitution tend to relatively minor. The structures of brannerite and thorutite might be considered as actinide analogues of the columbite structure, but distortions caused by U and Th in octahedral sites results in these two structure types being significantly different.

Polycrase group AB_2O_6**.** The polycrase structure type is comparable to that of the columbite group, except that the A site is a distorted cube (Fig. 1). Ti exceeds (Ta+Nb) in the B site of polycrase-(Y); Nb is dominant in the B site of euxenite-(Y) and vigezzite; and tantaeuxenite-(Y) and rynersonite are Ta-dominant in the B site (Table 3). Charge balance is maintained by Ca^{2+} replacing REE^{3+} at the A site. Euxenite-(Y) and tantaeuxenite-(Y) are compositionally intermediate between polycrase-(Y) and vigezzite and rynersonite, the latter two being Ca-dominant at the A site. This group occurs primarily as accessory minerals in granites and granite pegmatites (Gaines et al. 1997). All are commonly metamict (Table 3) owing to U (and Th) substitution at the A site, especially, it seems, in the Y-dominant minerals. However, only uranopolycrase contains U as an essential constituent (Table 1). Uranopolycrase was originally described from a pegmatite near Campo Village on Elba Island, Italy, and occurs as opaque, reddish brown, elongate [100] orthorhombic crystals that display good (100) cleavage (Aurisicchio et al. 1993). Uranopolycrase is "almost completely metamict" and heating to 900°C produces a sharp X-ray diffraction pattern indicating orthorhombic symmetry (*Pbcn*) (Aurisicchio et al. 1993). Uranopolycrase occurs

in a pegmatitic vein, where it is associated with uranmicrolite, euxenite-(Y), manganocolumbite, and titanowodginite. The recent structure determination of a crystalline polycrase-(Y) crystal from Malawi (Johnsen et al. 1999) verifies the iso-structural relationship between polycrase and uranopolycrase, and with synthetic $Y(Nb_{0.5}Ti_{0.5})_2O_6$ (von Weitzel and Schröcke 1980).

Samarskite group, ABO_4. Minerals of the samarskite group have Nb > Ta in the B site. The structures of the samarskite-group minerals are similar to that of wolframite, $MnWO_4$, a derivative of the α-PbO_2 structure (Graham and Thornber 1974; Warner and Ewing 1993). The samarskite group has the ideal formula $A^{3+}B^{5+}O_4$ (Warner and Ewing 1993), and the A sites are in octahedral coordination (Table 3). Hanson et al. (1999) reported detailed analyses of ishikawaite specimens and showed that this mineral is properly classified as a member of the samarskite group. There are three known members of the samarskite group of minerals, defined on the dominant A-site cation: samarskite-(Y) is Y dominant, ishikawaite is (U+Th) dominant, and calciosamarskite is Ca dominant (Hanson et al. 1999); however all contain substantial U and Th. An XRD study of a metamict samarskite was conducted by Keller and Wagner (1983), who reported the radial distribution function.

Fergusonite group ABO_4. The fergusonite group consists of REE-bearing Ta and Nb oxides, many of which are metamict and, therefore, commonly poorly characterized, with most available structural information derived from studies of heated material or synthetic analogues. The structure of the fergusonite group is comparable to that of samarskite group (wolframite structure type) but with large A sites (distorted cubes) (Fig. 1). Most of these minerals are monoclinic, although orthorhombic and tetragonal unit cells arise from cation ordering (Gaines et al. 1997). Fergusonite-(Nd) is reportedly tetragonal (Gong 1991b), and partially metamict fergusonite-(Y) may consist of both monoclinic and tetragonal forms (Gong 1991a,b). A Nd-dominant polymorph of fergusonite was described from a REE deposit in Proterozoic dolomite at Bayan Obo, Inner Mongolia, China, where it occurs as small (0.02-0.25 mm) irregular grains and prisms in association with fergusonite-(Ce) and fergusonite-(Nd), aeschynite-(Nd) , monazite, bastnaesite, riebeckite, ferroan dolomite, ilmenite, biotite, magnetite and pyrite (Weijun et al. 1983). It is proposed to be a monoclinic polymorph that the authors call "β-fergusonite-(Nd);" however, its definition as a new mineral is hampered by the fact that it is nearly metamict and is considered a questionable species (Nickel and Nichols 1992). Fergusonite-(Nd) contains approximately 1.1 wt % ThO_2 and 1.5 wt % UO_2. The B site in the fergusonite group is dominated by Nb, whereas Ta dominates in formanite; no Ti analogue is known (Table 3).

Pyrochlore group, $A_{1-2}B_2O_6(O,OH,F)$. The pyrochlore group is a particularly important group of Nb-Ta-Ti oxides that can contain substantial U. The structure of ideal pyrochlore, $A_{1-2}B_2O_6(O,OH,F)$, is a defect derivative of the fluorite structure type (Chakoumakos 1984, 1986). The structure is essentially a framework of B site octahedra with Ta, Nd, and Ti, and which can also contain Fe, Sn, W, and Sb (Fleischer and Mandarino 1999); Sb^{5+} can even dominate at the B site, as for roméite (Brugger et al. 1997). The A site is eight coordinated (distorted cube) and may contain alkalis, alkaline earths, REE and actinides. Charge balance is maintained in pyrochlore through cation substitutions at either A or B sites as well as through anionic substitutions. Three pyrochlore subgroups are defined, depending on the predominant cation in the B site. Niobium exceeds Ta in the pyrochlore subgroup, whereas Ta exceeds Nb in the microlite subgroup. Both the pyrochlore and microlite subgroups have (Ta + Nb) > 2Ti, whereas the betafite subgroup is characterized by 2Ti > (Ta + Nb) (Table 3). The compositions of most pyrochlores cluster near the pyrochlore-betafite join, with Ta less than 10 mol %, and near the microlite end member, with 30 mol % Nb or less and less than 15 mol % Ti. U

substitutes at the A site, and metamict pyrochlores are common. Although virtually all these minerals contain some U, only two minerals of the pyrochlore group contain U as an essential constituent: uranmicrolite and uranopyrochlore (Table 1). Pyrochlore has been studied as a potential actinide-bearing waste form and is a constituent of Synroc® and related crystalline ceramics being developed for nuclear waste disposal (Ringwood et al. 1988; Lumpkin et al. 1994). Numerous defect structures can be derived from the pyrochlore structure type (Lumpkin and Ewing 1988). Additional information on the pyrochlore structure can be found in Lumpkin and Ewing (1988), in Gaines et al. (1997) and by Burns (Chapter 2, this volume).

Zirconolite group, $A_2B_2O_7$. The structure of zirconolite, $CaZrTi_2O_7$, can be described as a derivative of the pyrochlore structure, with octahedrally coordinated B sites and A sites in distorted cubes. Zirconolite is monoclinic and has two distinct A sites, designated A (Ca) and A' (Zr) in Table 3. Zirconollite is Ti dominant at the B site, and Nb-dominant zirconolite minerals were identified from carbonatites in Kovdor (Williams and Gieré 1996); however, no Ta-dominant zirconolite-group minerals are known (Table 3). As for most other Ta-Nb-Ti oxides, U substitutes at the large cation sites, primarily for Ca at the A site in zirconolite; however, no U dominant zirconolite-group minerals are known. Nevertheless, U and Th substitution in zirconolite can be sufficient to induce substantial structural damage, and metamict zirconolites are not uncommon. In addition to its being an important accessory mineral in a wide variety of rocks, zirconolite has been studied as a potential actinide-bearing nuclear waste form (Vance et al. 1994; Lumpkin et al. 1994; Hart et al. 1996; Putnam et al. 1999; Woodfield et al. 1999). Gieré et al. (1998) suggest that redox conditions strongly influence cation substitutions in zirconolite; notably, ferric-ferrous ratios in crystallizing fluids can affect charge-balance. Williams and Gieré (1996) review numerous zirconolite occurrences and report chemical analyses. Mazzi and Munno (1983) clarified distinctions among zirconolite and zirkelite, and elucidated their structural relationships to the pyrochlore-group. Bayliss et al. (1989) further explain polytypism and "polytypoids" among zirconolite and related minerals.

Ixiolite and other α-PbO_2 structure types, MO_2. Ixiolite, $(Ta,Mn,Nb)O_2$, ashanite, $(Nb,Ta,Fe,Mn,V)_4O_8$, and zirkelite, $(Ti,Ca,Zr)O_{2-x}$, are structurally related to α-PbO_2, with octahedrally coordinated cation sites (Mazzi and Munno 1983; Warner and Ewing 1993). All three minerals may contain minor U (and Th). The papers by Mazzi and Munno (1983) and Bayliss et al. (1989) provide additional information on zirkelite and its relationship to zirconolite and the pyrochlore group.

Petschekite and liandratite. Both of these minerals are reportedly metamict and known from only one locality, a pegmatite in Madagascar (Mücke and Strunz 1978). Petschekite crystallizes when annealed, and Smith (1984) noted that the structure appears related to synthetic UTa_2O_8, a derivative of the U_3O_8 structure (Gasperin 1960). If so, petschekite may be more closely related to orthobrannerite than to other Nb,Ta oxides. Petschekite reported alters to a series of partly oxidized ($Fe^{2+} \rightarrow Fe^{3+}$), hydrous, Fe-depleted compounds (Mücke and Strunz 1978). Liandratite is the fully oxidized alteration product of petschekite and contains U^{6+}. It occurs as thin 1-2 mm-thick yellow to yellow-brown glassy coatings on the surfaces of petschekite crystals. Both minerals remain poorly described, and no data have been reported since their initial descriptions (Gaines et al. 1997).

U(IV) phosphates: rhabdophane group

Ningyoite. The rhabdophane group of phosphates are hexagonal phosphates with ideal formula $APO_4 \cdot H_2O$ (Bowels and Morgan 1984) or $APO_4 \cdot nH_2O$ ($0.5 \leq n \leq 1$) (Hikichi et al. 1989). The most common minerals of this group contain REE in the A site, although

four are known to contain actinides: ningyoite (A = U, Ca, Fe), grayite (A = Th, Pb, Ca), tristramite (A = Ca, U, Fe^{3+}), and brockite (A = Ca, Th, REE). Charge balance is maintained by substitutions of divalent cations at the A site or, possibly, by OH substitution for apical O atoms of PO_4 tetrahedra; Sharmová and Sharm (1994) suggested the formula $Ca_{2-x}U_x[P(O,OH)_4]_2 \cdot nH_2O$ for ningyoite (note that the formula for grayite in Dana's New Mineralogy (Gaines et al. 1997) is not charge balanced). Rhabdophane-group minerals have acicular habits, reflecting the ring-like structure of isolated PO_4 tetrahedra and A sites that form large channels parallel to the *c* axis; H_2O groups occupy sites within the channels. Ningyoite is orthorhombic, pseudo-hexagonal, due to doubling of the *b* cell edge. The structure of ningyoite has not been determined. Ningyoite is the most important U mineral at the Ningyo-toge mine in Japan, where it was first discovered (Muto et al. 1959), occurring as microcrystalline crusts and within cracks, rarely forming micrometer-sized crystals. Ningyoite has also been found in the U ore district of northern Bohemia, Czech Republic (Sharmová and Scharm 1994), where it reportedly forms a continuous solid-solution series with brockite: $Ca_{2-y}(U_{1-x}Th_x)_y[P(O,OH)_4]_2 \cdot nH_2O$. Sharmová and Scharm (1994) noted that many ningyoite crystals are P deficient, which they suggest is due to CO_3 and SO_4 replacing PO_4 groups. As noted above, Janeczek and Ewing (1996) proposed a limited solid solution between ningyoite and coffinite.

Vyacheslavite and lermontovite. Lermontovite occurs in reduced hydrothermal deposits in the Kola Peninsula, Russia, where it is associated with Tl minerals ("Tl ochre"), molybdenum sulfates and marcasite (Gaines et al. 1997). Lermontovite is remarkably similar to vyacheslavite, which has nearly the same nominal formula, being slightly more hydrated (Table 1). Both minerals display similar physical and optical properties, although their optical orientations and crystal habits differ. Vyacheslavite was described from an undisclosed location in Uzbekistan, where it occurs on quartz associated with pyrite (Belova et al. 1984).

Other U(IV) minerals

Numerous minerals contain U as a minor substituent and some are listed in Table 2. U^{4+} and Th^{4+} may substitute freely for one another, and Th-bearing minerals are especially important among those minerals that contain U. Many of these are included in discussions of various mineral groups above (e.g. thorianite and thorite). The structurally related REE phosphates of the ***monazite group*** and ***xenotime*** are also important U- and Th-bearing minerals in many granitic rocks, with U and Th substituting for primarily LREE in monazite and HREE in xenotime, through appropriate charge-balance substitutions (Förster 1998a,b; Hanchar et al. 1999; Finch et al. 1999c), and, as noted, coffinite may form a limited solid solution with xenotime (Janeczek and Ewing 1996). We will not attempt to completely describe all minerals with minor U in detail. They are described in Dana's New Mineralogy (Gaines et al. 1997) and additional references are provided for some minerals listed in Table 2. Additional mineralogical information is also available in Fleischer's Glossary of Mineral Species (Mandarino 1999) and Mineral Reference Manual (Nickel and Nichols 1992). Of particular note, however, are a group of chemically similar Th silicates discussed below.

Ekanite, steacyite, thornasite, iraqite-(La) and related Th silicates: Four of these minerals are structurally related, based on rings of silicate tetrahedra. Thorium is an essential constituent in ekanite, steacyite, and thornasite, whereas it is a minor substituent in iraqite, substituting for REE (Table 2). Ekanite and steacyite have often been confused (the structure of steacyite was even reported as that of ekanite; Gaines et al. 1997). The structure of ekanite (and possibly thornasite) is based on two-dimensional infinite sheets of puckered four-member rings of SiO_4 tetrahedra; that of steacyite and iraqite-(La) are based on isolated four-member rings of tetrahedra. Thorium and other cations occupy interstitial sites coordinated by SiO_4, O atoms, and in some cases, OH and H_2O groups. These minerals are commonly metamict and may contain substantial amounts of U^{4+} in substitution for Th^{4+} (Diella and Mannucci 1986). Ekanite is known to form gem-quality material (Gauthier and Fumey 1988), although it is not advisable to wear such radioactive jewelry for long! These minerals occur as accessory minerals in a variety of felsic rocks and granite pegmatites. Numerous occurrences are described for ekanite and steacyite (Gaines et al. 1997); thornasite is known only from Mount St.-Hillarie, Quebec (Ansell and Chao 1987), and iraqite-(La) occurs in granite near a dolomite contact at Shakhi-Rash Mt. in northern Iraq (Livingstone et al. 1976).

An unnamed Th-silicate, $Th_2(Ca,Ba)(Si_9O_{22})(OH)_2 \cdot nH_2O$, conditionally called "thorsite" (Lazebnik et al. 1985,1994), but closely resembling metamict ekanite and steacyite in many respects, was described from calcite carbonatites in the Murun massif, where it is associated with thorite, quartz, K-feldspar, aegerine, titanite, tinaksite, apatite, and dalyite. The translucent yellow grains are highly radioactive and X-ray amorphous, presumably metamict; relict prism faces on grains suggest originally tetragonal symmetry. X-ray powder data for heated material (900°C) resemble those of huttonite. The authors note that heating metamict ekanite (though only to 650°C) also leads to crystallization of huttonite. "Thorsite" has not been accepted as a valid mineral name, and similarities to ekanite and steacyite suggest that "thorsite" may not be a distinct species (Table 2).

An unnamed U-bearing Ca-Th silicate, $Ca_{3.5}(Th,U)_{1.5}(SiO_4)_3(OH)$, was described by Jamtveit et al. (1997) from a regionally metamorphosed shale-limestone xenolith in the Skrim plutonic complex, Oslo Rift, southern Norway, where it apparently forms during prograde reactions of hydrothermal fluids on apatite (T = 820-870°C). This mineral apparently has the apatite type structure and occurs with other silicate apatites, along with wollastonite, melilite, phlogopite, titanian grossular, kalsilite, nepheline, perovskite, and other minerals.

Uranyl minerals

The most oxidized state for U in nature is U^{6+}, and in oxidizing, aqueous environments, U^{6+} always bonds strongly to two O atoms, forming the approximately linear uranyl ion, UO_2^{2+}. In the absence of fluoride, the (hydrated) uranyl ion is the dominant aqueous species in most waters below a pH of approximately 5. At higher pH, the uranyl ion hydrolyzes, forming a number of aqueous hydroxide complexes, according to the general hydrolysis reaction,

$$UO_2^{2+} + yH_2O \Rightarrow UO_2(OH)_y + yH^+ ,$$

and in more U-rich solutions, polymeric U complexes become increasingly important:

$$xUO_2^{2+} + yH_2O \Rightarrow (UO_2)_x(OH)_y^{2x-y} + yH^+$$

These hydroxy complexes are moderately weak solution complexes, and in most groundwaters dissolved carbonate combines with UO_2^{2+} to form uranyl carbonate solution complexes (Langmuir 1978; Grenthe et al. 1992; Clark et al. 1995; also see Murphy and Shock this volume). The uranyl carbonate complexes are quite stable in most groundwaters, and most dissolved U in near-surface groundwaters is probably present as uranyl carbonate complexes (Langmuir 1978; Clark et al. 1995). Where sulfide minerals are undergoing oxidation and dissolution in the presence of U minerals, uranyl sulfate complexes can be important. These, too, are stable solution complexes, and dissolved sulfate can be an important factor for the transport of U in some low pH groundwaters. Most other oxyanions that form complexes with UO_2^{2+} form relatively insoluble uranyl

oxysalt minerals. Among these are uranyl silicates, phosphates, vanadates, arsenates, and molybdates.

The paragenesis of many uranyl minerals can be understood in terms of local groundwater chemistry, the relative solubilities of minerals, and the stabilities of relevant solution complexes. Most uranyl carbonates and sulfates are soluble in dilute groundwaters, precipitating where evaporation is significant. Uranyl oxyhydroxides are substantially less soluble than most uranyl carbonates (with the notable exception of rutherfordine), and can precipitate in abundance if solution complexes other than OH^- are absent. Most uranyl silicates, phosphates, vanadates and arsenates are relatively insoluble, but require dissolved Si, P, V^{5+} and As, which may be derived from a variety of sources. Dissolved silica is a common constituent of many natural waters and, not surprisingly, the uranyl silicates, uranophane and ß-uranophane, are the most common uranyl minerals in nature (Frondel 1958; Smith 1984). Phosphate is another common constituent in many groundwaters, and uranyl phosphates are also common; however, these minerals present some interesting problems for those attempting to understand their paragenesis (Murakami et al. 1997; see below). Figure 2 summarizes uranyl mineral paragenesis for most important uranyl mineral groups from weathered U deposits in the Colorado Plateau, USA, as originally set forth by Garrels and Christ (1959) more that forty years ago. Their conclusions remain valid today and are relevant to many uranyl-mineral occurrences worldwide.

Uranyl oxyhydroxides

The uranyl oxyhydroxides (Table 4) can be represented by the general formula

$$M_n[(UO_2)_xO_y(OH)_z](H_2O)_m$$

where M represents divalent cations, commonly Ca^{2+}, Pb^{2+}, Ba^{2+}, and Sr^{2+}, although K^+-bearing phases are also known. The compositions of known uranyl oxyhydroxides are plotted in Figure 3, which shows mole fractions of MO as a function of total H_2O (the mole fraction of UO_3 is $[1 - MO + H_2O]$). Because some H_2O in uranyl oxyhydroxides occurs as H_2O groups in interlayer positions with the M cations, there is a general decrease in total H_2O as MO increases. This trend also reflects decreasing OH^- in the structural sheets that compensates increased interlayer cation occupancies.

The uranyl oxyhydroxides form in U-rich aqueous solutions and develop early during the oxidation and corrosion of uraninite-bearing ore deposits, most commonly at or near the surface of corroded uraninite. Alteration of uranyl oxyhydroxides is ubiquitous, and the question of their long-term stability under various environmental conditions is pertinent to understanding the often complex assemblages of uranyl minerals found at many U deposits. The formation and alteration of uranyl oxyhydroxides can, in part, determine reaction paths and uranyl-minerals paragenesis at weathered U deposits, which help to control dispersion and fixation of U in many dilute groundwaters.

Significant progress has been made in our knowledge of this group of minerals in the 15 years since the review by Smith (1984). This has come with the advent of improved analytical methods, most notably the introduction of charge-coupled device (CCD) detectors for X-ray diffraction (Burns 1998b). The use of CCD detectors permits accurate structure determinations of very small crystals and of minerals with large unit cells, both of which are common problems among the uranyl minerals (see Burns 1998b for a discussion of the use of CCD detectors in X-ray structure analysis). Two new uranyl oxyhydroxides have been named since the review by Smith (1984), although Ondrus et al. (1997c) report several new unnamed species, which are listed in Table 4. One new mineral is the Pb-uranyl oxyhydroxide sayrite, discussed with other Pb minerals below. The other is

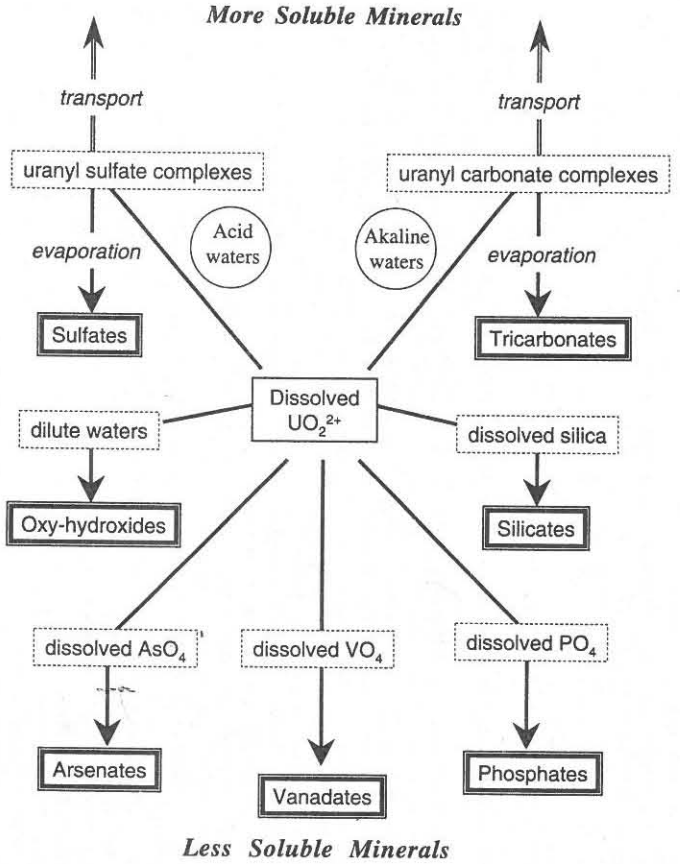

Figure 2. Schematic representation of the paragenesis of several important uranyl-mineral groups. Dissolved UO_2^{2+} is derived from the oxidative dissolution of U-bearing minerals and the arrows indicate interactions with additional dissolved species. Arrows pointing downwards indicate precipitation, and those pointing upwards indicate transport. Minerals are shown with more soluble species above those with generally lower solubilities; for qualitative comparison only (modified after Garrels and Christ 1959).

protasite, a rare hydrated Ba-uranyl oxyhydroxide from the Shinkolobwe mine, where it forms bright orange pseudohexagonal plates flattened on {010} with good {010} cleavage (Pagoaga et al 1986). The structure of protasite is monoclinic (*Pn*), though almost dimensionallyorthorhombic ($\beta = 90.4°$), with edge- and corner-sharing U polyhedra forming structural sheets parallel to (010) (Pagoaga et al. 1987). Protasite, which closely resembles fourmarierite in color and habit, is associated with Pb-uranyl oxyhydroxides and uranophane. The synthetic equivalent of protasite has been known for some time (Protas 1959), as has the compositionally similar Ca-analogue, although the Ca-analogue of protasite is unknown as a mineral.

At the time of Smith's (1984) review, the uranyl peroxides, studtite and metastudtite, were considered rare; however, both minerals have now been identified from a large number of localities, including the Shinkolobwe mine in Shaba, southern Democtratic Republic of Congo, the Kobokobo pegmatite in western Democratic Republic of Congo, the Menzenschwand U mine, and U deposits in Lodève, France, sometimes in large

Table 4. Uranyl oxy-hydroxides

Name	*Formula*	*Comments*
Agrinierite*	$(K_2,Ca,Sr)(UO_2)_3O_2(OH)_3(H_2O)_4$	structure similar to protasite, Cahill & Burns (1999)
Bauranoite*	$BaO{\cdot}UO_3{\cdot}4{\cdot}5H_2O$	ill defined; Belova et al. (1985)
Becquerelite*	$Ca(UO_2)_6O_4(OH)_6(H_2O)_8$	Pagoaga et al. (1987), Cejka et al. (1998a)
Billietite*	$Ba(UO_2)_6O_4(OH)_6(H_2O)_8$	Pagoaga et al. (1987), Cejka et al. (1998a); structure refinement, Finch et al. (in prep.)
Calciouranoite*	$(Ca,Ba,Pb,K_2,Na_2)O{\cdot}UO_3{\cdot}5H_2O$	amorphous; ill defined; compare wölsendorfite, bauranoite, clarkeite; Belova et al. (1985)
Clarkeite*	$(Na,Ca)(UO_2)(O,OH)(H_2O)_m$ (n = 0-1)	cf. calciouranoite, bauranoite, wölsendorfite; Gaines et al. (1997); compositional zoning, Finch & Ewing (1997); compare synthetic $K_5[(UO_2)_{10}O_8(OH)_5](H_2O)$ of Burns & Hill (199b)
Compreignacite*	$K_2(UO_2)_6O_4(OH)_6(H_2O)_7$	Gaines et al. (1997); Ondrus et al. (1997b); similar to becquerelite, Burns (1998b)
Curite*	$Pb_{1.5+x}(UO_2)_4O_{4+2x}(OH)_{3-2x}(H_2O)$ ($0 < x < 0.15$)	Gaines et al. (1997); Cejka et al. (1998a); variable Pb content, Li & Burns (1999a); Burns & Hill (1999a)
"Dehydrated schoepite"*	$(UO_2)O_{0.15-x}(OH)_{1.5+2x}$ ($0 < x < 0.25$)	dehydration of schoepite & metaschoepite; forms series with α-$UO_2(OH)_2$; Christ & Clark (1960); Finch et al. (1998)
Fourmarierite*	$Pb(UO_2)_4O_3(OH)_4(H_2O)_4$	Deliens (1977a); Piret & Deliens (1985); Gaines et al. (1997); variable Pb content, Li & Burns (in prep.)
Ianthinite*	$U^{4+}(UO_2)O_4(OH)_6(H_2O)_9$	mixed-valence U species; Burns et al. (1997b)
Masuyite*	$Pb[(UO_2)_3O_3(OH)_2](H_2O)_3$	recent structure suggests possibility for Pb:U variability (Burns & Hanchar 1999). Formula is that of "grooved masuyite"; $4PbO{\cdot}9UO_3{\cdot}10H_2O$ also reported as "type masuyite" with distinct X-ray powder pattern (Deliens & Piret 1996); synthetic analogue is $3PbO{\cdot}8UO_3{\cdot}10H_2O$ (Protas 1959; Noe-Spirlet & Sobry 1974). Christ & Clark (1960); Deliens (1977a); Deliens et al. (1984) Finch & Ewing (1992); Ondrus et al. (1997b).
Metacalciouranoite*	$(Ca,Ba,Pb,K,Na)O{\cdot}UO_3{\cdot}2H_2O$	amorphous; ill defined; compare wölsendorfite, bauranoite, clarkeite; Belova et al. (1985)
Metaschoepite*	$(UO_2)_8O_2(OH)_{12}(H_2O)_{10}$	uncertain formula; Christ & Clark (1960), Debets & Loopstra (1963), Ondrus et al. (1997b); Finch et al. (1998)
Metastudtite	$UO_4{\cdot}2H_2O$	Peroxide; Deliens & Piret (1983b); Gaines et al. (1997)
Meta-vandendriesscheite	$PbO{\cdot}7UO_3{\cdot}(12-x)H_2O$ (?)	ill defined; structure probably similar to vandendriesscheite; Christ & Clark (1960)
Paraschoepite*	$UO_3{\cdot}nH_2O$ (?) ($n \approx 2$)	ill defined; questionable species; Finch et al. (1992, 1997, 1998)
Protasite	$Ba(UO_2)_3O_3(OH)_2(H_2O)_3$	very rare; compare masuyite; Pagoaga et al. (1987); Cejka et al. (1998a)
Rameauite	$K_2Ca(UO_2)_6O_4(OH)_6(H_2O)_6$	Gaines et al. (1997)
Richetite*	$M_4Pb_{8.5}[(UO_2)_{36}O_{36}(OH)_{24}](H_2O)_{41}$	Variable H_2O? M is probably a transition-metal; e.g. Fe^{2+}, Burns (1998a); Piret & Deliens (1984); Ondrus et al. (1997b)
Sayrite	$Pb_2(UO_2)_5O_6(OH)_2(H_2O)_4$	Piret et al. (1983); Gaines et al. (1997)
Schoepite*	$(UO_2)_8O_2(OH)_{12}(H_2O)_{12}$	Finch et al. (1996); Finch et al. (1997), Finch et al. (1998)
Studtite*	$UO_4{\cdot}4H_2O$	Peroxide; Cejka et al. (1996a)
Uranosphaerite*	$Bi_2O_3{\cdot}2UO_3{\cdot}3H_2O$	ill defined; Kolitschn (1997); Gaines et al. (1997)
Vandenbrandeite*	$Cu(UO_2)(OH)_4$	Cejka (1994); Gaines et al. (1997)
Vandendriesscheite*	$Pb_{1.57}(UO_2)_{10}O_6(OH)_{11}(H_2O)_{11}$	Christ & Clark (1960); Deliens (1977a); Gaines et al. (1997); Burns (1997)
Wölsendorfite*	$(Ca,Ba)_xPb_{2-x}[(UO_2)_{14}O_{19}(OH)_4](H_2O)_{12}$ ($x \leq 1$?)	structure of barian wölsendorfite by Burns (1999e): $Pb_{0.18}Ba_{0.36}(UO_2)_{14}O_{19}(OH)_4(H_2O)_{12}$; compare calciouranoite, bauranoite, clarkeite. Deliens (1977a); Beddoe-Stephens & Secher (1977); Belova et al. (1985); Gaines et al. (1997)
Unnamed*	Hydrated uranyl hydroxide	Mineral "A" of Frondel (1956); hydrothermal origin; minor Pb, K, Th, Ca, Sr; Korzeb et al. (1997); Foord et al. (1997)
Unnamed*	Hydrated uranyl hydroxide	Amber brown crystals, with minor Pb; synthetic analogue: PDF 15-569; Threadgold (1960); Ondrus et al. (1997c)
Unnamed*	Hydrated uranyl oxide hydroxide	olive yellow; compare dehydrated schoepite; Ondrus et al. (1997c)

* New or supplemental data or not listed in Dana's New Mineralogy (Gaines et al. 1997).

Figure 3. Compositions of the uranyl oxyhydroxides as a function of the molecular proportions of MO and H_2O (M = Ca, Pb, Ba, Sr, K_2). The Pb- uranyl oxyhydroxides are indicated by black-filled diamonds, richetite and wölsendorfite, which may contain cations besides Pb, are indicated with slightly lighter shadings. Pb-free uranyl oxyhydroxides are represented as lightly filled squares. Labels are as follows. Sp: schoepite; MS: metaschoepite; DS: "dehydrated schoepite:" Vdr: vandendriesscheite; Bq: becquerelite; Bl: billietite (Bl*: partly dehydrated billietite of Pagoaga et al. 1987); Cmp: compreignacite; Rch: richetite; Fm: fourmarierite; Agr: agrinierite; Rm: rameauite; MC: masuyite (Burns and Hanchar 1999; "gooved masuyite" of Deliens and Piret 1996); Pr: protasite; M(syn) synthetic analogue of masuyite (Protas 1959); MT: "type masuyite" of Deliens and Piret (1996); Syr: sayrite; W: wölsendorfite; Clk: clarkeite; Cur (ss): curite (solid solution indicated by shaded line at left; Li and Burns 1999; third diamond at right from curite of Taylor et al. 1981); CaU: calciouranoite; BaU: Bauranoite; Vb: vandenbrandeite; Usp: uranosphaerite.

quantities (e.g. at Menzenschwand). The structures of these two minerals are unknown, but the unit-cell parameters and space group of studtite suggest it is topologically similar to α-$UO_2(OH)_2$ (Taylor 1971), with alternate rows of U atoms missing along [001]. By placing a U atom at (0,0,0) in space groups *C2/m* (studtite) and *Immm* (metastudtite), X-ray powder diffraction patterns can be calculated that match well with data published for natural studtite (Debets 1963; Cejka et al. 1996a) and metastudtite (Debets 1963; Deliens and Piret 1983b). X-ray examinations of natural studtite commonly reveal mixtures of studtite and meta-studtite as well as other minerals, such as lepersonnite and oxyhydroxidesfourmarierite, the latter commonly occurring as thread-like inclusions within studtite and metastudtite crystals (Deliens and Piret 1983b).

The structure of ianthinite was reported by Burns et al. (1997b), and the formula differs slightly from that originally reported (Bignand 1955; Guillemin and Protas 1959) by being more reduced (U^{4+}:U^{6+} = 2:4 rather than U^{4+}:U^{6+} = 1:5). The structure determination by Burns et al. (1997b) was not of optimal quality, with an agreement index (R) of 9.7 %, and additional refinement may help clarify the details of the structure. Ianthinite is rarely found, but because it oxidizes readily in air to schoepite, it may be a common precursor to schoepite and metaschoepite (Deliens et al. 1984). Pearcy et al. (1994) identified ianthinite as an early oxidation product of uraninite at the Nopal I mine near Peña Blanca, Mexico.

A recent structure determination of schoepite (Finch et al. 1996) indicates that the composition is equivalent to that determined by Billiet and de Jong (1935), $4UO_3{\cdot}9H_2O$,

rather than the previously accepted composition of synthetic preparations with slightly less water, $UO_3 \cdot 2H_2O$ (Christ and Clark 1960; Christ 1965). The synthetic compound apparently corresponds to metaschoepite (Christ and Clark 1960; Debets and Loopstra 1963; Finch et al. 1998), the structure of which has reportedly been determined (M Weller, pers. comm.). Finch et al. (1997) compare the X-ray powder diffraction pattern calculated for schoepite with X-ray powder diffraction data for several minerals and synthetic compounds related to schoepite. The dehydration of schoepite was described by Finch et al. (1992, 1998) (see below), who proposed a structural formula for "dehydrated schoepite", a common dehydration product of schoepite and metaschoepite in nature (Christ and Clark 1960). Paraschoepite, an inadequately described mineral (Schoep and Stradiot 1947; Christ and Clark 1960), may not be a valid species (Finch et al. 1997, 1998) and requires further study.

The structure of compreignacite was determined recently, demonstrating that it contains a sheet similar to the structure of becquerelite (Burns 1998c), and indicating that there is one less H_2O in the formula than previously accepted (Table 4).

New data for clarkeite help to clarify the formula. Clarkeite crystallizes during metasomatic replacement of pegmatitic uraninite by late-stage, oxidizing hydrothermal fluids. Samples are zoned compositionally: clarkeite, which is Na-rich, surrounds a K-rich core (commonly with remnant uraninite) and is surrounded by more Ca-rich material. Clarkeite is hexagonal ($R\bar{3}m$). The structure of clarkeite is based on anionic sheets with composition $[(UO_2)(O,OH)_2]$, and these are bonded to each other through interlayer cations and water molecules. The ideal formula for clarkeite is $Na[(UO_2)O(OH)](H_2O)_{0-1}$, although it commonly contains additional elements, including K, Ca, and Th. The structure of a hexagonal synthetic K-uranyl oxyhydroxide, $K_5[(UO_2)_{10}O_8(OH)_9](H_2O)$, recently reported by Burns and Hill (1999b), may be structurally related to clarkeite and the "K-rich phase" that forms near the cores of clarkeite (Finch and Ewing 1997).

New data on mineral "A" described by Frondel (1956) were reported by Foord et al. (1997), and some details on its paragenesis at the Ruggles and Palermo pegmatites are discussed by Korzeb et al. (1997). This material may be a mixture of metaschoepite and "dehydrated schoepite," and more data are needed to clarify the structural details of mineral "A." = HEISENBERGITE

An extensive study natural and synthetic samples of becquerelite, billietite and protasite was reported by Cejka et al. (1998b), who demonstrated that billietite contains eigth interlayer H_2O groups, rather than the four reported by Pagoaga et al. (1987). This is consistent with a recent structure refinement for billietite (Finch et al. in prep.).

Although a large number of uranyl oxyhydroxide minerals are known, none contains Na or Mg. Such phases have been synthesized, and reports of Na-uranyl oxyhydroxides are especially common in the literature (e.g. Diaz Arocas and Grambow 1997); these display close structural similarities to schoepite and metaschoepite (Diaz Arocas and Grambow 1997). Their lack of occurrence in nature probably reflects their high solubilities. Several Mg-uranyl oxyhydroxides have been synthesized, and all are structurally related to becquerelite and protasite: $Mg[(UO_2)_6O_6(OH)_4]_2 \cdot 4H_2O$ and $Mg_3[(UO_2)_6O_5(OH)_5]_2 \cdot 19H_2O$ (Vdovina et al. 1984) and $Mg[(UO_2)_6O_4(OH)_6] \cdot 10H_2O$ (Vochten et al. 1991). Vochten et al. (1991) also synthesized two Ni^{2+} and Mn^{2+} uranyl oxyhydroxides and measured their solubilities along with that of the Mg compound. They concluded that the Mg compound was approximately as soluble as synthetic becquerelite (Vochten and Van Haverbeke 1990), whereas the Ni and Mn compounds were more so. Vochten et al. (1991) concluded that Mg, Ni, and Mn uranyl oxyhydroxides should be stable in natural groundwaters and

may occur as minerals. None has been found yet.

A synthetic Ca-uranyl oxyhydroxide was described from experiments with U-doped cements that has the empirical formula $CaO \cdot 4UO_3 \cdot 7H_2O$, and which appears to be structurally related to becquerelite (Moroni and Glasser 1996; Skakle et al 1997). The Ca:U ratio (1:4) is the same as the Mg:U ratio of the more Mg-rich uranyl oxyhydroxide synthesized by Vdovina et al. (1984), and is similar to the Ba:U ratio of protasite (1:3); however, no Ca-uranyl oxyhydroxide with a similar Ca:U ratio is known as a mineral.

Pb-uranyl oxyhydroxides

Structure determinations for several Pb-uranyl oxyhydroxides, vandendriesscheite, fourmarierite, masuyite, richetite, and wölsendorfite, have greatly improved our understanding of this enigmatic group of minerals. Masuyite and, especially, vandendriesscheite are common at oxidized U deposits; whereas richetite is exceedingly rare.

Vandendriesscheite. Vandendriesscheite is one of the most common Pb-bearing uranyl oxyhydroxides, occurring at numerous uraninite deposits exposed to weathering environments (Frondel 1956, 1958). Christ and Clark (1960) reported that, like schoepite, vandendriesscheite undergoes spontaneous, irreversible dehydration with structural modifications, although they did not determine water contents. Oriented inclusions of extraneous phases, such as masuyite, within vandendriesscheite crystals may complicate interpretations of XRD data. The recent structure determination for vandendriesscheite revises the formula slightly (Burns 1997), although it is not clear how the crystal examined is related to meta-vandendriesscheite as described by Christ and Clark (1960) (Table 4).

Fourmarierite. Fourmarierite has been confused in the past with vandendriesscheite and wölsendorfite (Frondel 1958; Deliens 1977a). These minerals display similar X-ray powder diffraction patterns. The structure determination of fourmarierite clarifies the formula (Piret 1983), and additional detail on its structure is provided by Burns (this volume).

Richetite. Richetite's dark color prompted Frondel (1958) to suggest that some U is reduced; however, XPS analyses verified that U in richetite is fully oxidized (Piret and Deliens 1984). This is consistent with the recent structure determination, which verifies that richetite is related to becquerelite, but with a complex interlayer containing cations in addition to Pb, possibly Fe (Burns 1998a); this may explain its dark color. The new structural formula indicates that the richetite crystal studied by Burns (1998a) contained significantly more H_2O than material described by Piret and Deliens (1984). The reason for this apparent discrepancy is uncertain, but richetite may exhibit variable hydration states without significant structural differences (cf. curite). The fact that richetite is rare may be a reflection of unusual conditions required for its formation. Richetite, like wölsendorfite, which also contains interlayer cations in addition to Pb, does not form a series with other Pb-uranyl oxyhydroxides but requires a unique paragenesis. The precise composition of richetite remains uncertain, and further work is needed to clarify the formula (Burns 1998a). Richetite has been reported from the Shinkolobwe mine in Shaba, Democtratic Republic of Congo (Deliens et al. 1981) and at Jáchymov, Czech Republic (Ondrus et al. 1997b); specimens from the two localities display subtle differences in unit-cell parameters. Its color (dark brown to tan), strong pleochroism, and triclinic symmetry help distinguish richetite from other Pb-uranyl oxyhydroxides. X-ray powder diffraction data for richetite are reported by Piret and Deliens (1984) and by Ondrus et al. (1997b). Burns (this volume) discusses the structure of richetite in more detail.

Masuyite. The composition of masuyite has long been uncertain. Piret et al. (1983) noted that masuyite from Shinkolobwe is heterogeneous, with variations in Pb:U ratios and XRD powder spectra. Deliens and Piret (1996) report two compositions for masuyite, $PbO{\cdot}3UO_3{\cdot}4H_2O$ ("grooved" masuyite) and $4PbO{\cdot}9UO_3{\cdot}10H_2O$ ("type" masuyite). These bracket the composition of the synthetic analogue, $3PbO{\cdot}8UO_3{\cdot}10H_2O$ (Protas 1959; Noe-Spirlet and Sobry 1974). Finch and Ewing (1992a, 1992b) reported masuyite inclusions within vandendriesscheite crystals with the composition $PbO{\cdot}3UO_3{\cdot}4H_2O$. Burns and Hanchar (1999) report the crystal structure for masuyite with this same composition, demonstrating that it is isostructural with protasite, although the presence of an additional cation site in the interlayer may permit compositional variability.

Sayrite. The only new Pb-uranyl oxide hydrate described since Smith's (1984) review, sayrite, a very rare Pb-uranyl oxyhydroxide, occurs at the Shinkolobwe U mine in close association with other Pb-uranyl oxyhydroxides, masuyite and richetite, as well as becquerelite and uranophane (Piret et al. 1983). Sayrite (monoclinic, space group $P2_1/c$) forms reddish orange to yellow-orange prismatic crystals (optically biaxial negative) flattened on {-102} and elongated along [010], with perfect (-102) cleavage parallel to the structural sheets. Compositionally, it lies between masuyite and curite (Fig. 3).

Curite. A structural examination of thirteen curite crystals showed that curite displays a limited range of interlayer Pb occupancies but no evidence for OH^- ions in interlayer positions (Li and Burns 1999), as proposed by Mereiter (1979) and Taylor et al. (1981). Charge balance for different Pb occupancies is maintained through $OH^- \Leftrightarrow O^{2-}$ substitution in the structural sheets, and curite can be represented by the general formula $Pb_{1.5+x}[(UO_2)_4O_{4+x}(OH)_{3-2x}](H_2O)$ $(0 < x < 0.15)$ (Li and Burns 1999a). Cejka et al. (1998a) provide a comprehensive review of analytical data for curite and report new chemical analyses, X-ray powder-diffraction data, IR data and thermal analyses. Burns and Hill (1999a) report the structure of a synthetic Sr-bearing analogue of curite.

Wölsendorfite and related minerals. The structure of a barian wölsendorfite was recently reported by Burns (1999e), demonstrating that wölsendorfite is structurally related to other uranyl oxyhydroxides of the protasite group but with a structural sheet that has a considerably more complex anion topology. Belova et al. (1985) report chemical and X-ray diffraction data for four compositionally similar uranyl oxyhydroxide minerals wölsendorfite, calciouranoite, metacalciouranoite, and bauranoite. They consider these four to comprise a structurally related group with solid solution between minerals rich in Ca, Ba and Pb. Except for wölsendorfite, these minerals are known only from unspecified occurrences in the former Soviet Union. Calciouranoite and bauranoite are not generally well crystallized (Rogova et al. 1973, 1974), and X-ray powder-diffraction data originally reported for these two minerals are for samples heated to 900°C. Powder patterns of heated material closely resemble synthetic anhydrous Ca and Ba uranates structurally related to clarkeite (Loostra and Rietveld 1969) but structurally distinct from wölsendorfite and other uranyl oxyhydroxides. X-ray diffraction patterns reported by Belova et al. (1985) show considerable variation (with some unindexed lines), and assignment of group status to these minerals is probably premature. Fayek et al. (1997) reported finding an unidentified uranyl oxyhydroxide at the Cigar Lake U deposit, where uranyl minerals reportedly occur as colloform bands along the outer edges of fine-grained botryoidal uraninite and single uraninite grains, as well as occurring in small veins that cut across uraninite and coffinite. Isobe et al. (1992b) reported Ca-free wölsendorfite from the Koongarra U deposit in Northern Territories, Australia.

Uranyl carbonates

Uranium carbonates (Tables 5 and 6) may precipitate where evaporation is significant or where the fugacity of CO_2 is greater than atmospheric (Garrels and Christ 1959; Hostetler and Garrels 1962; Finch and Ewing 1992b; Finch 1997a). Uranyl di- and tri-carbonates tend to form only where evaporation is high. Most of these minerals are ephemeral, dissolving readily when re-exposed to fresh water. Uranyl carbonate complexes in solution are quite stable and are probably the most important solution complexes responsible for U migration in oxidizing environments (Langmuir 1978; Clark et al. 1995). They are important in near-neutral to alkaline waters (pH > 7), and precipitation of uranyl tricarbonate minerals usually reflects evaporation of alkaline waters (Fig. 2). On the other hand, the monocarbonates rutherfordine, joliotite, blatonite, urancalcarite and wyartite probably precipitate from fresh water where (at least local) pCO_2 values are elevated relative to atmospheric values ($pCO_2 > 10^{-3.5}$ atm). Elevated pCO_2 most commonly results from organic respiration, transpiration and decomposition. Such waters tend to have relatively acid pH values (pH < 6 or 7). Unlike the uranyl di- and tri-carbonates, the uranyl monocarbonates are relatively insoluble. The solubility of rutherfordine, for example, is comparable to that of schoepite (Grenthe et al. 1992), and rutherfordine may persist in some environments for several tens to hundreds of thousands of years (Finch et al. 1996). Understanding the structural and thermodynamic stabilities of U carbonates is particularly germane to our ability to manage U-contaminated sites and our understanding of potential radionuclide behavior around a high-level waste repository (Clark et al. 1995; Finch 1997a) because of the potentially high mobility of U in carbonate-bearing groundwaters (Hostetler and Garrels 1962; Langmuir 1978; Grenthe et al. 1992). Uranyl carbonates may be important in actinide-contaminated soils and certain high-level nuclear-waste repositories (e.g. the proposed repository at Yucca Mountain) because they may be sinks for ^{14}C (Murphy 1995), transuranic actinides (Burns et al. 1997a; Wolf et al. 1997) and possibly certain fission-products (Finch and Ewing 1991; Wronkiewicz et al. 1996).

Only three uranyl carbonates with no cations besides U and C are known, rutherfordine, joliotite and blatonite, and all are monocarbonates. Rutherfordine and joliotite were discussed by Smith (1984). A recent structure refinement of rutherfordine indicates that there are two polytypes of rutherfordine with space groups *Pmmn* (Christ et al. 1955) and *Imm*2 (Finch et al. 1999). Thermal and IR analyses of synthetic and natural uranyl monocarbonates, including rutherfordine, indicate variable amounts of OH and H_2O in some of these phases, with minor modifications to the structure (Cejka et al. 1988). Blatonite, $UO_2CO_3{\cdot}H_2O$, was recently described from the Jomac mine in San Juan County, Utah (Vochten and Deliens 1998) Blatonite occurs as fibrous bundles of finely acicular, canary-yellow crystals within gypsum seams in siltstones of the Triassic Shinarump Conglomerate and is associated with the uranyl minerals boltwoodite, coconinoite, metazeunerite, and rutherfordine, as well as azurite, malachite, brochantite, smithsonite and carbonate-cyanotrichite. Blatonite is hexagonal or trigonal; Vochten and Deliens (1998) report XRD and IR data. Walenta (1976) studied the dehydration of joliotite, $UO_2CO_3{\cdot}2H_2O$, and found that heating increased the refractive indices and caused diffraction peaks to become more diffuse; however, data from the dehydration of joliotite do not resemble those of blatonite, leading Vochten and Deliens (1998) to conclude that blatonite is not a simple dehydration product of joliotite and therefore cannot be described as "meta-joliotite."

The structure of wyartite, $Ca(CO_3)U^{5+}(UO_2)_2O_4(OH)(H_2O)_7$, was reported by Burns and Finch (1999), who demonstrated that it contains U^{5+}, rather than U^{4+} as originally reported (Guillemin and Protas 1959), making wyartite the first mineral known to contain pentavalent U. This may have important implications for the stability of the UO_2^+ ion in

Table 5. Miscellaneous uranyl carbonates

Name	*Formula*	*Comments*
Albrechtschraufite*	$MgCa_4(UO_2)(CO_3)_3F_2(H_2O)_{17}$	compare schröckingerite; Mereiter (1984); Ondus et al. (1997a)
Astrocyanite-(Ce)	$Cu_2(REE)_2(UO_2)(CO_3)_5(OH)_2(H_2O)_{1.5}$	compare shabaite; Piret & Deliens (1990); Gaines et al. (1997)
Blatonite*	$UO_2CO_3{\cdot}H_2O$	not produced by dehydration of joliotite; Vochten & Deliens (1999)
Bijvoetite-(Y)*	$(REE)_2(UO_2)_4(CO_3)_4(OH)_6(H_2O)_{11}$	Deliens & Piret (1982a); Gaines et al. (1997); Li & Burns (1999b)
Fontanite	$Ca(UO_2)_3(CO_3)_4(H_2O)_3$	Deliens & Piret (1992), Gaines et al. (1997)
Joliotite	$UO_2CO_3{\cdot}nH_2O$ $(n \approx 2)$	Gaines et al. (1997)
Kamotoite-(Y)	$Y_2(UO_2)_4(CO_3)_3O_4(H_2O)_{14.5}$	Gaines et al. (1997)
Lepersonnite-(Gd)	$Ca(REE)_2(UO_2)_{24}(CO_3)_6Si_4O_{12}(H_2O)_{60}$	Deliens & Piret (1982a); Gaines et al. (1997)
Roubaultite	$Cu^{2+}{}_2(UO_2)_3(CO_3)_2O_2(OH)_2(H_2O)_4$	Ginderow & Cesbron (1985); B&97, Gaines et al. (1997)
Rutherfordine*	UO_2CO_3	two polytypes (*Pmmn* & *Imm*2); Christ et al. (1955), Frondel (1958); Cejka & Urbanec (1988); Gaines et al. (1997); Finch et al. (1999); Vochten & Blaton (1999)
Schröckingerite	$NaCa_3(UO_2)(CO_3)_3(SO_4)F(H_2O)_{10}$	compare albrechtschraufite; Urbanec & Cejka (1979b); Mereiter (1986); Gaines et al. (1997)
Shabaite-(Nd)	$Ca(REE)_2(UO_2)(CO_3)_4(OH)_2(H_2O)_6$	compare astrocyanite; Deliens & Piret (1990a), Gaines et al. (1997)
Sharpite	$Ca(UO_2)_6(CO_3)_5(OH)_4(H_2O)_6$	Cejka et al. (1984); Gaines et al. (1997)
Urancalcarite	$Ca_2(UO_2)_3(CO_3)(OH)_6(H_2O)_3$	oxidation product of wyartite (?); Deliens & Piret (1984b); Gaines et al. (1997)
Voglite*	$Ca_2Cu(UO_2)(CO_3)_4(H_2O)_6$ or $Ca_2Cu(UO_2)(CO_3)_3(OH)_2(H_2O)_4$ [PD79]	Jachymov: $Ca_2Cu(UO_2)_2(CO_3)_2O_3$; Ondrus et al. (1997b); Urbanec & Cejka (1979b); Piret & Deliens (1979); Gaines et al. (1997)
Wyartite*	$CaU^{5+}(CO_3)(UO_2)O(OH)_4(H_2O)_7$	Gaines et al. (1997); Smith (1984); mixed U^{5+}-U^{6+}; structure determination reveals first known U^{5+} mineral; Burns & Finch (1999)
"Wyartite II"*	$CaU^{5+}(CO_3)(UO_2)O(OH)_4(H_2O)_3$	Clark (1960); mixed U^{5+}-U^{6+}; dehydration product of wyartite, structure similar to wyartite, unpublished data
Unnamed*	$Ca_2Cu(UO_2)_2(CO_3)_2O_3(H_2O)_3$ or $Ca_2Cu(UO_2)_2(CO_3)_2(OH)_6$	compare voglite; Ondrus et al. (1997c)
Unnamed*	$Ca_5Cu(UO_2)_4(CO_3)_6(OH)_8(H_2O)_4$	"pseudo-voglite"; Ondrus et al. (1997c)
Unnamed*	hydrated Ca-Cu-uranyl carbonate	Ondrus et al. (1997c)

* New or supplemental data or not listed in Dana's New Mineralogy (Gaines et al. 1997).

Table 6. Uranyl dicarbonates (UO_2:CO_3 = 1:2) and tricarbonates (UO_2:CO_3 = 1:3)

Name	*Formula*	*Comments*
Andersonite*	$Na_2Ca(UO_2)(CO_3)_3(H_2O)_6$	synthetic intermediate with liebigite also known; Cejka et al. (1987); Urbanec & Cejka (1979b); Vochten et al. (1994); Gaines et al. (1997)
Bayleyite	$Mg_2(UO_2)(CO_3)_3(H_2O)_{18}$	Frondel (1958); Gaines et al. (1997)
Grimselite	$K_3Na(UO_2)(CO_3)_3(H_2O)$	Gaines et al. (1997)
Liebigite*	$Ca_2(UO_2)(CO_3)_3(H_2O)_{11}$	synthetic intermediate with andersonite also known; Urbanec & Cejka (1979b); Vochten et al. (1994); Gaines et al. (1997)
Metazellerite*	$Ca(UO_2)(CO_3)_2(H_2O)_n$ $(n < 5)$	dicarbonate; dehydration product of zellerite; Gaines et al. (1997); Ondrus et al. (1997b)
Rabbittite	$Ca_3Mg_3(UO_2)_2(CO_3)_6(OH)_4(H_2O)_{18}$	Frondel (1958); Gaines et al. (1997); Ondrus et al. (1997b)
Swartzite	$CaMg(UO_2)(CO_3)_3(H_2O)_{12}$	Gaines et al. (1997)
Unnamed*	$Na_4(UO_2)(CO_3)_3$	may be structurally distinct from the synthetic analogue; Douglass (1956); Ondrus et al. (1997c)
Widenmannite*	$Pb_2(UO_2)(CO_3)_3$	Walenta (1976); Gaines et al. (1997)
Zellerite*	$Ca(UO_2)(CO_3)_2(H_2O)_5$	dicarbonate; Gaines et al. (1997); Ondrus et al. (1997b)
Znucalite*	$CaZn_{12}(UO_2)(CO_3)_3(OH)_{22}(H_2O)_4$ or $CaZn_{11}(UO_2)(CO_3)_3(OH)_{20}(H_2O)_4$	possible compositional variability; Ondrus et al. (1990); Chiappero & Sarp (1993); Ondrus et al. (1997b); Gaines et al. (1997)

* New or supplemental data or not listed in Dana's New Mineralogy (Gaines et al. 1997).

anoxic U-rich waters (Langmuir 1978), because U^{5+} is considered unstable in aqueous solutions, disproportionating to U^{4+} plus U^{6+}, especially in acid media. Whether wyartite forms from thermodynamically stable UO_2^+-bearing waters, or whether UO_2^+ in these solution persists metastably is not known; however, the crystal structure apparently stabilizes U^{5+} in the mineral. The crystal structure of a dehydration product of wyartite, wyartite II, $Ca(CO_3)U^{5+}(UO_2)_2O_4(OH)(H_2O)_{3.4}$, originally described by Clark (1960), has also been determined (unpublished data), and it is also consistent with U^{5+} in structural sites.

Deliens and Piret (1984b) described urancalcarite from the Shinkolobwe mine in Shaba, Democratic Republic of Congo, where it is found on uraninite, and is associated with uranophane, masuyite and wyartite. Urancalcarite is orthorhombic (*Pbnm* or $Pbn2_1$), forming bright yellow crystals that occur as radiating aggregates to 4 mm in diameter. Individual crystals form fibers elongated on [001] and flattened on (100), and display no cleavage. Unit-cell parameters of urancalcarite resemble those of the mixed-valence uranyl carbonates wyartite and wyartite II. Similarities between the mixed-valence carbonates and fully oxidized urancalcarite resemble similarities between the mixed-valence uranyl oxyhydroxide, ianthinite, and fully oxidized schoepite. The structural sheets in these mixed-valence minerals posses the β-U_3O_8 anion topology (cf. Miller et al. 1996; Burns et al. 1996) and have similar dimensions in the plane of the structural sheets (Table 7). Schoepite and urancalcarite have similar cell dimensions in the plane of their structural sheets, suggesting that urancalcarite has structural sheets similar to those in schoepite (Table 7). Ianthinite oxidizes to schoepite, with little or no lattice strain (Schoep and Stradiot 1947), the implication being that wyartite (or wyartite II) may oxidize to urancalcarite. The U:Ca:C ratios in urancalcarite (3:1) are identical to those in wyartite and wyartite II, so their compositions are similar. Whether urancalcarite might form by the oxidation of pre-existing wyartite or wyartite II is uncertain; however, both minerals commonly occur together (Deliens and Piret 1984b).

Fontanite, $Ca(UO_2)_3(CO_3)_4(H_2O)_3$, is orthorhombic (*Pmnm*, $Pmn2_1$, or $P2_1nm$: *a* 15.337; *b* 17.051; *c* 6.931 Å), and occurs as bright yellow, elongated [001], platy (010), lath-shaped crystals in pelitic rocks of Permian age, in the weathered zone of the Rabejac U deposit in Lodève, Hérault, France, where it is associated with billietite and uranophane (Deliens and Piret 1992). The unit-cell parameters are similar to those of urancalcarite (*a* 15.42; *b* 16.08; *c* 6.970 Å), although the composition is not.

Znucalite is a uranyl tricarbonate that occurs with gypsum, hydrozincite, aragonite, sphalerite, galena, pyrite and other minerals as a weathering product from uraninite-bearing mine tailings (Ondrus et al. 1990), and with hydrozincite, calcite and gypsum on the surfaces of mine workings and adits (Ondrus et al. 1997b). Znucalite forms porous, fine-grained coatings and aggregates of minute scaly white to yellow-green crystals that are reportedly triclinic (Ondrus et al. 1997b). At Jáchymov, Czech Republic, znucalite is noted to be absent from weathered sulfide-bearing veins, where pH values can drop below ~4. Chiappero and Sarp (1993) report that znucalite from the French U deposits Mas d'Alary and Lodève is orthorhombic (space group unknown). At the French occurrences, znucalite occurs as submillimetric sperules of elongate [001], platy (010) crystals with perfect {010} cleavage, and is biaxial negative. The composition of the crystals from France, $CaZn_{11}(UO_2)(CO_3)_3(OH)_{20}\cdot 4H_2O$, apparently differs slightly from that reported by Ondrus et al. (1990): $CaZn_{12}(UO_2)(CO_3)_3(OH)_{22}\cdot 4H_2O$. The UO_2:CO_3 ratio (1:3) suggests that the structure of znucalite contains uranyl tricarbonate ions $(UO_2)(CO_3)_3$, with water and cations occupying structural interstices, as for most other uranyl tricarbonates. It seems reasonable that znucalite may display some compositional variability without significantly changing the underlying structural framework.

Table 7. Unit-cell parameters of selected orthorhombic Ca-uranyl carbonates (Å)

	uranyl carbonates		*uranyl oxy-hydroxides*	
	wyartite	*urancalcarite**	*ianthinite*	*schoepite*
a	11.2706	15.42	11.473	16.813
b	7.1055	6.97	7.178	14.337
c	20.807	16.08	30.39	14.731
V (Å^3)	1666.3	1728.2	2502.7	3550.9
sp. grp.	$P2_12_12_1$	*Pmcn* or $P2_1cn$	$P2_1ca$	$P2_1ca$

*Note: Unit-cell parameters of urancalcarite ianthinite and schoepite are transposed *a c b*, to compare with wyartite; *c* is always perpendicular to the plane of the sheets.

There are five recently described uranyl carbonates that contain essential REE. The rare REE-uranyl carbonate, bijvoetite, occurs close to uraninite with sklodowskite, uranophane, lepersonnite, oursinite, becquerelite, curite, studtite and rutherfordine in the lower part of the oxidation zone at Shinkolobwe mine (Deliens and Piret 1982). Bijvoetite is orthorhombic (C-centered), forming elongated [110] yellow {001} tablets with good {001} cleavage. Bijvoetite is pleochroic (colorless to dark yellow) and, unlike most known uranyl minerals, is optically biaxial positive. Lepersonnite, a REE-uranyl carbonate-silicate, orthorhombic (*Pnnm* or *Pnn*2), forms long (~1 mm), slender, bright yellow crystals in close proximity to uraninite in the lower part of the oxidation zone at Shinkolobwe mine. Associated uranyl minerals include sklodowskite, uranophane, bijvoetite, oursinite, becquerelite, curite, rutherfordine and studtite—with which lepersonnite has sometimes been confused (Deliens and Piret 1982). Three REE bearing carbonates have been reported from the Kamoto-Est Cu-Co deposit west of Kalwezi, near Kivu in southern Shaba province, Democratic Republic of Congo. Astrocyanite-(Ce) is an oxidation product of uraninite, associated with uranophane, kamototite-(Y), françoisite-(Nd), shabaite-(Nd), masuyite, and schuilingite-(Nd), $PbCu^{2+}(REE)(CO_3)_3(OH)(H_2O)_{1.5}$ (Deliens and Piret 1990b). Named for its habit and striking color, the hexagonal (*P6/mmm* or subgroup) crystals occur as blue to blue-green, millimeter-sized rosettes of micaceous to platy {001} tablets, rarely occasionally as isolated tabular blue crystals, translucent to opaque, optically uniaxial negative, and strongly pleochroic (blue to colorless). Another REE carbonate from Kamoto, shabaite-(Nd) occurs with uraninite, kamotoite-(Y), uranophane and schuilingite-(Nd). Shabaite is monoclinic(*P*2, *Pm* or $P2_1/m$), optically biaxial negative, and commonly forms rosettes (to 5 mm) of pale yellow, elongated [100] micaceous flakes {010} (Deliens and Piret 1990a). The third REE carbonate from Kamoto, kamotoite-(Y), forms bladed yellow crystals and fine-grained crusts on uraninite; it is monoclinic ($P2_1/n$), optically biaxial negative, strongly pleochroic (colorless to yellow) and has two good cleavages, {001} and {-101}, commonly occurring as crusts or yellow blades on uraninite (Piret and Deliens 1986).

Ondrus et al. (1997b) report voglite with two distinct compositions from Jáchymov, Czech Republic, along with several compositionally similar Ca-Cu-uranyl carbonates (Table 5). X-ray data show similarities to published data but with characteristic differences. Clearly additional work is required to clarify the composition of this mineral (or minerals), as reported stoichiometries display a range of U:C ratios (Frondel 1958; Piret and Deliens 1979; Ondrus et al. 1997b) (Table 5).

Ondrus et al. (1997c) also report an unnamed anhydrous Na-uranyl tri-carbonate,

$Na_4(UO_2)(CO_3)_3$ from Jáchymov, where it forms minute earthy aggregates (~100 μm) on surfaces. The mineral is apparently structurally distinct from the synthetic phase with the same composition (Douglass 1956).

Roubaultite was originally described as a cupric uranyl oxyhydroxide (Cesbron et al. 1970), but a structural analysis demonstrated that it is a uranyl carbonate (Ginderow and Cesbron 1985), revising the formula from that reported by Smith (1984). The occurrence and paragenesis of roubaultite are described by Smith (1984) and by Deliens et al. (1981, 1990).

Elton and Hooper (1992) describe new occurrences for andersonite and schröckingerite from the Geevor mine, Cornwall, England, where these two tri-carbonates form on the walls of the 17-level of the mine. Schöckingerite occurs as greenish-yellow globules; andersonite, which is less common, forms bright yellow, pseudocubic crystals to 3 mm. Other U minerals at this mine include johannite and a zippeite-like mineral.

Uranyl silicates

The uranyl silicates (Table 8) are moderately insoluble in most natural groundwaters. Because of the ubiquity of dissolved Si in most groundwaters, uranyl silicates are the most abundant group of uranyl minerals. Uranophane, the most common uranyl mineral and possibly the most common U mineral after uraninite, precipitates from near neutral to alkaline groundwaters that contain dissolved Si and Ca. When exposed to dilute meteoric waters (low carbonate and pH below ~7), uranophane may be replaced by soddyite (Deliens 1977b; Finch 1994), a phenomenon also observed in experimental dissolution studies of uranophane in deionized water (Casas et al. 1994). Sklodowskite is replaced by kasolite where radiogenic Pb that accumulates within the sklodowskite reaches sufficient levels to be exsolved and reprecipitated as kasolite (Isobe et al. 1992). This appears to be independent of changes in water compositions, but is rather a result of the durability of sklodowskite, which persists long enough to accumulate radiogenic Pb in substantial amounts. Replacement of other uranyl silicates is not well documented, a reflection, perhaps, of their durability. Uranophane and soddyite can persist in some environments for more than one hundred thousand years (Finch et al. 1996).

Several especially Si-rich minerals are known, the most important being the weeksite group with a U:Si ratio of 2:5 (Rastsvetaeva et al. 1997; Burns 1999b) (Table 8). These minerals are relatively rare and occur in arid environments, which may reflect evaporation of Si-rich waters of relatively high pH, in which dissolved polymeric silicate species may reach quite elevated concentrations (Stumm and Morgan 1981; Dent Glasser and Lachowski 1980). Unlike the uranyl carbonates and sulfates, however, weeksite-group minerals apparently do not dissolve so readily upon re-exposure to fresh water. Like uranophane, when exposed to carbonate-free waters, these minerals might lose some Ca and Si preferentially, altering to more U-rich minerals such as uranophane or soddyite. In more alkaline, carbonate-rich waters, they may lose U preferentially, altering to amorphous or microcrystalline silica.

Uranosilite, with a U:Si ratio (1:7) far lower than any other known uranyl silicates, is found at the Menzenschwand U deposit, where it occurs on quartz and is intimately intergrown with studtite and uranophane (Walenta 1974, 1983). Uranosilite forms finely acicular, yellowish white orthorhombic ($P22_12_1$, *Pmmb* or *Pmcb*) crystals, that are optically biaxial negative. Heating causes no change in the X-ray powder diffraction pattern but lowers the refractive indices, which is explained by the loss of a small amount of "zeolitic water" (Walenta 1983). Uranium(VI) in uranosilite almost certainly occurs as the uranyl ion, and the structure of uranosilite may be that of a silicate framework with UO_2^{2+}

Table 8. Uranyl silicates

Name	*Formula*	*Comments*
Soddyite	$(UO_2)_2SiO_4(H_2O)_2$	Gaines et al. (1997); Vochten et al. (1995a); Moll et al. (1995)
Uranosilite	$(UO_2)Si_2O_{15}(H_2O)_n$ $(0 < n < 1)$	Rare; Walenta (1983)
Ursilite	$(Mg,Ca)_4(UO_2)_4(Si_2O_5)_5(OH)_6(H_2O)_{15}$	probably equivalent to haiweeite; Chernikov et al. (1957); Smith (1984)
Lepersonnite-(Gd)	$Ca(Gd,Dy)_2(UO_2)_{24}(CO_3)_6Si_4O_{12}(H_2O)_{60}$	Gaines et al. (1997)
"Pilbarite"	$PbO{\cdot}ThO_2{\cdot}UO_3{\cdot}2SiO_2{\cdot}4H_2O$ (?)	species not verified; Frondel (1958)
Unnamed *	$2CaO{\cdot}2UO_3{\cdot}6SiO_2{\cdot}10H_2O$ "$Ca_2(UO_2)_2(Si_2O_5)_3{\cdot}10H_2O$"	Ondrus et al. (1997c); proposed formula for synthetic analogue is unbalanced; Moroni & Glasser (1995); Skakle et al. (1997)
Uranophane Group	$M^{m+}[(UO_2)(SiO_3OH)]_m(H_2O)_n$	
Boltwoodite*	$K(UO_2)(SiO_3OH)(H_2O)_{1.5}$	Stohl & Smith (1981); Pu Congjian (1990); Gaines et al. (1997); Vochten et al. (1997c); Na-K solid solution, Burns (1998c), Na/K-Cs ion exchange, Burns (1998a)
Cuprosklodowskite	$Cu(UO_2)_2(SiO_3OH)_2(H_2O)_6$	Frondel (1958); Smith (1984)
Kasolite	$Pb(UO_2)(SiO_4)(H_2O)$	Frondel (1958); Stohl & Smith (1981); Gaines et al. (1997)
Na-boltwoodite*	$(Na,K)(UO_2)(SiO_3OH)(H_2O)_{1.5}$	Stohl & Smith (1981); Gaines et al. (1997); Burns (1998c); Vochten et al. (1997c)
Oursinite*	$(Co,Mg)(UO_2)_2(SiO_3OH)_2(H_2O)_5$	rare; Deliens & Piret (1983a); Gaines et al. (1997)
Sklodowskite*	$Mg(UO_2)_2(SiO_3OH)_2(H_2O)_6$	Frondel (1958); Gaines et al. (1997)
Swamboite	$U^{6+}(UO_2)_6(SiO_3OH)_6(H_2O)_{30}$	Deliens & Piret (1981a); Gaines et al. (1997)
Uranophane-α	$Ca(UO_2)_2(SiO_3OH)_2(H_2O)_5$	most common uranyl mineral; Frondel (1958); Ginderow (1988); Gaines et al. (1997)
Uranophane-β*	$Ca(UO_2)_2(SiO_3OH)_2(H_2O)_5$	common mineral but never synthesized; Viswanathan & Harnett (1986); Cesbron et al. (1993); Gaines et al. (1997); Palenzona & Selmi (1998)
Weeksite Group	$M^{m+}(UO_2)_2(Si_5O_{13})(H_2O)_4$	
Haiweeite*	$Ca(UO_2)_2[Si_5O_{12}(OH)_2](H_2O)_{4.5}$	Stohl & Smith (1981); structure reported by Rastsvetaeva et al. (1997); Burns (1999f)
Metahaiweeite	$Ca(UO_2)_2[Si_5O_{12}(OH)_2](H_2O)_n$ $(n < 5)$	ill defined; structural formula inferred; Gaines et al. (1997)
Mg-haiweeite*	$Mg(UO_2)_2[Si_5O_{12}(OH)_2](H_2O)_n$	Structural formula inferred; Smith (1984)
Weeksite*	$K_{1-x}Na_x(UO_2)_2(Si_5O_{13})(H_2O)_4$ $(x = 0.4)$	Stohl & Smith (1981); Baturin & Sidorenko (1985), Vochten et al. (1997a); Jackson & Burns (1999)

* New or supplemental data or not listed in Dana's New Mineralogy (Gaines et al. 1997).

ions occupying structural interstices, similar to the framework uranyl tellurite cliffordite, and suggesting the structural formula $(UO_2)Si_7O_{15}{\cdot}nH_2O$. The conditions necessary for the precipitation of uranosilite are unknown, although the fact that it occurs with studtite suggests that it may be stable only in highly oxidizing environments and in waters with low carbonate concentrations. No data are available on its stability or solubility, although it is relatively insoluble in weak hydrochloric acid (Walenta 1983).

Slender yellow crystals of swamboite occur at the Swambo U mine in Shaba, Democratic Republic of Congo, where it is associated with soddyite and curite. Swamboite is monoclinic ($P2_1/a$). Optical properties, crystal habit and unit-cell data demonstrate its close structural relationship to uranophane, but the ideal formula, $U^{6+}_{0.33}H^+_2(UO_2)_2(SiO_4)_2(H_2O)_{10}$, derived by analogy with the uranophane-group, is difficult to reconcile with the uranophane structure. The structural roles and chemical forms of the additional U^{6+} (presumably as the UO_2^{2+} ion) and H^+ ions (possibly as part of acid $(SiO_3OH)^{3-}$ groups) are uncertain, although the large cell, with Z = 18, suggests a complex ordering of interlayer constituents. Compositionally similar to soddyite, with which it is associated, swamboite and soddyite must precipitate under similar conditions, and the coexistence of these two uranyl silicates suggests that slight changes in groundwater chemistry may be sufficient to shift from the stability regime of one mineral to the other. Soddyite has a higher U:Si ratio (2:1) than swamboite (1.167:1), suggesting that swamboite is stable relative to soddyite in waters with higher activities of orthosilicic acid.

Deliens and Piret (1983a) report oursinite from the Shinkolobwe mine, Shaba, Democratic Republic of Congo, where it occurs with soddyite, kasolite, schoepite and curite. Oursinite occurs as pale yellow acicular [001] crystals that form radial aggregates. Crystal habit, optical properties and X-ray diffraction data indicate that oursinite is structurally related to the uranophane-group minerals, with a unit cell that resembles that of sklodowskite. The Co and Ni in oursinite are derived from the oxidation of primary Co- and Ni-sulfides in the host rocks at Shinkolobwe.

New structure determinations show that neither polymorph of uranophane contains H_3O^+ (hydroxonium), as previously proposed by Stohl and Smith (1981). Charge balance is maintained by acid silica tetrahedra instead (Ginderow 1988, Viswanathan and Harnett 1986). The structure of boltwoodite contains the alpha-uranophane type sheet, with K and Na in the interlayer. Burns (1998d) demonstrated solid solution between boltwoodite and Na-boltwoodite. The structure is apparently compatible with a range of cation occupancies within the interlayer. Vochten et al. (1997c) synthesized Na-boltwoodite, demonstrating by spectroscopy that the structure contains acid $(SiO_3OH)^{3-}$ groups, rather than H_3O^+ ions as previously reported, consistent with the structure determination (Burns 1998d). The existence of H_3O^+ in uranyl mineral structures is commonly proposed but has not been convincingly demonstrated. Vochten et al. (1997c) used the synthetic Na-boltwoodite as starting material for the synthesis of several structurally related uranophane-group silicates. Burns (1999a) obtained Cs-substituted boltwoodite by immersing natural boltwoodite single crystals in Cs-rich solutions. Burns (1999a) demonstrated that the Cs replaced K and Na in the interlayer by cation exchange, rather than by dissolution and re-precipitation, a testament to the stability of the structural unit in boltwoodite. The demonstration of Cs exchange in boltwoodite has significant potential implications for the retention of Cs released from corroded spent nuclear fuel, because, under conditions relevant to the proposed high-level waste repository at Yucca Mountain, Na-boltwoodite is a major corrosion product of spent UO_2 fuel (Finch et al. 1999b).

Haiweeite has been poorly understood, with symmetry variously reported as monoclinic or orthorhombic. Based on single-crystal XRD data for a crystal of haiweeite

from Teofilo Otoni, Minas Gerais, Brazil, Rastsvetaeva et al. (1997) report the structural formula for haiweeite as $Ca(UO_2)_2[Si_5O_{12}(OH)_2]{\cdot}4.5H_2O$, which was confirmed recently by a more precise structure refinement (Burns 1999b). This is slightly different from the formula that had been accepted, $Ca(UO_2)_2Si_6O_{15}{\cdot}5H_2O$ (Cejka and Urbanec 1990; Nickel and Nichols 1992; Mandarino 1999). Smith (1984) suggested that "ursilite," $(Mg,Ca)_4(UO_2)_4(Si_2O_5)_{5.5}(OH)_5{\cdot}13H_2O$ (Chernikov et al. 1957) is equivalent to haiweeite (or Mg-haiweeite); however, "ursilite" is not considered a valid species according to Mandarino (1999). Weeksite contains the same structural sheets as haiweeite, but the sheets are bonded directly to each other, forming a framework structure (Baturin and Sidorenko 1985). Low valence cations and water molecules are located in channels within the framework.

Ondrus et al. (1997c) reported an unnamed uranyl silicate from Jáchymov, Czech Republic, which forms thin coatings of tabular yellow crystals, and is associated with liebigite, voglite, gypsum, rösselite, and an unnamed hydrated Cu-Ca-uranyl carbonate. The phase described by Ondrus et al. (1997c) displays an X-ray powder diffraction pattern similar to that of a Ca-uranyl silicate synthesized from U-loaded cement (Moroni and Glasser 1995; Skakle et al. 1997). The natural and synthetic compounds both appear to be distinct from haiweeite. The formula suggested by Skakle et al (1997) for the uranyl silicate, $Ca_2(UO_2)_2(Si_2O_5)_3{\cdot}10H_2O$, cannot be correct, as it is not charge-balanced. Alternative formulas may be $Ca_2(UO_2)_2Si_6O_{16}{\cdot}10H_2O$ [cf. "ursilite" and the synthetic K-U silicate of Plesko et al. (1992) or, $Ca_2(UO_2)_2(Si_4O_{10})_2{\cdot}nH_2O$, by analogy with a synthetic K-Na-uranyl silicate described by Burns et al. (1999)].

Several studies have been reported on synthetic uranyl silicates. The synthesis of minerals and related compounds can provide important insights into the conditions of mineral formation and their structural relationships. Alpha-uranophane has been synthesized (Nguyen et al. 1992; Cesbron et al. 1993); however no successful synthesis of _-uranophane has been reported, despite concentrated efforts to do so (Cesbron et al. 1993). This is a curious dilemma because β-uranophane is the more common of the two known uranophane polymorphs at several U deposits (Frondel 1958; Palenzona and Selmi 1998), including the Nopal I U deposit in Peña Blanca, northern Mexico (Pearcy et al. 1994). Hydrothermal reaction of synthetic U-bearing borosilicate glass resulted in the formation of a previously unknown compound, $KNa_3(UO_2)_2(Si_4O_{10})_2(H_2O)_4$ (Burns et al. 1999). This novel uranyl silicate may be relevant to hydrothermal U(VI) occurrences, such as near Spruce Pine, North Carolina, Ruggles mine, Grafton, New Hampshire, and near Rajputana, India (Frondel and Meyrowitz 1956; Korzeb et al. 1997). This compound has a U:Si ratio of 1:4, placing it intermediate between haiweeite-group minerals (2:5) and uranosilite (1:7).

Burns et al (1999) discuss how the crystal structure of the synthetic $KNa_3(UO_2)_2(Si_4O_{10})_2{\cdot}4H_2O$ provides insight into the structural connectivities of uranyl silicates. Si tetrahedra become increasingly polymerized as Si:U ratios increase, with linkages between Si and U polyhedra depending on the U:Si ratio. In soddyite (U:Si = 2:1) each Si tetrahedron shares two of its edges with U polyhedra, whereas in structures with U:Si = 1:1 only one edge of each Si tetrahedron is shared with a U polyhedron, and each tetrahedron links to another U polyhedron by sharing vertices. In structures with a 2:5 ratio, some Si tetrahedra share a single edge with a U polyhedron, whereas others share none. In synthetic $KNa_3(UO_2)_2(Si_4O_{10})_2{\cdot}4H_2O$ (U:Si = 1:4), U polyhedra and Si tetrahedra share only vertices; however, all four equatorial vertices of the U polyhedra are shared with Si tetrahedra in adjacent sheets.

During a study to examine phase relationships among uranyl silicates and uranyl

oxyhydroxides at elevated temperatures, Plesko et al. (1992) synthesized several uranyl silicates in sealed tubes at 200 to 300°C and 30 MPa, including weeksite and a K-uranyl silicate with a U:Si ratio close to that of the synthetic K-Na-uranyl silicate of Burns et al. (1999): $K_2O{\cdot}4UO_3{\cdot}15SiO_2$. However, Plesko et al. (1992) performed their syntheses in a Na-free system. The phase synthesized by Plesko et al. (1992) appears structurally distinct from, and contains less alkali than, synthetic $KNa_3(UO_2)_2(Si_4O_{10})_2{\cdot}4H_2O$. Plesko et al. (1992) found that, under the conditions of their experiments, the only uranyl silicates in the system K_2O-UO_3-SiO_2-H_2O are soddyite, boltwoodite, weeksite and $K_2O{\cdot}4UO_3{\cdot}15SiO_2$.

Uranyl phosphates and arsenates

Uranyl phosphates and arsenates (Tables 9-13) constitute by far the most diverse group of uranyl minerals, with approximately 70 species described. Dissolved phosphate is a common constituent of many groundwaters, and the uranyl phosphates have a correspondingly wide distribution in nature. Their genesis, however, apears to be somewhat unique and is discussed in more detail in a separate section below. Uranyl arsenates precipitate where dissolved AsO_4 is available, which is most commonly where arsenide minerals and As-bearing sulfide minerals are being oxidized. Thus, uranyl arsenates commonly occur in the same localities as uranyl sulfates. However, unlike the sulfates, uranyl arsenates are quite insoluble in most natural waters. In fact, they are structurally related to uranyl phosphates and display virtually identical physical properties, including low solubilities. Many phosphates and arsenates show substantial substitution of P and As in structural sites (see Burns this volume), and complete solid solution may be possible between some end members. A large number of uranyl phosphates and arsenates has been described since Smith's (1984) review. One particularly interesting occurrence is the uraniferous quartz-albite-muscovite pegmatite at Kobokobo, near Kivu, in western Democratic Republic of Congo, where at least ten uranyl phosphates occur, most of which also contain Al (Deliens and Piret 1980). Kobokobo is the type locality for nine of these: kamitugaite, triangulite, althupite, moreauite, ranunculite, threadgoldite, phuralumite, vanmeerscheite and metavanmeerscheite (Deliens et al. 1981, 1984, 1990). Furongite also occurs at Kobokobo (Deliens and Piret 1985). Uranyl phosphates not discussed by Smith (1984) are described below within their respective structural groups.

Uranyl phosphates and arsenates can be divided into at least three structurally and chemically related groups. The autunite and meta-autunite groups are tetragonal or pseudotetragonal with U:P and U:As ratios of 1:1 (Tables 9 and 10). The phosphuranylite group (Table 11) is based on a structural sheet with U:P = 3:2. A small but interesting group are uranyl phosphates and arsenates with U:P and U:As ratios of 1:2 (Table 12), most of which are triclinic and may be structurally related to the arsenates walpurgite and orthowalpurgite (Mereiter 1982; Krause et al. 1995). Several phosphates and arsenates that are not so readily categorized are listed in Table 13.

Autunite and meta-autunite groups (Tables 9 and 10). These two mineral groups are the most numerous of the phosphates and arsenates, with approximately 40 species known. They are common in a wide variety of deposits (Frondel 1958; Smith 1984), and probably control U concentrations in many groundwaters. Four new autunite-group minerals and the redefinition of one described before 1984 have been reported since Smith's (1984) review.

Vochtenite is found at the Basset mine, southeast of Camborne, Cornwall, England, where it occurs as aggregates of approximately square, monoclinic (space group unknown) brown crystals with one perfect {010} cleavage; optical properties, crystal habit, and the UO_2:PO_4 ratio clearly indicate that vochtenite is a member of the autunite-group (Zwaan et al. 1989). Vochtenite is associated with chalcopyrite, chalcocite, and cassiterite, and minor

Table 9. Autunite group of phosphates and arsenates (U:P = 1:1) $M^{m+}[(UO_2)(PO_4)]_m(H_2O)_n$ (n = 10–12)

Name	*Formula*	*Comments*
Autunite	$Ca[(UO_2)(PO_4)]_2(H_2O)_{10\text{-}12}$	Frondel (1958); Gaines et al. (1997)
Sabugalite	$Al[(UO_2)_4(HPO_4)(PO_4)_3](H_2O)_{16}$	Monoclinic; compare threadgoldite, uranospathite, ranunculite; Frondel (1958); Gaines et al. (1997)
Uranospathite	$AlH[(UO_2)(PO_4)]_4(H_2O)_{40}$	Compare threadgoldite, sabugalite, ranunculite; Walenta (1978); Smith (1984); Gaines et al. (1997)
Saléeite*	$Mg[(UO_2)(PO_4)]_2(H_2O)_{10}$	Murakami (1996a); Vochten & Van Springel K (1996); Murakami et al. (1997); Gaines et al. (1997)
Torbernite	$Cu[(UO_2)(PO_4)]_2(H_2O)_8$	Gaines et al. (1997)
Uranocircite	$Ba[(UO_2)(PO_4)]_2(H_2O)_8$	Gaines et al. (1997)
Arsenuranospathite	$AlH(UO_2)_4(AsO_4)_4(H_2O)_{40}$	Smith (1984); Gaines et al. (1997)
Heinrichite	$Ba[(UO_2)(AsO_4)]_2(H_2O)_{10\text{-}12}$	Smith (1984); Gaines et al. (1997)
Kahlerite	$Fe^{2+}[(UO_2)(AsO_4)]_2(H_2O)_{10\text{-}12}$	only qualitative chemical analysis reported; Frondel (1958); Gaines et al. (1997)
Kirchheimerite	$Co[(UO_2)(AsO_4)]_2(H_2O)_{12}$	Smith (1984); Gaines et al. (1997)
Novácekite	$Mg[(UO_2)(AsO_4)]_2(H_2O)_{8\text{-}12}$	Frondel (1958); Gaines et al. (1997)
Trögerite	$(UO_2)_3(AsO_4)_2(H_2O)_{12}$ or possibly $[H(UO_2)(AsO_4)]_2(H_2O)_8$	ill defined; cf. synthetic "H-uranospinite"; Frondel (1958); Smith (1984); Gaines et al. (1997)
Uranospinite	$Ca[(UO_2)(AsO_4)]_2(H_2O)_{10}$	Ca-free analogue synthesized: "H-uranospinite"; Frondel (1958); Gaines et al. (1997)
Zeunerite	$Cu[(UO_2)(AsO_4)]_2(H_2O)_{16}$	Frondel (1958); Gaines et al. (1997)

* New or supplemental data or not listed in Dana's New Mineralogy (Gaines et al. 1997).

Table 10. Meta-autunite group of phosphates and arsenates (U:P = 1:1) $M^{m+}[(UO_2)(PO_4)]_m(H_2O)_n$ $(2 < n < 8)$

Name	*Formula*	*Comments*
Bassetite	$Fe[(UO_2)(PO_4)]_2(H_2O)_8$	Vochten et al. (1984); Gaines et al. (1997)
Chernikovite	$(H_3O)[(UO_2)(PO_4)]_2(H_2O)_8$	"hydrogen autunite"; Gaines et al. (1997)
Lehnerite	$Mn[(UO_2)(PO_4)]_2(H_2O)_8$	Mücke (1988); Gaines et al. (1997)
Meta-autunite	$Ca[(UO_2)(PO_4)]_2(H_2O)_6$	Gaines et al. (1997)
Meta-autunite II*	$Ca[(UO_2)(PO_4)]_2(H_2O)_2$	questionable species; Smith (1984)
Meta-ankoleite	$K_2[(UO_2)(PO_4)]_2(H_2O)_6$	Gaines et al. (1997)
Metatorbernite*	$Cu[(UO_2)(PO_4)]_2(H_2O)_6$	Stergiou et al. (1993); Calos & Kennard (1996); Gaines et al. (1997)
Meta-uranocircite	$Ba[(UO_2)(PO_4)]_2(H_2O)_8$	Gaines et al. (1997)
Meta-uranocircite II	$Ba[(UO_2)(PO_4)]_2(H_2O)_6$	questionable species; Gaines et al. (1997)
Na-autunite	$(Na_2,Ca)[(UO_2)(PO_4)]_2(H_2O)_8$	Smith (1984); Gaines et al. (1997)
Przhevaskite	$Pb[(UO_2)(PO_4)]_2(H_2O)_4$	ill defined; Gaines et al. (1997)
Ranunculite	$AlH(OH)_2[(UO_2)(PO_4)](H_2O)_4$ or possibly $Al(OH)_2[(UO_2)(PO_4)](H_2O)_5$	compare sabugalite, uranospathite; Gaines et al. (1997)
Threadgoldite	$Al(OH)[(UO_2)(PO_4)]_2(H_2O)_8$	Smith (1984); K-S82; Gaines et al. (1997)
Uramphite	$(NH_4)_2[(UO_2)(PO_4)]_2(H_2O)_{4-6}$ (?)	from oxidized coal deposits (Russia); Gaines et al. (1997)
Vochtenite	$(Fe^{2+},Mg)Fe^{3+}[(UO_2)(PO_4)]_4(OH)(H_2O)_{12-13}$	Zwaan et al. (1990); Gaines et al. (1997)
Abernathyite	$K_2[(UO_2)(AsO_4)]_2(H_2O)_8$	Frondel (1958); Gaines et al. (1997)
Metaheinrichite	$Ba[(UO_2)(AsO_4)]_2(H_2O)_8$	Frondel (1958); Gaines et al. (1997)
Metakahlerite	$Fe^{2+}[(UO_2)(AsO_4)]_2(H_2O)_8$	Mn^{2+} and Fe^{3+} analogues have been synthesized; Gaines et al. (1997)
Metalodevite	$Zn[(UO_2)(AsO_4)]_2(H_2O)_{10}$	Smith (1984); Gaines et al. (1997)
Metanovácekite	$Mg[(UO_2)(AsO_4)]_2(H_2O)_{4-8}$	polymorph of seelite ?; Frondel (1958); Smith (1984); Bachet et al. (1991); Gaines et al. (1997)
Na-uranospinite	$(Na_2,Ca)[(UO_2)(AsO_4)]_2(H_2O)_5$	Frondel (1958); Gaines et al. (1997)
Seelite	$Mg(UO_2)(AsO_3)_x(AsO_4)_{1-x}(H_2O)_7$ $(x = 0.7)$	Arsenate-arsenite; polymorph of metanovácekite?; Bachet et al. 1991); Bariand et al. (1993); Gaines et al. (1997)
Meta-uranospinite*	$Ca[(UO_2)(AsO_4)]_2(H_2O)_8$	two polymorphs (18 & 17 Å) ?; Frondel (1958); Gaines et al. (1997); Ondrus et al. (1997b)
Metazeunerite	$Cu[(UO_2)(AsO_4)]_2(H_2O)_8$	Frondel (1958); Gaines et al. (1997)
Unnamed*	$Ni[(UO_2)(AsO_4)]_2(H_2O)_{6-8}$	XRD of synthetic analogue: PDF 12-586; Ondrus et al. (1997c)
Unnamed*	$(H_3O)(UO_2)_2(AsO_4)_2(H_2O)_8$ or possibly $(UO_2)_2(HAsO_4)_2(AsO_4)(H_2O)_{10}$	"hydronium uranospinite" (compare trögerite); Ondrus et al. (1997c)

* New or supplemental data or not listed in Dana's New Mineralogy (Gaines et al. 1997).

bassetite.

Lehnerite is found in the Hagendorf pegmatite, Oberpfalz, Germany, where it occurs in close association with altered zweiselite, $(Fe^{2+},Mn^{2+})_2(PO_4)F$, and rockbridgeite, $(Fe^{2+},Mn^{2+})Fe^{3+}_4(PO_4)_3(OH)_5$, as well as with morinite, carlhintzeite, pachnolite and fluellite (Mücke 1988). Lehnerite is monoclinic ($P2_1/n$), forming bronze-yellow to yellow, micaceous, pseudotetragonal plates (to 1 mm), flattened on (010) and layered perpendicular to [010]; it is optically biaxial negative with perfect {010} cleavage. The optical properties of lehnerite crystals vary from core to rim, with the optic axial angle ($2V$) decreasing and extinction becoming more oblique toward crystal edges. The outermost edges of crystals have axial planes perpendicular to the axial-plane orientation at the core, with intermediate zones being uniaxial. These changes in optical properties are explained by variations in H_2O contents (Mücke 1988).

Seelite is known from both the Rabejac U deposit in Lodève and the Talmessi mine in central Iran, where it forms bright yellow, pleochroic (colorless to yellow), tabular, elongate [010] monoclinic ($C2/m$) crystals, flattened on (100) (Bariand et al. 1993). The formula, originally reported as $Mg[UO_2)(AsO_4)]_2(H_2O)_4$ for a crystal from Talmessi (Bachet et al. 1991), but revised to $Mg[UO_2)(AsO_3)_x(AsO_4)_{1-x}]_2(H_2O)_7$ ($x \cong 0.7$), based on the chemistry and structure of a crystal from Lodève, indicates that it is the first known mixed-valence uranyl arsenite-arsenate and a member of the meta-autunite group. Lambor (1994) suggested that seelite might be the tetragonal polymorph of metanovacekite. Seelite is the As analogue of saléeite (Table 9).

Sodium meta-autunite, $Na_2(UO_2)_2(PO_4)_2{\cdot}6\text{-}8H_2O$, can be reversibly hydrated to form fully hydrated sodium autunite, $Na_2(UO_2)_2(PO_4)_2{\cdot}10\text{-}16H_2O$ (Tschernikov and Organova 1994). Both minerals are tetragonal ($P4/nmm$). Sodium meta-autunite forms rapidly in air from sodium autunite .

Chernikovite, the new mineral name for "hydrogen autunite," occurs as thin, transparent, micaceous plates, elongated [010], with perfect (001) cleavage. Chernikovite is pale yellow to lemon green and fluoresces an intense yellow green in ultraviolet light; it is weakly pleochroic. Chernikovite is known from a number of localities (Atencio 1988), including Perus (Sao Paolo) Brazil, where it occurs as oriented inclusions within autunite and meta-autunite. These uranyl phosphates are found in fractures within pegmatitic granites at the Perus occurrence. Finch and Ewing (1992b) tentatively identified chernikovite from the Shinkolobwe mine, where oriented flakes of chernikovite appear to have formed epitaxially on pre-existing curite. Finch and Ewing (1992b) suggest that chernikovite is a precursor to later-formed uranyl phosphates, and that it may replace uranyl oxyhydroxides in P-bearing groundwaters where P concentrations are lower than required to precipitate uranyl phosphates directly from solution. If true, chernikovite may be an important, though potentially short-lived, mineral in the paragenesis of U phosphate minerals.

Phosphuranylite group (Table 11). This group of minerals includes 16 mostly orthorhombic uranyl phosphates, with U:P equal to 3:2. The U:P ratio refers to that of the structural sheets, as there are exceptions: a few minerals in this group contain U in interlayer positions, such as phosphuranylite. The phosphuranylite group contains structural sheets with composition $[(UO_2)_3(O,OH)_2(PO_4)_2]$. Unit-cell dimensions within the plane of the structural sheets in phosphuranylite-group minerals are ~7 and ~17.3 Å (or multiples thereof). In addition to the phosphates, a few minerals without P are structurally related to the phosphuranylite group, including the uranyl selenites guilleminite (Cooper and Hawthorne 1995), haynesite (Cejka et al. 1999), and piretite (Vochten et al. (1996) (see Table 18, below) and probably the arsenate hügelite (Table 11). The structural unit in

Table 11. Phosphuranylite group (U:P = 3:2) $(M^{n+})_m[(UO_2)_3(O,OH)_2(PO_4)_2]_{(p-m)/2}(H_2O)_n$

Name	*Formula*	*Comments*
Althupite	$ThAl(OH)(UO_2)[(UO_2)_3O_2(PO_4)_2]_2(H_2O)_{17}$	Gaines et al. (1997)
Bergenite	$(Ba,Ca)_2[(UO_2)_3O_2(PO_4)_2](H_2O)_{6.5}$	Gaines et al. (1997)
Dewindtite	$Pb_3[(UO_2)_3O(OH)(PO_4)_2]_2(H_2O)_{12}$	Piret et al. (1990); Gaines et al. (1997)
Dumontite	$Pb_2[(UO_2)_3O_2(PO_4)_2](H_2O)_5$	Gaines et al. (1997)
Hügelite*	$Pb_2[(UO_2)_3O_2(AsO_4)_2](H_2O)_5$	As-analogue of dumontite (formula inferred); Gaines et al. (1997)
Françoisite-(Nd)	$(REE)[(UO_2)_3O(OH)(PO_4)_2](H_2O)_6$	Gaines et al. (1997)
"Kivuite"*	$(Th,Ca,Pb)(H_3O)_2(UO_2)_4(PO_4)_2(OH)_8(H_2O)_5$ (?)	ill defined, discredited species; Nickel & Nichols (1992); Gaines et al. (1997)
Mundite	$Al(OH)[(UO_2)_3(OH)_2(PO_4)_2](H_2O)_{5.5}$	$Al[(UO_2)_3O(OH)(PO_4)_2](H_2O)_{6.5}$ DP81b, Gaines et al. (1997)
Phosphuranylite*	$Ca(UO_2)[(UO_2)_3(OH)_2(PO_4)_2]_2(H_2O)_{12}$ or $KCa(H_3O)_3(UO_2)[(UO_2)_3O_2(PO_4)_2]_2(H_2O)_8$	D&91, PP91, Gaines et al. (1997)
Phuralumite	$Al_2(UO_2)_3O_2(PO_4)_2(OH)_2(H_2O)_{12}$	Gaines et al. (1997)
Phurcalite	$Ca_2[(UO_2)_3O_2(PO_4)_2](H_2O)_7$	Gaines et al. (1997)
Renardite	$Pb(UO_2)_4(PO_4)_2(OH)_4(H_2O)_7$ possibly $Pb(UO_2)[(UO_2)_3O_2(PO_4)_2](H_2O)_9$	Possible mixture (dewindtite + phosphuranylite); Deliens et al. (1990),Gaines et al. (1997)
Upalite	$Al[(UO_2)_3O(OH)(PO_4)_2](H_2O)_7$	Gaines et al. (1997)
Vanmeerssche ite	$U^{6+}(UO_2)_3(PO_4)(OH)_6(H_2O)_4$	Piret & Deliens (1982b); Gaines et al. (1997)
Meta-vanmeersscheite	$U^{6+}(UO_2)_3(PO_4)(OH)_6(H_2O)_2$	Piret & Deliens (1982b); Gaines et al. (1997)
Yingjiangite	$K_2Ca(UO_2)_7(PO_4)_4(OH)_6(H_2O)_6$ or $K_2Ca(UO_2)[(UO_2)_3O(OH)(PO_4)_2]_2(H_2O)_8$	Similar to phosphuranylite; $K \Leftrightarrow H_2O$ exchange?; Chen et al. (1990); Gaines et al. (1997)

*New or supplemental data or not listed in Dana's New Mineralogy (Gaines et al. 1997).

phosphuranylite-type structures is composed of sheets with a strong linear component, reflected in the physical properties: cleavage parallel to the layers (17.3 × 7 plane), and crystals are commonly elongated along [100] (in the 17.3 Å direction).

Phosphuranylite is one of a few minerals with U in interlayer positions. Demartin et al. (1991) demonstrated that phosphuranylite from Sardinia contains K in interlayer positions, $KCa(H_3O)_3(UO_2)[(UO_2)_3O_2(PO_4)_2]_2(H_2O)_8$, which is slightly different from the composition reported for a crystal from the Shinkolobwe mine: $Ca(UO_2)(UO_2)_3(OH)_2(PO_4)_2(H_2O)_{12}$ (Piret and Piret-Meunier 1991). In order to explain charge balance, Demartin et al. (1991) proposed that hydroxonium ions (H_3O^+) also occur in the interlayer; however, the evidence for H_3O^+ is not convincing, especially given the apparent disorder of interlayer constituents in this mineral (Piret and Piret-Meunier 1991; Demartin et al. 1991).

Althupite was described from the pegmatite at Kobokobo, Kivu, Democratic Republic of Congo, where it occurs with beryl and columbite as thin, transparent yellow tablets (to 0.1 mm); triclinic ($P1$), elongated [001] and flattened on (001), optically biaxial negative and pleochroic (pale yellow to dark yellow); the structure has been determined (Piret and Deliens 1987).

Vanmeerscheite and meta-vanmeerscheite both occur with studtite at the Kobokobo pegmatite, forming orthorhombic ($P2_1mn$) yellow plates, elongated on [001] with good {010} cleavage (subordinate {100} cleavage); it is optically biaxial negative (Piret and Deliens 1982). Both minerals are believed to contain phosphuranylite-type structural sheets parallel to (010) (Piret and Deliens 1982).

Another member of the phosphuranylite group, yingjiangite occurs as golden yellow to yellow, compact microcrystalline aggregates (Chen et al. 1990). The IR spectrum indicates both OH and H_2O groups in the structure, and X-ray powder diffraction demonstrates a close structural similarity to phosphuranylite; yingjiangite is orthorhombic ($C222_1$), optically biaxial negative, length slow and pleochroic (colorless to yellow). Described as an alteration product in an oxidized zone that contains uraninite and uranothorite from Yingjiang County, Yunnan Province, China, yingjiangite is associated with studtite, calcurmolite, tengchongite, and autunite. Zhang et al. (1992) reported chemical analyses of material from Xiazhuang U deposit, Guangdong Province, China, confirming the formula $(K_2,Ca)(UO_2)_7(PO_4)_4(OH)_6{\cdot}6H_2O$, and orthorhombic symmetry ($Bmmb$) originally reported (Chen et al. 1990). Yingjiangite bears close structural and chemical similarities to phosphuranylite, possibly with K^+ replacing some interlayer H_2O (or H_3O^+).

Françoisite-(Nd) was described from the Kamoto-est Cu-Co-deposit near Kolwezi, Democratic Republic of Congo, where it occurs as yellow, tabular (010), elongated [001] crystals (monoclinic, $P2_1/c$), and is associated with uraninite, schoepite, uranophane, curite, kamotoite-(Y) and schuilingite-(Nd) (Piret et al. 1988). The structure determination verifies françoisite is a member of the phosphuranylite group (Piret et al. 1988).

Single-crystal structure determinations demonstrate that dewindtite (Piret et al. 1990) and dumontite (Piret and Piret-Meunier 1988) are both members of the phosphuranylite group. The close chemical and structural similarity of dumontite to hügelite (Table 11) suggests that hügelite is also a phosphuranylite-group mineral, with possible formula $Pb_2[(UO_2)_3O_2(AsO_4)_2]{\cdot}5H_2O$. A crystal structure determination and electron microprobe analysis of phurcalite from São Paulo, Brazil, showed this mineral to be a member of the phosphuranylite group (Atencio et al. 1991). Braithwaite et al. (1989) report phurcalite from Dartmoor in southwest England and demonstrate that "nisaite," described from Nisa,

Portugal, is equivalent to phurcalite (nisaite was never accepted by the IMA as a valid species), and Singh (1999) report phurcalite from Putholi in Rajasthan, India. A recent review of phurcalite occurrences is provided by Walenta (1993a) who also describes a new occurrence of phurcalite from the Schmiedestollen-Halde, Wittechen, in central Schwarzwald, Germany. In another paper, Walenta (1993b) reports on established and discredited mineral species in the German Schwarzwald, a compilation of interest for more than the discussion of U minerals. Steen (1998) describes U and Pb mineralization near Sulzburg in the south Schwarzwald, Germany.

Walpurgite group (Table 12). These are compositionally and structurally similar minerals with U:P or U:As ratios of 1:2. Although they display many similarities, many of their structures are still unknown, and their classification here as a single mineral group remains to be demonstrated.

Krause et al. (1995) reported orthowalpurgite from a mine dump at Schmiedestollen, Wittichen, Germany, where it occurs as transparent yellow, orthorhombic (*Pbcm*), tabular, elongate [100] crystals (to 0.3 mm) flattened on {010}, also forming fan-shaped aggregates to 1 mm. Orthowalpurgite is associated with preisingerite, $Bi_3(AsO_4)_2O(OH)$, quartz, and anatase; it is isochemical with walpurgite.

Birch et al. (1988) described ulrichite from a granite quarry near Lake Boga, Victoria, Australia, where it occurs as radiating sprays of apple-green to lime-green acicular crystals (to 1 mm) and as flat prisms (monoclinic *C2/m*), optically biaxial (probably negative). Ulrichite is found in miarolitic cavities in a pegmatoidal granite along with chalcosiderite, turquoise, torbernite, saléeite, as well as fluorite, cyrilovite, libethenite, apatite, and an unidentified Fe phosphate.

Furongite was originally described from a U deposit in western Hunan, China, where it occurs in strongly weathered carbonaceous shales in association with autunite, limonite, halloysite, opal, evansite and variscite (Hunan 230 Laboratory 1976). Furongite was subsequently described from the Kobokobo quartz-beryl pegmatite, where it occurs with other Al-uranyl phosphates, principally triangulite and moreauite (Deliens and Piret 1985b). Furongite, which is triclinic (P1), occurs as bright yellow masses of optically biaxial negative tabular crystals with three perfect cleavages, and apparently displays some compositional variability, with slight changes in Al, and large differences in H_2O contents (Table 13). The formula is close to $Al_2(UO_2)(PO_4)_2(OH)_2{\cdot}8H_2O$ (Gaines et al. 1997; Mandarino 1999), with Kobokobo material being less hydrated (~1.5 H_2O instead of 8); H_2O loss begins at 38°C. The composition and space group resemble those of walpurgite-type minerals (Table 12). However, Shen and Peng (1981) reportedly determined the structure (but did not publish their results or data), describing furongite as a sheet-type structure with "a lot of water" between the structural sheets; the structure reportedly supports the more complex formula (Table 13).

Some uranyl phosphates are not readily categorized, having compositions and structures distinct from the phosphuranylite and walpurgite, autunite and meta-autunite groups (Table 13). Kamitugaite is a Pb-Al-uranyl phosphate-arsenate (P > As) from the pegmatite at Kobokobo, Kivu, Democratic Republic of Congo, where it occurs as thin yellow plates (to 0.5 mm) and tufts on the surfaces of quartz grains, triclinic, with two cleavages, (010) and (001). It is optically biaxial negative, as for most other uranyl phosphates of the (meta)autunite and phosphuranylite groups; however, cleavage and unit-cell data suggest that it is not structurally related to any known uranyl phosphates or arsenates (Deliens and Piret 1984a). Kamitugaite is associated with other uranyl phosphates such as triangulite, threadgoldite and dumontite, as well as the uranyl peroxide studtite.

Table 12. Walpurgite group of phosphates and arsenates (U:P = 1:2) $M^{2+}[(UO_2)(PO_4)_2](H_2O)_n$

Name	*Formula*	*Comments*
Hallimondite	$Pb[(UO_2)(AsO_4)_2]$	Smith (1984); Gaines et al. (1997)
Orthowalpurgite	$(BiO)_4[(UO_2)(AsO_4)_2](H_2O)_2$	Krause et al. (1995); Gaines et al. (1997)
Parsonsite	$Pb_2[(UO_2)(PO_4)_2](H_2O)_2$	Frondel (1958); Gaines et al. (1997); structure determination indicates presence of uranyl phosphate chains, Burns (1999c)
Pseudo-autunite	$Ca_2[(UO_2)_2(PO_4)_4](H_2O)_9$	discredited; inadequate data; Gaines et al. (1997)
Ulrichite	$CaCu^{2+}[(UO_2)(PO_4)_2](H_2O)_4$	Frondel (1958); Gaines et al. (1997)
Unnamed	$(BiO)_4[(UO_2)(PO_4)_2](H_2O)_2$	phosphate analogue of walpurgite ?; Smith (1984); Ondrus et al. (1997c)
Walpurgite	$(BiO)_4[(UO_2)(AsO_4)_2](H_2O)_2$	Mereiter (1982); Gaines et al. (1997)

*New or supplemental data or not listed in Dana's New Mineralogy (Gaines et al. 1997).

Table 13. Miscellaneous uranyl phosphates and arsenates

Name	*Formula*	*Comments*
Arsenuranylite	$Ca(UO_2)_4(AsO_4)_2(OH)_4(H_2O)_6$ possibly $Ca(UO_2)[(UO_2)_3O_2(AsO_4)_2](H_2O)_8$	Possible phosphuranylite structure type; Smith (1984); Gaines et al. (1997)
Asselbornite	$(Pb,Ba)(BiO)_4(UO_2)_6(AsO_4)_2(OH)_{12}(H_2O)_3$	Sarp et al. (1983); Gaines et al. (1997)
Coconinoite	$Fe^{3+}{}_2Al_2(UO_2)_2(PO_4)_4(SO_4)(OH)_2(H_2O)_{20}$	Compare xiangjiangite; $SO_4 \Leftrightarrow PO_4$?; Gaines et al. (1997)
Furongite*	Approximately $Al_2(OH)_2[(UO_2)(PO_4)_2](H_2O)_8$	Akita, Japan: $Al_{13}(UO_2)_7(PO_4)_{13}(OH)_{14}(H_2O)_{58}$; Shen & Peng (1981); Kivu, DRC: $Al_2(UO_2)_7(PO_4)_3(OH)(H_2O)_{13.5}$, Deliens & Piret (1985); Deliens et al. (1990); Gaines et al. (1997). Compare with walpurgite group (Table 12)
Kamitugaite	$PbAl(UO_2)_5([P,As]O_4)_2(OH)_9(H_2O)_{9.5}$	Deliens & Piret (1984a), Gaines et al. (1997)
Moreauite	$Al_3(UO_2)(PO_4)_3(OH)_2(H_2O)_{13}$	Gaines et al. (1997)
Triangulite	$Al_3(OH)_5[(UO_2)(PO_4)]_4(H_2O)_5$	Deliens & Piret (1982c); Gaines et al. (1997)
Xiangjiangite	$(Fe^{3+},Al)(UO_2)_4(PO_4)_2(SO_4)_2(OH)(H_2O)_{22}$	Compare coconinoite; $SO_4 \Leftrightarrow PO_4$?; Gaines et al. (1997)

*New or supplemental data or not listed in Dana's New Mineralogy (Gaines et al. 1997).

Triangulite, $Al_3[(UO_2)(PO_4)]_2(OH)_5 \cdot 5H_2O$, occurs in the oxidized zone of the Kobokobo pegmatite (Deliens and Piret 1982b). Its structure is triclinic and is apparently distinct from known uranyl phosphates. It bears a compositional similarity to the synthetic compound, $Ba_3[(UO_2)(PO_4)(PO_3OH)]_2 \cdot xH_2O$ (Guesdon and Raveau 1998), which does not possess autunite-type structural sheets. Triangulite occurs as bright yellow triangular crystals and as mm-sized nodules and is most commonly associated with phosphuranylite, meta-autunite and ranunculite. Crystals are flattened on (010), and elongated [001], and display two good cleavages: (010) and (001).

Deliens and Piret (1985) described moreauite from the Kobokobo pegmatite, where it is associated with furongite, ranunculite and phosphosiderite. Moreauite crystals (monoclinic, space group $P2_1/c$) are greenish yellow and form books of flattened plates, on (001), with perfect {001} cleavage (optically biaxial negative). Crystals of moreauite are commonly partially dehydrated, and the reported formula corresponds to fully hydrated moreauite. The structure of moreauite is unknown; however, the composition and unit-cell data suggest that it is not structurally related to either the autunite and meta-autunite groups, or to the phosphuranylite group.

Sarp et al. (1983) identified asselbornite from Schneeberg, Saxony, Germany, where it occurs within quartz-rich gangue minerals and is associated with β-uranophane, uranospinite, and uranosphaerite. Asselbornite forms translucent brown to lemon-yellow cubic (*I*-centered) crystals up to 0.3 mm across. Martin and Massanek (1995) reported orange crystals of asselbornite associated with zeunerite and uranophane in the Schneeberg area of Saxony, Germany.

Recent chemical analyses of a coconinoite specimen from an unspecified locality within the Kizylkhum Formation demonstrate the predominance of Al: $Al_4(UO_2)_2(PO_4)_4(SO_4)(OH)_2 \cdot 18H_2O$ (Belova et al. 1993), which contrasts with the original description of coconinoite from the Colorado Plateau, for which Al and Fe occur in approximately equal molar proportions: $Fe^{3+}{}_2Al_2(UO_2)_2(PO_4)_4(SO_4)(OH)_2 \cdot 20H_2O$ (Young et al. 1966). Combined electron and X-ray diffraction analyses confirm that coconinoite is monoclinic (*C*2/*c* or *Cc*) as originally reported (Belova et al. 1993).

Uranyl vanadates, molybdates, tungstates

Uranyl vanadates (Table 14) comprise perhaps the most insoluble of uranyl minerals (Garrels and Christ 1959; Langmuir 1978; Smith 1984). Uranyl vanadates are important U ores in the Colorado Plateau of the US (Finch 1996). Uranyl vanadates are so stable that it is likely that they will form wherever dissolved U comes in contact with waters containing dissolved vanadate ions. The uranyl vanadates occur where reduced U minerals (e.g. uraninite, coffinite or brannerite) and reduced V minerals (e.g. montroseite) are undergoing oxidation. Vanadium(V) may also be derived from rocks that contain reduced V, such as organic-rich shales and other clay-rich rocks. The stabilities of the uranyl vanadates is manifested in their potential longevity. Some of the carnotite-group minerals have reported ages of 350 Ka (Kaufman and Ku 1989) No new uranyl vanadates have been described since the review by Smith (1984), although Paulis (1992) described curienite from Abertamy near Jáchymov, Czech Republic, where it occurs on a phyllite fragment penetrated by a quartz-sphalerite-galena-uraninite vein.

Uranyl molybdates (Table 15) are locally important as ore minerals, and are also common as accessories in roll-front deposits and other deposits where uraninite and Mo-bearing minerals are being weathered. Molybdenum in these minerals occurs as Mo^{6+}, and U may be of mixed valence, U^{4+} and U^{6+}. The paragenesis of many of these minerals remains uncertain and many are poorly described. Uranyl molybdates are potentially more

Table 14. Uranyl vanadates

Name	*Formula*	*Comments*
Carnotite	$K_2(UO_2)_2(V_2O_8)(H_2O)_3$	Carnotite group; Frondel (1958); Gaines et al. (1997)
Curiénite	$Pb(UO_2)_2(V_2O_8)(H_2O)_5$	Carnotite group; Smith (1984); Paulis (1992); Gaines et al. (1997)
Ferghanite*	$(UO_2)_3(V_2O_8)(H_2O)_6$ (?)	Not verified; possible carnotite group mineral; Frondel (1958)
Francevillite	$(Ba,Pb)(UO_2)_2(V_2O_8)(H_2O)_5$	Carnotite group; Gaines et al. (1997)
Fritzscheite	$Mn^{2+}(UO_2)_2(V_2O_8)(H_2O)$	Carnotite group; Frondel (1958); Gaines et al. (1997)
Margaritasite	$(Cs,K)_2(UO_2)_2(V_2O_8)(H_2O)_n$ (n ~ 1-3)	Carnotite group; Gaines et al. (1997)
Rauvite*	$Ca(UO_2)_2V_{10}O_{28}(H_2O)_{16}$	ill defined; possibly isostructural w/ pascoeite; Frondel (1958); Smith (1984)
Sengierite	$Cu_2(UO_2)_2(V_2O_8)(OH)_2(H_2O)5$	Carnotite group; Gaines et al. (1997)
Strelkinite	$Na_2(UO_2)_2(V_2O_8)(H_2O)_6$	Carnotite group; Gaines et al. (1997)
Tyuyamunite	$Ca(UO_2)_2(V_2O_8)(H_2O)_8$	Carnotite group; Frondel (1958); Gaines et al. (1997)
Metatyuyamunite	$Ca(UO_2)_2(V_2O_8)(H_2O)_3$	Carnotite group; Frondel (1958); Gaines et al. (1997)
Vanuralite*	$Al(UO_2)_2(V_2O_8)(OH)(H_2O)_{11}$	Carnotite group; Gaines et al. (1997)
Metavanuralite	$Al(UO_2)_2(V_2O_8)(OH)(H_2O)_8$	Carnotite group; Gaines et al. (1997)
Vanuranylite	$(H_3O,Ba,Ca,K)_{1.6}(UO_2)_2(V_2O_8)(H_2O)_4$	ill defined; possible carnotite-group mineral; Gaines et al. (1997)
Uvanite	$(UO_2)_2V_6O_{17} \cdot 15H_2O$	ill defined; Frondel (1958); Gaines et al. (1997)

* New or supplemental data or not listed in Dana's New Mineralogy (Gaines et al. 1997).

Table 15. Uranyl molybdates, tungstates, niobate-tantalate

Name	*Formula*	*Comments*
Calcurmolite	$Ca(UO_2)_3(MoO_4)_3(OH)_2(H_2O)_{11}$	Gaines et al. (1997)
Cousinite	$Mg(UO_2)_2(MoO_4)_2(OH)_2(H_2O)_5$	Gaines et al. (1997)
Deloryite	$Cu^{2+}{}_4(UO_2)(MoO_4)_2(OH)_6$	Sarp & Chiappero (1992); Gaines et al. (1997)
Irginite	$(UO_2)Mo_2O_7(H_2O)_3$	alteration product of umohoite; Gaines et al. (1997)
Moluranite	$H_4U^{4+}(UO_2)_3(MoO_4)_7(H_2O)_{18}$	Gaines et al. (1997)
Tengchongite	$Ca(UO_2)_6(MoO_4)_2O_5(H_2O)_{12}$	Gaines et al. (1997)
Umohoite	$(UO_2)MoO_4(H_2O)_4$	minor Mg, Ni, Ca; Frondel (1958); Gaines et al. (1997)
Uranotungstite	$(Ba,Pb,Fe^{2+})(UO_2)_2(WO_4)(OH)_4(H_2O)_{12}$	Walenta (1985); Gaines et al. (1997)
Liandratite	$U^{6+}(Nb,Ta)_2O_8$	Oxidation product of of petschekite (Table 1); possible α-U_3O_8 structure derivative; compare with UTa_2O_8; Gasperin (1960); Smith (1984); Gaines et al. (1997)

* New or supplemental data or not listed in Dana's New Mineralogy (Gaines et al. 1997).

abundant than currently appreciated due to confusion (by color) with reduced U minerals. U-molybdates commonly coexist as fine-grained masses (Smith 1984; Gaines 1997).

Two new uranyl molybdates have been described since Smith (1984). Deloryite (Table 15) is monoclinic (*C*2, *Cm* or *C*2/*m*) and occurs as dark green rosettes of tabular (010) elongate [001] crystals, transparent to opaque, and displaying three cleavages (Sarp and Chiappero 1992). Deloryite was described from the Cap Garonne mine near Le Pradet, Var, France, where it occurs with metazeunerite, atacamite, paratacamite, malachite, tourmaline, and barite on quartz gangue. Unit-cell dimensions of deloryite are similar to those of the Cu-uranyl selenite, derricksite, suggesting a structural relationship.

Chen et al. (1986) described the hydrated uranyl molybdate, tengchongite, from Tengchong County, Yunan province, China, where it occurs in a migmatitic gneiss. Tengchongite is orthorhombic ($A2_122$) [*a* 15.616; *b* 13.043; *c* 17.716 Å] and forms yellow (biaxial negative) irregular grains, flattened on {001} with perfect (001) cleavage. Closely associated with studtite, and calcurmolite, tengchongite has a higher U:Mo ratio (3:1) than other known uranyl molybdates. Notably, the IR spectrum indicates that the structure contains H_2O groups but no OH^- ions. Both structurally and compositionally, tengchongite resembles an orthorhombic Cs- and Ba-bearing uranyl molybdate identified from corrosion experiments on spent UO_2 fuel (Buck et al. 1997).

A single-crystal structure determination for synthetic iriginite (Serezhkin etal. 1973), combined with more recent TEM data (Vishnev et al. 1991), confirm orthorhombic symmetry ($Pca2_1$), and indicate the structural formula $(UO_2)[Mo_2O_7(H_2O)_2](H_2O)$, similar to the composition reported for natural iriginite, $(UO_2)Mo_2O_7{\cdot}H_2O$ (Epstein 1959) but with more H_2O.

Uranyl tungstates (Table 15). There is only one known uranyl tungstate, uranotungstite, which is known from two localities in the Black Forest: Menzenschwand (Southern Black Forest) and the Clara mine near Oberwolfach (Central Black Forest) (Walenta 1985). Specimens from the two localities have different compositions. Material from Menzenschwand contains approximately equal molar proportions of Fe, Ba and Pb, whereas uranotungstite from the Clara mine has no Pb and only a trace of Ba. Uranotungstite is orthorhombic (optically biaxial negative) and forms spherulitic clusters of yellow, orange or brownish, lath-shaped crystals. Crystals have a perfect {010} cleavage and are pleochroic (colorless to yellow) perpendicular to the cleavage. Molon (1990) provides a synopsis of mineral paragenesis at the Clara mine, including that of uranotungstite.

Uranyl sulfates, selenites, tellurites

Uranyl sulfates (Table 16) are important only where sulfides are being oxidized, providing dissolved sulfate to groundwater that can complex with UO_2^{2+} to form stable uranyl sulfate complexes in solution. Evaporation is required to precipitate uranyl sulfates. Waters from which uranyl sulfates precipitate tend to be somewhat acidic, with pH values below approximately 6 (Garrels and Christ 1959; Ondrus et al. 1997a) (Fig. 2). Like uranyl di- and tri-carbonates, most uranyl sulfates are ephemeral and redissolve upon exposure tofresh water. Uranyl sulfates occur where uranyl carbonates are absent (and vice versa), a reflection of the different pH ranges over which uranyl sulfate and uranyl carbonate complexes are important (Ondrus et al. 1997a). Synthesis experiments on uranyl sulfates suggest that a "slow decrease in solution pH" is required for the precipitation of zippeite (-group minerals), otherwise uranyl oxyhydroxides tend to form, decreasing the activities of dissolved U species (Frondel et al. 1976; Brindley and Bastanov 1982).

Table 16. Uranyl sulfates

Name	*Formula*	*Comments*
Coconinoite*	$Fe^{3+}{}_2Al_2(UO_2)_6(PO_4)_4(SO_4)(OH)_2(H_2O)_{20}$	compare xiangjiangite; Smith (1984); Gaines et al. (1997)
Deliensite*	$Fe(UO_2)_2(SO_4)_2(OH)_2(H_2O)_3$	Vochten et al. (1997b)
Jáchymovite*	$(UO_2)(SO_4)(OH)_{14}(H_2O)_{13}$	compare uranopilite; C&96b
Johannite	$Cu(UO_2)_2(SO_4)_2(OH)_2(H_2O)_{6\text{-}8}$	Frondel (1958); Gaines et al. (1997); Ondrus et al. (1997b)
Rabejacite	$Ca(UO_2)_4(SO_4)_2(OH)_6(H_2O)_6$	DP93; Gaines et al. (1997); Ondrus et al. (1997b)
Schrökingerite	$NaCa_3(UO_2)(CO_3)_3(SO_4)F(H_2O)_{10}$	Frondel (1958); Gaines et al. (1997)
Uranopilite*	$(UO_2)_6(SO_4)(OH)_{10}(H_2O)_{12}$	compare jáchymovite; Gaines et al. (1997); Ondrus et al. (1997b)
Meta-uranopilite	$(UO_2)_6(SO_4)(OH)_{10}(H_2O)_5$	reversible dehydration of uranopilite; Gaines et al. (1997); Ondrus et al. (1997b)
Xiangjiangite	$(Fe^{3+},Al)(UO_2)_4(PO_4)_2(SO_4)_2(OH)(H_2O)_{22}$	compare coconinoite; Gaines et al. (1997)
Unnamed*	Hydrated Ca-uranyl sulfate	"pseudo-johannite"; Ondrus et al. (1997c)
Unnamed*	$(Fe,Mg)_2(UO_2)_4(SO_4)_2(OH)_8(H_2O)_3$	"ferro-zippeite"; Ondrus et al. (1997c)
Unnamed*	Hydrated Mg-Fe-K-uranyl-sulfate	"pseudo-Mg-zippeite"; Ondrus et al. (1997c)
Unnamed	Hydrated Pb-uranyl sulfate	few data; Ondrus et al. (1997c)
Zippeite Group	$M^{2+}{}_2(UO_2)_6(SO_4)_3(OH)_{10}(H_2O)_n$ *or*	$M^{n+}{}_m[(UO_2)_2(SO_4)(OH)_3]_{(p\cdot m)}(H_2O)_n$
Zippeite*	$K_4(UO_2)_6(SO_4)_3(OH)_{10}(H_2O)_4$	synthetic analogue, $K[(UO_2)_2(SO_4)(OH)_3](H_2O)$ (Vochten et al. 1995b); Frondel (1958); Frondel et al. (1976)
Co-zippeite	$Co_2(UO_2)_6(SO_4)_3(OH)_{10}(H_2O)_{16}$	Frondel et al. (1976); Gaines et al. (1997)
Mg-zippeite	$Mg_2(UO_2)_6(SO_4)_3(OH)_{10}(H_2O)_{16}$	Frondel et al. (1976); Gaines et al. (1997); Ondrus et al. (1997b)
Na-zippeite	$Na_4(UO_2)_6(SO_4)_3(OH)_{10}(H_2O)_4$	Frondel et al. (1976); Gaines et al. (1997); Ondrus et al. (1997b)
Ni-zippeite	$Ni_2(UO_2)_6(SO_4)_3(OH)_{10}(H_2O)_{16}$	Frondel et al. (1976); Gaines et al. (1997)
Zn-zippeite	$Zn_2(UO_2)_6(SO_4)_3(OH)_{10}(H_2O)_{16}$	Frondel et al. (1976); Gaines et al. (1997)

* New or supplemental data or not listed in Dana's New Mineralogy (Gaines et al. 1997).

Several new uranyl sulfates have been described since Smith's (1984) review. Jáchymovite was described from Jáchymov, Czech Republic, where it occurs as translucent yellow acicular crystals (monoclinic $P2_1$ or $P2_1/m$), with good {010} cleavage, forming coatings on uraninite-bearing dolomite veins, and is associated with uraninite, uranopilite, and gypsum (Cejka et al. 1996b). The formula for jáchymovite, $(UO_2)_8(SO_4)(OH)_{14}\cdot 13H_2O$, is similar to that of uranopilite, $(UO_2)_6(SO_4)(OH)_{10}\cdot(12\text{-}13)H_2O$ (Table 16), and X-ray diffraction data are probably necessary to distinguish these minerals with confidence. Jensen et al. (1997) identified uranopilite (tentatively, by microprobe analysis) from the Bangombé natural fission reactor in Gabon, where it is a recent alteration product of uraninite.

Rabejacite, found at both Rabejac and Mas de d'Alary in Lodève, Herault, France, forms bright yellow to amber-yellow spherulitic aggregates and individual tablets flattened on {001} (to 0.1 mm) (Deliens and Piret 1993). Rabejacite is orthorhombic (space group unknown: *a* 8.73; *b* 17.09; *c* 15.72 Å), optically biaxial negative, and strongly pleochroic (pale yellow to sulfur yellow). Rabejac is associated with gypsum, and other uranyl minerals derived from the oxidative dissolution of uraninite, including fontanite, billietite, and uranophane. Deliensite was also discovered at the Mas d'Alary U deposit in Lodève, Hérault, France, where it occurs as spherical aggregates of submillimeter-sized pale yellow to grayish white, tabular, orthorhombic (*Pnnm* or *Pnn*2) crystals (Vochten et al. 1997b). Deliensite is associated with uraninite, gypsum and pyrite, and results from the oxidative dissolution of uraninite and primary sulfides.

The composition and unit-cell parameters of zippeite-group minerals may need revision in light of the crystal-structure study of synthetic zippeite by Vochten et al. (1995b) (Table 16). They showed that the structural formula for synthetic zippeite, $K(UO_2)_2(SO_4)(OH)_3\cdot H_2O$, is significantly different from the previously accepted formula, $K_4(UO_2)_6(SO_4)_3(OH)_{10}\cdot 16H_2O$ (Frondel et al. 1976). Minerals of the zippeite group are thought to be orthorhombic; however, the synthetic crystal examined by Vochten et al. (1995b) was monoclinic. Re-examination of this mineral group is in order, a potentially daunting challenge given the extremely small grain sizes and pulverulent habits common to most zippeite-group minerals.

Uranyl selenites (Table 17) occur where Se-bearing sulfide minerals are undergoing oxidation and dissolution. Selenium in all known uranyl minerals occurs as Se(IV), in the form of the selenite ion, SeO_3^{2-}, although there seems no reason not to expect the existence of Se(VI) minerals under sufficiently oxidizing conditions. These would probably be as soluble (and as ephemeral) as uranyl sulfates, and might be confused with them. No data are available on the solubilities of these minerals, only six of which are known. Two-thirds of the uranyl selenites are from the Musonoi deposit in southern Shaba, Democratic Republic of Congo, where Se is derived from the oxidation of seleniferous digenite, Cu_9S_5 (Deliens et al. 1981). Two new uranyl selenites have been described since Smith's (1984) review.

A structure determination of guilleminite by Copper and Hawthorne (1995) revises the structural formula slightly and demonstrates that the structural unit of guilleminite is similar to that of the phosphuranylite-group minerals.

Piretite is found at the Shinkolobwe mine in the Democratic Republic of Congo, where it occurs as lemon-yellow tablets, orthorhombic ($Pmn2_1$ or *Pmnm*), with good {001} cleavage, and is optically biaxial negative (Vochten et al. 1996). Piretite forms crusts on the surfaces of uraninite crystals and is also associated with masuyite (or similar Pb-uranyl oxyhydroxide minerals). The composition, physical properties, and unit-cell parameters of piretite indicate a close structural relationship with guilleminite (Cooper and Hawthorne 1995) and suggests that piretite has a phosphuranylite-type structural sheet.

Table 17. Uranyl selenites and tellurites

Name	*Formula*	*Comments*
Demesmaekerite	$Cu_5Pb_2(UO_2)_2(SeO_3)_6(OH)_6(H_2O)_2$	Gaines et al. (1997)
Derricksite	$Cu_4(UO_2)(SeO_3)_2(OH)_2$	Gaines et al. (1997)
Guilleminite*	$Ba[(UO_2)_3O_2(SeO_3)_2](H_2O)_3$	Phosphuranylite structure type; Gaines et al. (1997); Cejka et al. (1995, 1999)
Haynesite	$(UO_2)_3(OH)_2(SeO_3)_3(H_2O)_5$	Phosphuranylite structure type; Gaines et al. (1997); Cejka et al. (1999)
Marthosite	$Cu(UO_2)_3(OH)_2(SeO_3)_3(H_2O)_7$	Gaines et al. (1997)
Piretite*	$Ca(UO_2)_3(OH)_2(SeO_3)_2(H_2O)_4$	Possible phosphuranylite structure type; Vochten et al. (1996)
Cliffordite	UTe_3O_9	Smith (1984); Gaines et al. (1997)
Moctezumite	$Pb(UO_2)(TeO_3)_2$	Swihart et al. (1993); Gaines et al. (1997)
Schmitterite	$(UO_2)TeO_3$	Smith (1984); Gaines et al. (1997)

* New or supplemental data or not listed in Dana's New Mineralogy (Gaines et al. 1997).

Haynesite was described from the Repete mine near Blanding, Utah, where it occurs in mudstones and sandstones with boltwoodite and andersonite, as well as gypsum and calcite (Deliens and Piret 1991). Haynesite is orthorhombic (*Pnc*2 or *Pncm*) and occurs as amber-yellow, elongate [001] tablets or acicular crystals in rosettes; individual crystals display perfect {010} cleavage. The chemical formula, unit-cell parameters, and physical properties suggest that haynesite contains structural sheets similar to those found in guilleminite and the phosphuranylite group of uranyl phosphates, and a preliminary structure determination suggests that this is true (Burns, pers. comm.). Infrared data for haynesite are reported by Cejka et al. (1999) and compared with other uranyl selenites (also see Cejka, Chapter 12 this volume).

Uranyl tellurites (Table 17). The three known uranyl tellurites all occur at the San Miguel and Moctezuma mines in Moctezuma, SON, Mexico, although schmitterite is also known from the Shinkolobwe mine in southern Democratic Republic of Congo. They occur where sulfides are undergoing oxidation, which probably provide Te. All uranyl tellurites are anhydrous. The structures of all three are known, the most recent being reported for moctezumite by Swihart et al. (1993) (also see Burns et al. 1996, and Burns this volume). Few details are known about the conditions of their formation, although moctezumite reportedly alters pseudomorphously to schmitterite, and both schmitterite and moctezumite are more soluble in dilute HCl than cliffordite is (Gaines 1965). Thermodynamic data have been reported recently for synthetic cliffordite (Mishra et al. 1998) and synthetic schmitterite (Mishra et al. 1998; Singh et al. 1999).

ALTERATION OF REDUCED URANIUM MINERALS

Except for coffinite and brannerite, most U^{4+} minerals occur as accessory minerals in granitic igneous rocks, pegmatites, and aluminous metamorphic host rocks. Alteration of U-bearing accessory minerals is a major factor affecting U concentrations in groundwaters emanating from exposed granite terranes. Most U-bearing accessory minerals are formed under reducing conditions, crystallizing from deep-seated Si-rich magmas or hydrothermal fluids. Where uplifted and exposed to percolating meteoric waters, these minerals are commonly destabilized, and U^{4+} may be oxidized, lost from the crystalline host, and enter

into aqueous solution as the uranyl ion or its complexes. Because U^{4+} is readily oxidized at near-atmospheric O fugacities, and because the uranyl ion, UO_2^{2+}, can form many stable solution complexes, U is potentially mobile in oxidizing aqueous solutions, whereas other elements, such as Th and REE, commonly incorporated into U^{4+}-bearing accessory minerals during crystallization are generally less amenable to aqueous transport. Differences in aqueous mobilities of U and its erstwhile companion elements readily explain why U that is mobilized from Th- and REE-bearing minerals is so commonly segregated from these other, less-mobile elements. Uraninite deposited from low-temperature U-bearing groundwaters are nearly always devoid of Th and REE (Berman 1957; Frondel 1958).

Initial alteration of most U^{4+} minerals probably occurs as U^{4+} oxidizes to U^{5+} or U^{6+} without significantly affecting the structure. Accumulation of radiogenic Pb, He, and U^{6+} (the latter also caused by "auto-oxidation") may contribute to destabilization of some U^{4+} minerals, although the degree to which this is important has rarely been addressed. Of course, the importance of these effects in a mineral depends on the mineral's age and concentrations of radioactive elements. On the other hand, the effects of radioactive decay in U- (and Th-) bearing minerals caused by alpha-recoil damage commonly exceeds most detectable effects of compositional changes. Notably, the UO_2 structure is remarkably resilient to alpha-decay damage, due to rapid annealing kinetics (Stout et al. 1988; Janeczek and Ewing 1991), which is one reason why UO_2 was chosen as a nuclear fuel. Many minerals are significantly less resilient to radiation damage, and metamictization (radiation-induced amorphization), partial or complete, can have a profound influence on the geochemical durability of most radioactive minerals.

Geochemical alteration of pyrochlore-group minerals was described in a series of papers by Lumpkin and Ewing (1992a, 1995, 1996). They have shown that microlite, pyrochlore and betafite are subject to cation and anion exchange and incongruent dissolution when exposed to a wide range of aqueous fluids in a variety of environments: from deep hydrothermal (to ~650°C and 5 kbar) to near-surface weathering environments. The A-site cation mobility is limited by ionic charge and radius, with the high field-strength cations, REE^{3+}, Th^{4+} and U^{4+}, being least mobile. Actinides are essentially retained in microlite, pyrochlore and most betafite samples for periods up to ~1.4 Ga. Preferential loss of some cations from betafite shifts the composition towards the stability field of liandratite, uranopyrochlore and rutile (or anatase). Betafite may undergo extensive incongruent dissolution and recrystallization, and exhibit U loss under "extreme conditions." Alteration of the pyrochlore group minerals depends in part on grain size, radiation damage and micro-fracturing, as well as fluid flow and duration of exposure to fluids. Pyrochlore-group minerals exposed to lateritic weathering experience cation exchange at a rate that exceeds mineral dissolution, which is primarily controlled by the stability of the Nb-Ta-Ti octahedral framework. Electron energy-loss spectroscopy (EELS) was used to identify Ce oxidation states in a partly altered pyrochlore sample (Xu and Wang 1999). Cerium and other REE occur as trivalent ions in unaltered regions, whereas Ce is oxidized to Ce^{4+} in a neighboring altered region of the pyrochlore. The oxidation of Ce was reportedly accompanied by losses of REE, U, and radiogenic Pb during alteration.

Uraninite alteration under reducing conditions

Uraninite is by far the most important U mineral in terms of abundance, wide-spread occurrence, and economic value. Coffinite and brannerite are of secondary importance, both geochemically and economically (Finch 1996). Because of its importance to U geochemistry, a rather detailed discussion of uraninite alteration is provided here.

Ancient uraninite commonly consists of two cubic phases with slight but distinct differences in unit-cell parameters (Janeczek and Ewing 1992a; Janeczek and Ewing 1991a), an effect that appears to be caused by segregation of Pb-rich and Pb-poor uraninite, with the larger unit cell corresponding to the Pb-rich phase (Janeczek 1993). In strongly reducing environments ancient uraninite may recrystallize as fine-grained Pb-depleted, Si-enriched material from precursor Pb-rich, Si-poor coarsely crystalline material (Janeczek and Ewing 1992b; Kotzer and Kyser 1993; Fayek et al. 1997). Recrystallization of ancient uraninite in reducing environments may be most affected by the combination of two effects of radioactive decay of U: (1) destabilization of uraninite by decreased U content and increased Pb content (upwards of 20 wt % PbO has been reported in some specimens of uraninite), and (2) increased U^{6+}:U^{4+} ratios caused by "auto-oxidation," which increasingly destabilizes uraninite under reducing conditions. The rate at which synthetic UO_{2+x} dissolves exceeds that of UO_2 in reducing waters above pH 5 (Janeczek and Ewing 1992c). Variations in Si contents within uraninite demonstrate the important role of groundwaters during uraninite alteration under reducing conditions, and incipient coffinite is common in many uraninite specimens that have recrystallized in reducing, Si-rich groundwaters (Janeczek and Ewing 1995; Fayek et al. 1998).

Uraninite is sparingly soluble at normal pHs in dilute, reducing groundwaters (Langmuir 1978; Parks and Pohl 1988). The solubility of uraninite increases with temperature and dissolved F, Cl and CO_2 (Giblin and Appelyard 1987; Keppler and Wyllie 1990), and dissolved U^{4+} concentrations in Na-K-Ca-Cl brines are an order of magnitude higher than in fresh waters (Giblin and Appelyard 1987). U^{4+}-fluoride complexes are stable below pH 4, contributing to potentially significant migration of U in reducing groundwaters. The influence that impurity elements in uraninite may have on uraninite dissolution under reducing conditions is uncertain. Grandstaff (1976) reports that increased Th concentrations increase the dissolution rate, whereas Posey-Dowty et al. (1987) found no effect. Janeczek and Ewing (1992c) examined uraninite from Cigar Lake in Saskatchewan, Canada, and Oklo, Gabon, and found evidence for extensive dissolution and replacement of uraninite. Replacement by U-free minerals such as illite, chalcopyrite and apatite suggests that the amount of U that migrated was substantial. Janeczek and Ewing (1992c) attribute much of this alteration to hydrothermal interactions, although they note that radiolysis (the radiolytically induced decomposition of water) may have been a factor by increasing redox conditions at the uraninite-water interface, particularly at Oklo (Dubessy et al. 1988; Meere and Banks 1997; Savary and Pagel 1997; Janeczek this volume). Kotzer and Kyser (1993) showed that most uraninite at the Cigar Lake deposit has been recrystallized, possibly through migration and reprecipitation. Janeczek (this volume) notes that uraninite of secondary origin from the Francevillian FA sandstone at Bangombé often can be distinguished from primary uraninite within the nearby natural reactor only on the basis of $^{235}U/^{238}U$ ratios. A recent experimental study comparing the dissolution of synthetic UO_2 and natural uraninite suggests that "the mobilization of U in reducing environments can occur by only slight changes [in] the surrounding conditions, even if the [uraninite] is chiefly in its reduced form" (Casas et al. 1998).

Coffinitization of uraninite. The alteration of uraninite to coffinite is common (Smits 1989; Janeczek 1991; Janeczek and Ewing 1992a,b), although it is not always well understood whether, when uraninite initially precipitated in Si-rich groundwaters, coffinite was not thermodynamically stable, or whether coffinite formation is kinetically inhibited. The factors that determine whether uraninite or coffinite form are poorly understood. Uraninite certainly crystallizes from Si-rich groundwaters under reducing conditions, as well as from higher temperature Si-rich hydrothermal and magmatic fluids. Perhaps certain impurity cations stabilize uraninite relative to coffinite in some Si-rich groundwaters.

Because uraninite always contains some oxidized U, whereas coffinite may not, we can see that coffinite is more stable than uraninite in strongly reducing waters according to the simplified reaction:

$$UO_{2+x} + SiO_{2(aq)} \Rightarrow USiO_4 + 1/2\ xO_2$$

The alteration of uraninite to coffinite may arise from an increase in dissolved silica, destabilizing existing uraninite. In addition, radiation-induced changes to the composition of uraninite can destabilize uraninite, which, in reducing groundwaters with adequate dissolved silica, combined with slow release of U from uraninite, favors crystallization of coffinite. Many elements commonly contained in uraninite are not compatible in the coffinite structure. For example Pb commonly precipitates as galena where S^{2-} activities are sufficient.

Radiogenic helium. Coarsely crystalline uraninite may display high concentrations of voids, due to accumulation of radiogenic He (Stout et al. 1988; Finch 1994; L. Thomas pers. comm.) (Fig. 4a). Voids are concentrated along sub-grain boundaries and dislocations, where present, but are also distributed throughout homogenous crystals. The role of increased strain due to the accumulation of radiogenic He is uncertain, but this may contribute to destabilization and subsequent recrystallization of some uraninite, as well as to the alteration of other radioactive minerals. Finch (1994) suggested that He voids in uraninite exposed to oxidizing groundwaters may also accelerate oxidative corrosion by increasing surface area and providing pathways for groundwater penetration (Fig. 4b).

Uraninite alteration under oxidizing conditions

The oxidative alteration of uraninite was described by Frondel (1958) as follows: first, partial oxidation of U^{4+} to U^{6+} without decomposition of the uraninite structure, although the uraninite commonly displays a change in color from black to dark brown and a change in luster from sub-metallic to "dull or pitch-like." At this stage and as alteration progresses, there is commonly "some degree of hydration, and U and especially Th may be [lost to groundwater]" relative to Pb (Frondel 1958). Further alteration, which Frondel (1958) considered as a "second type," resulted in the complete conversion of uraninite into uranyl minerals, the compositions of which depended primarily on the composition of local groundwaters.

By analogy with synthetic UO_2, it has been proposed by several authors that the early stages of oxidation and alteration of uraninite proceeds through intermediate U oxides such as U_3O_7 or U_3O_8 (Voultsidis and Clasen 1978; Posey-Dowty et al. 1987; Waber et al. 1990; Bruno et al. 1991; Sunder et al. 1996; Trocellier et al. 1998); however, crystalline compounds with these compositions are unknown in nature. It has been proposed that these oxides may occur as thin (~1 μm) layers on uraninite, but their existence has not been demonstrated (Janeczek et al. 1993). The formation of hydrated, X-ray amorphous U^{6+} hydroxides from uraninite has been postulated (Garrels and Christ 1959; Finch 1994), sometimes being given names such as "hydronasturan" and "urghite" (see Cejka and Urbanec 1990), but these are poorly described and not considered valid species.

The initial oxidation and subsequent dissolution of uraninite has not been studied in the same detail as the oxidation, dissolution and corrosion of synthetic UO_2 and UO_2 nuclear fuels (Forsyth and Werme 1992; Sunder et al. 1992; Gray et al. 1993; Einziger et al. 1992; Bruno et al 1992; Matzke 1992; Wronkiewicz et al. 1992, 1996). Because of structural similarities of uraninite and UO_2, the oxidation and corrosion of uraninite has often been assumed to be identical to that of synthetic UO_2 (Miller 1958; Parks and Pohl 1990). This is probably true to a limited degree, but elements besides U

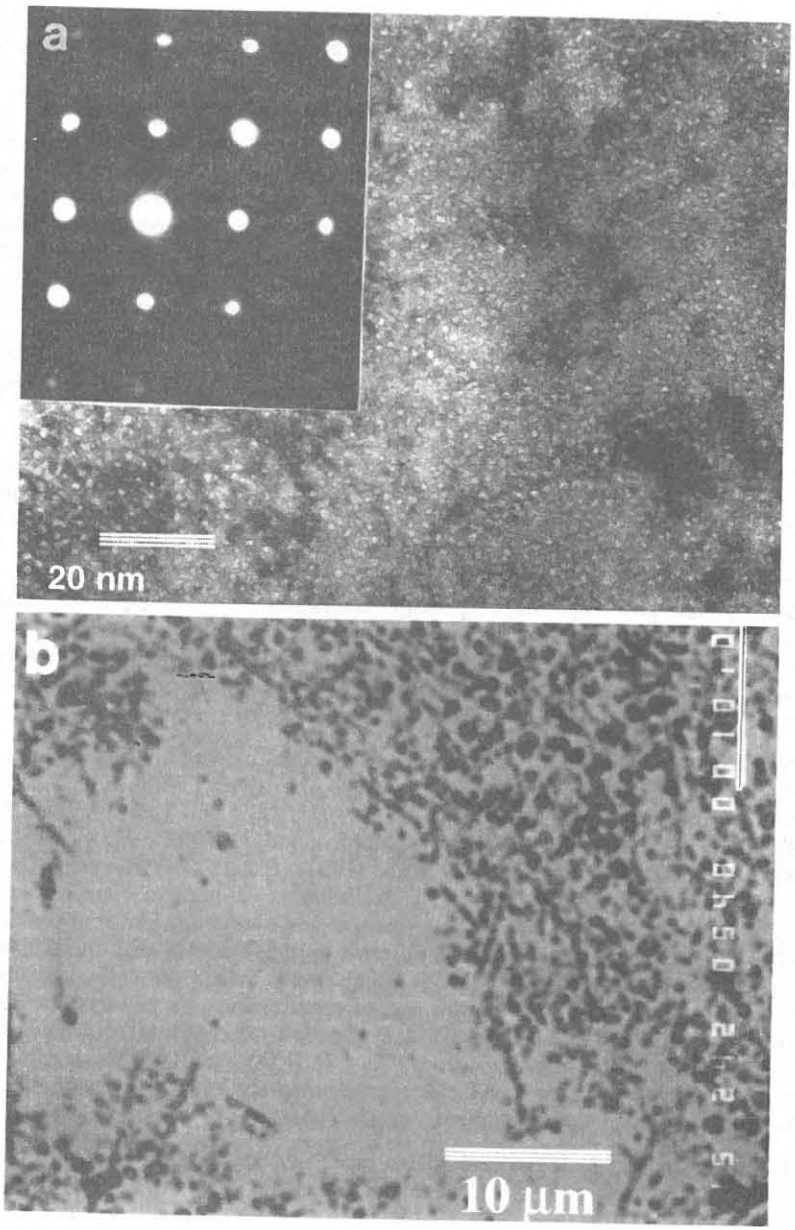

Figure 4. (a) Bright field TEM image of uraninite from Shinkolobwe mine, Shaba, Dem. Rep. Congo displaying mottled contrast attributed to inclusions of radiogenic-He produced during radioactive decay of U. Inset: SAED pattern along [001] illustrating cubic UO_2-type pattern. There is no indication of super-cell or ordering as might be expected for U_4O_9 or U_3O_7 (TEM photo courtesy of Larry Thomas). (b) Voids in altered uraninite grain possibly reflecting preferential dissolution of radiogenic-He bubbles (from Finch 1994).

and O can affect the alteration behavior of uraninite (Grandstaff 1976), of irradiated (spent) UO_2 fuels (Einziger et al. 1992; Thomas et al. 1993) and of doped U oxides (Anderson 1953; Anderson et al. 1954; Thomas et al. 1993).

The slow diffusion of oxygen into the UO_2 structure necessitates that most oxidation studies of UO_2 be performed at elevated temperatures (~150 to > 800°C). (The diffusion coefficient of oxygen in UO_2 at 25°C is on the order of 10^{-23} to 10^{-25} $m^2 \cdot s^{-1}$; Grambow 1989). Even slow kinetics of oxygen diffusion may be unimportant over geologic time spans, as interstitial sites in ancient uraninite probably become saturated with oxygen in all but the most reducing environments (Janeczek and Ewing 1992b). The question of whether U oxides that form in nature, especially during weathering, resemble those synthesized at elevated temperatures has been the subject of some debate (e.g. Janeczek et al. 1993).

The mechanisms by which synthetic UO_2 oxidizes in water may differ from those by which it oxidizes in dry air (Grambow 1989). For example, Grambow (1989) reports that the activation energy for weight gain in water is approximately one-third of that in dry air (21-42 $kJ \cdot mol^{-1}$ in water vs. ~109 kJ mol^{-1} in air). XPS has shown that the earliest stages of aqueous oxidation of synthetic UO_{2+x}, prior to dissolution, probably mimic those of air oxidation (Sunder et al. 1992; Sunder et al. 1997). Whether this is true for uraninite is uncertain, but recent studies indicate that the oxidation pathway of Gd-doped UO_2 and spent UO_2 fuels differ from that of pure UO_2 (Einziger et al. 1992; Thomas et al. 1993). Inferring the oxidation and corrosion behavior of uraninite from that of pure UO_2 must, therefore, be done carefully. Despite potential discrepancies, however, the oxidation of synthetic UO_2 is a useful analogue for the oxidation behavior of uraninite, and studies on the low temperature oxidation of UO_2 in aqueous solutions provide insight into crystal chemical and micro-structural changes occurring in uraninite during oxidative aqueous corrosion (Finch and Ewing 1992b; Wronkiewicz et al. 1996).

Oxidation of synthetic UO_2 in air. The initial oxidation of synthetic UO_2 to U_4O_9 ($UO_{2.25}$) in air above ~350°C has been studied extensively (Willis 1963; Belbeoch et al. 1967; Contamin et al.1972; Naito 1974; Willis 1978; Allen and Tempest 1982; Allen et al. 1982; Allen 1985; Allen et al. 1987; St A Hubbard, and. Griffiths 1987). The structural aspects of oxidation were summarized by Willis (1987). Excess oxygen enters unoccupied U-equivalent interstices in UO_2, displacing two adjacent oxygens to opposite interstices (Willis 1978). At the oxidation state $UO_{2.25}$, there is one excess oxygen atom per uraninite unit cell. In β-U_4O_{9-y}, oxygen occupies a different interstitial site in each of four adjacent cells in the three crystallographic directions giving rise to a $4a \times 4a \times 4a$ superstructure. Synthetic UO_{2+x} consists of two coexisting phases, representing a miscibility gap (Belbeoch et al. 1967; Naito 1974; Smith et al. 1982), and oxidation proceeds in a "step-wise" fashion as domains in the structure transform from $UO_{2.04}$ to U_4O_{9-y} ($y < 0.2$; Smith et al. 1982). The influence of these two phases on the electronic properties of UO_{2+x} strongly affects the dissolution of synthetic UO_{2+x} in oxidizing waters (Johnson and Shoesmith 1988).

McEachern and Taylor (1998) provide an especially thorough review of the oxidation of synthetic UO_2 below 400°C. The formation of crystalline U_4O_9 from synthetic UO_2 may be inhibited below ~250°C (Grambow 1989), which may be due to slow kinetics associated with long-range ordering of interstitial oxygens (Janeczek et al. 1993). Below 250°C, synthetic UO_2 oxidizes to a phase that is a tetragonal distortion of the fluorite structure with a composition near $UO_{2.33}$: α-U_3O_7 or β-U_3O_7. Evidence for the transient formation of β-U_4O_9 does exist, but the small change in stoichiometry between $UO_{2.25}$ and $UO_{2.33}$ may explain the rapid transformation of cubic U_4O_9 to tetragonal U_3O_7, perhaps before complete conversion of all domains of UO_{2+x} to U_4O_9. Further oxidation may crystallize orthorhombic U_3O_8 (commonly non-stoichiometric) when time or temperature (or both) are

sufficient. No stable phases between tetragonal U_3O_7 and orthorhombic U_3O_8 exist at ambient pressures. Continued oxidation of U_3O_8 to UO_3 does not occur, although the reasons for this are not fully understood (McEachern and Taylor 1998). At elevated temperatures (~800°C) UO_3 decomposes to non-stoichiometric U_3O_8 through O loss.

Oxidation of doped UO_2 and spent UO_2 fuels in air. The dry air oxidation of spent UO_2 fuel differs from that of unirradiated UO_2 in several respects. The primary difference between the two materials is that spent fuel contains impurities, such as fission products and transuranic elements, and the effects of radiation-induced changes on the structure of spent fuel can be important (Matzke 1992). The oxidation of spent fuel below 150°C produces disordered cubic U_4O_{9+x} (γ-U_4O_9) (Thomas et al. 1989). The fluorite-type structure is maintained to at least an O:U ratio of 2.4 (Einziger et al. 1992; Thomas et al. 1993). The oxidation of spent UO_2 fuel to γ-U_4O_9 proceeds along a reaction front that advances from grain boundaries into the centers of grains without significant strain. The smaller unit cell volume of γ-U_4O_9 causes shrinkage cracks at grain boundaries and embrittlement of the fuel. Further oxidation in dry air leads to crystallization of a hexagonal polymorph of U_3O_8, although the onset of formation is delayed to longer times or higher temperatures compared with formation of orthorhombic α-U_3O_8 during oxidation of undoped UO_2 (McKeachern et al. 1998) There is no evidence for tetragonal U_3O_7 at any stage in the oxidation sequence of spent fuels (Thomas et al. 1989; Thomas et al. 1993) or Gd-doped UO_2 (Thomas et al. 1993).

Understanding the disparate oxidation behaviors of UO_2 and doped-UO_2 (or spent UO_2 fuel) depends on understanding the role of the non-uranium cations in the UO_2 structure. Many of these cations have valences below 4+ (e.g. Sr^{2+}, Gd^{3+}), others do not oxidize readily (Th^{4+}); these elements can stabilize the UO_2 structure (Grandstaff 1976). The persistence of cubic U_4O_{9+x} to O:U ratios close to 2.4 probably explains the nucleation and growth of U_3O_8 without intermediate formation of tetragonal U_3O_7 (Thomas et al. 1993) since the O:U ratio of $UO_{2.4}$ exceeds that of U_3O_7. The reason that hexagonal U_3O_8 forms during dry-air oxidation of spent fuel, rather than orthorhombic α-U_3O_8, which forms from pure UO_{2+x}, is not understood (Thomas et al. 1993). Additional comparisons between synthetic UO_2 and spent UO_2 fuels are discussed by Janeczek et al. (1995) and by Janeczek (this volume).

Oxidation of uraninite. The dry-air oxidation of uraninite at elevated temperatures (150-300°C) is similar to that described for spent UO_2 fuel and doped synthetic UO_2. Cubic symmetry is maintained up to 300°C during air oxidation of untreated uraninite. No tetragonal distortions are evident, nor is crystalline U_3O_8 detected (Janeczek and Ewing 1991a ; Janeczek et al. 1993). By contrast, uraninite that was pre-annealed at 1200°C in H_2 gas for 24 hours forms cubic U_4O_9, followed by crystallization of orthorhombic α-U_3O_8 when oxidized in air at 300°C (Janeczek et al. 1993). In neither case, however, is tetragonal U_3O_7 observed. As for spent fuel and doped UO_2, the formation of hexagonal U_3O_8 is apparently inhibited during dry-air oxidation of uraninite. Thus, as for spent UO_2 fuels and doped synthetic UO_2, formation of tetragonal U_3O_7 and orthorhombic U_3O_8 are not formed during the dry-air oxidation of unannealed uraninite.

The initial oxidation of uraninite may result in a reduced unit cell parameter, as noted for oxidized spent fuel, although the effect of other cations may offset this to varying degrees (Janeczek 1993). The upper limit on the amount of U^{5+} or U^{6+} that can be accommodated in uraninite is unknown and probably depends strongly on the original composition. Reported U^{6+}:U^{4+} ratios for uraninite commonly exceed the highest expected for U_4O_9, without loss of cubic symmetry (Frondel 1958; Berman 1957; Janeczek and Ewing 1992b). Despite such high U^{6+}:U^{4+} ratios, interstitial O probably does not exceed

1/8 of U-equivalent sites in uraninite (Janeczek and Ewing 1992b), equal to the interstitial O occupancy in synthetic U_4O_9, and the actual number of O interstitials in uraninite may be less if interstitial sites are also occupied by cations such as Pb, Ca or REEs. Recalculation of reported uraninite formulas by accounting for impurity elements generally gives O:U ≤ 2.25, as expected (Janeczek et al. 1993).

The effects described above for the oxidation of uraninite provide no clear indication of how oxidation affects the physical properties of uraninite and what role these changes play in the dissolution of uraninite in oxidizing groundwaters. Reduced unit-cell parameters caused by oxidation could result in the formation of gaps between uraninite grains, increasing surface areas and providing pathways for groundwater penetration. There is no clear evidence, however, for a transformation of the type: $UO_{2+x} \Rightarrow U_4O_{9+x}$ in natural uraninite. This may be because most uraninite is already partially oxidized at the time of formation, and may also reflect how the accumulation of radiogenic Pb (and other large cations) can offset unit-cell shrinkage caused by partial oxidation. Where uraninite with two different unit-cell sizes have been reported within a single sample, this has been attributed to the segregation of radiogenic Pb, rather than oxidation (Janeczek and Ewing 1992c; Janeczek et al. 1993).

Replacement of uraninite by uranyl minerals

When in contact with oxidizing water, U oxides above U_4O_9 cannot form from synthetic UO_2, because the kinetics of dissolution in oxidizing waters are orders of magnitude faster than those of dry-air oxidation and dissolution dominates (Posey-Dowty et al. 1987; Shoesmith and Sunder 1991; Shoesmith et al. 1998). This is consistent with the observation that cubic uraninite is the mineral most often found in contact with the corrosion rind formed by oxidation in water (Frondel 1958; Finch and Ewing 1992b). Rapid oxidative dissolution of uraninite can lead to quite elevated concentrations of dissolved U, and the precipitation of uranyl oxyhydroxides appears to be kinetically favored over precipitation of more complex uranyl minerals (Finch and Ewing 1992b; Finch 1994). The reasons for kinetic constraints on the precipitation of many uranyl minerals are uncertain. Precipitation of uranyl oxyhydroxides may require little atomic rearrangement of uranyl solution complexes (Evans 1963) compared with atomic rearrangements required to precipitate uranyl silicates or phosphates. Many uranyl tricarbonate solution complexes might be expected to precipitate as minerals without much atomic rearrangement, because their structures contain the uranyl tricarbonate ion, $(UO_2)(CO_3)_3^{4-}$. However, U concentrations required to precipitate most uranyl carbonates (and sulfates) are much higher than for uranyl oxyhydroxides (with the exception of rutherfordine). Uranyl oxyhydroxides may therefore have the lowest solubilities among those minerals for which precipitation kinetics do not present significant barriers to nucleation. Given that the early-formed uranyl minerals are kinetic (i.e. metastable) products, it is not surprising that they are pervasively altered by continued interaction with groundwaters from which they precipitated.

Thus, the uranyl oxyhydroxides comprise an especially important group of uranyl minerals because they commonly form early during the oxidative dissolution of reduced U minerals. The uranyl oxyhydroxides that form earliest during the oxidation of uraninite are ianthinite, schoepite, becquerelite, vandendriesscheite and fourmarierite (Snellling 1980; Finch and Ewing 1992b; Pearcy et al. 1994; Finch 1994). Schoepite and becquerelite are also the first phases to form from Si-saturated waters during corrosion experiments on synthetic UO_2 at 90°C (Wronkiewicz 1992, 1996).

Finch and Ewing (1992b) described a simplified reaction for the early-stage oxidative

corrosion of uraninite at Shinkolobwe (written with all U retained in schoepite and vandendriesscheite):

$$\begin{aligned} &U^{4+}_{0.48}U^{6+}_{0.39}(Y,Ce)_{0.02}Pb_{0.09}Ca_{0.02}O_{2.27} \\ &+ 0.24\ O_2 \\ &+ 1.57\ H_2O \\ &+ 0.10\ H^+ \end{aligned} \quad \rightarrow \quad \begin{aligned} &0.03375\ [(UO_2)_8O_2(OH)_{12}](H_2O)_{12} \\ &+ 0.06\ Pb_{1.5}[(UO_2)_{10}O_3(OH)_{11}](H_2O)_{11} \\ &+ 0.02\ Ca^{2+} \\ &+ 0.02\ (Y,Ce)^{3+} \end{aligned}$$

The minerals on the right, schoepite and vandendriesscheite, are common corrosion products formed early in contact with dissolving uraninite. In Ca-bearing water, becquerelite will also form, at the expense of some or all schoepite, depending on the activity ratio $\{Ca^{2+}\}/\{H^+\}^2$ (cf. Fig. 7, below). If pO_2 levels drop, due to consumption of oxygen by uraninite oxidation or from organic influences, the mixed valence oxyhydroxide, ianthinite, may replace schoepite in the above reaction. Little is known about the conditions necessary for the formation of ianthinite, but it may be a common initial oxidation product of uraninite (Finch and Ewing 1994; Pearcy et al. 1994; Burns et al. 1997b), subsequently oxidizing in air to schoepite. The above reaction represents a somewhat simplified view of the natural system, being written without dissolved silica, carbonate or other complexing ligands. However, even in silica saturated solutions, uranyl silicates do not play an important role during the initial stages of uraninite corrosion (Frondel 1956; Wronkiewicz 1992, 1996; Pearcy et al. 1994). Slightly alkaline carbonate waters tend to solubilize U, although a significant amount of U remains in solids near the dissolving uraninite in most weathered uraninite deposits (Frondel 1956; Frondel 1958; Finch and Ewing 1992b).

Continued interaction between groundwaters and the early-formed uranyl oxyhydroxides results in their replacement by uranyl silicates (and carbonates) and increasingly Pb-rich uranyl oxyhydroxides (Frondel 1956; Finch and Ewing 1991; Finch and Ewing 1992b). The most common uranyl minerals to persist after uraninite has been essentially replaced at the Shinkolobwe mine are soddyite and curite, where pseudomorphic replacement of uraninite by approximately equal volumes of curite plus soddyite is common (Schoep 1930; Finch 1994). At Koongarra, where Mg-chlorites are abundant, uraninite alteromorphs are commonly composed of curite and sklodowskite (Isobe et al. 1992). In the somewhat drier environment at the Nopal I U mine near Peña Blanca, Mexico, alteromorphs after Pb-poor Tertiary-age uraninite are commonly composed of uranophane, soddyite, and minor weeksite (Pearcy et al. 1994). Although kasolite is a persistent uranyl mineral that withstands prolonged groundwater interaction, kasolite is not known to replace uraninite, but instead tends to fill veins that may transect uraninite alteromorphs. Kasolite commonly fills veins within uraninite early during alteration (Isobe et al. 1992; Finch 1994), probably owing to the availability of Pb from dissolving galena located along uraninite grain and subgrain boundaries. These kasolite veins can persist even after the surrounding uraninite has been entirely replaced by uranyl minerals. They do not, however, comprise a substantial volume of the alteromorphs (Isobe et al. 1992; Finch 1994).

Elton and Hooper (1995) described a rich assemblage of supergene U, Pb, and Cu minerals at a coastal exposure near Low Warren, Cornwall, England. These minerals were produced by the action of surface waters and sea spray on uraninite, chalcocite and chalcopyrite. Elton and Hooper (1995) identified three zones of mineralization in terms of the major alteration minerals found in each.

1. Rutherfordine, boltwoodite, and vandendriesscheite closely associated with the uraninite, along with minor trögerite and an unidentified Ca-REE uranyl

carbonate.

2. Central part of the exposure with few U minerals, but there are several Cu-bearing products of chalcocite alteration.
3. Kasolite, wölsendorfite, widenmannite, dewindtite, and an unidentified "basic" Pb uranyl carbonate.

ALTERATION OF URANYL MINERALS

Thermodynamic background

Uraninite can be a remarkably heterogeneous mineral, with a composition and microstructure that can vary widely among samples from different localities, or even among specimens from within a single occurrence (Janeczek and Ewing 1992b,c, Janeczek and Ewing 1995). Thermodynamics of uraninite may be difficult to generalize, and the synthetic pure oxides, UO_2 and U_4O_9, are necessary surrogates in geochemical codes. The influences that impurity elements may have on thermodynamic stabilities are poorly understood. Elements such as Ca^{2+} and Th^{4+}, as well as U that is more oxidized than U^{4+}, may increase the stability range of uraninite to higher oxidation potentials relative to pure oxides; elements incompatible in the uraninite structure, notably radiogenic Pb^{2+}, probably decrease uraninite stability. Accumulation of radiogenic Pb may affect thermodynamic stabilities of all U minerals of sufficient age. A recent study comparing solubilities of several uraninite samples and synthetic UO_2, suggests that synthetic UO_2 and natural uraninite have comparable solubilities in reducing groundwater, and in the near-neutral pH range (5 to 7) variability among uraninite samples can exceed differences between uraninite and synthetic UO_2 (Casas et al. 1998). The thermodynamics of coffinite are also poorly known, and impurities such as REE, P and Ca, will influence its stability (Hansley and Fitpatrick 1989; Janeczek and Ewing 1996). For the most part, thermodynamic stabilities of other U^{4+}-bearing minerals remain poorly constrained. This is also true of most uranyl minerals. The solubilities of uranyl minerals, measured in terms of total dissolved U, span several orders of magnitude: from as low as 10^{-9} to 10^{-8} mol·L^{-1} for some uranyl phosphates, arsenates and vanadates, to as high as perhaps 10^{-3} to 10^{-2} mol·L^{-1} for uranyl carbonates and sulfates (Langmuir 1978). Despite their importance in controlling U concentrations in U-rich waters, reliable thermodynamic data are available for fewer than ten of the more than 160 uranyl minerals known (Robie et al. 1979; Hemingway 1982; Vochten and Van Haverbeke 1990; Grenthe et al. 1992; Nguyen et al. 1992; Casas et al. 1994, 1997).

The lack of thermodynamic data for uranyl minerals is not due to a lack of effort. Many studies have been done on the solubilities and other thermodynamic properties of U minerals. However, natural samples are rarely pure; minerals are often fine-grained and intimately intergrown at even a sub-micron scale. Variations in composition, including hydration state, are common and can lead to large differences in measured parameters. Studies of the thermodynamics of synthetic phases are useful, but for many of these, accurate thermodynamic measurements are hampered by kinetic effects, and mixed or amorphous phases are common in laboratory studies. Synthetic phases do not always correspond to known minerals, and, due in part to inadequate knowledge about the compositions of many uranyl minerals, the degree to which synthetic phases are representative of minerals may be uncertain.

Measured and estimated thermodynamic parameters

The desire to understand the thermodynamics of U minerals focused early on trying to describe geochemical conditions favorable for concentration of U in economic deposits.

Hostetler and Garrels (1962) were perhaps the first to predict mineral-solution equilibria for low-temperature U-rich waters. Their study provided important insights into the occurrences of U deposits and the conditions under which U is transported in and precipitated from groundwaters. Langmuir (1978) published a comprehensive study of U thermodynamics, and applied his results successfully to understanding a wide variety of U-mineral occurrences. Out of necessity, many of Langmuir's data were estimated. The United States Geological Survey recognized the need for thermodynamic data for the great number of U minerals, leading to the work by Hemingway (1982), which focussed on the formation of coffinite and uraninite deposits. Hemingway (1982) used the method of Chen (1975) to estimate many of the Gibbs free energies of formation values for U many minerals; however, Chen's method works best if a large number of thermodynamic data can be used for the calculation, and such was not the case for U minerals at that time. Despite some inaccurate estimates, data reported by Langmuir (1978) and Hemingway (1982) were remarkably successful at helping to understand U-mineral occurrences. Estimates of Gibbs free energies of formation for some anhydrous phosphates were published by Van Genderen and Van der Weijden (1984), who used the method developed by Tardy and Garrels (1976, 1977); however, Van Genderen and Van der Weijden (1984) ignored the contribution of structurally bound H_2O in uranyl phosphates.

During the 1980s, the emphasis on U geochemistry began to shift. Demand for nuclear energy diminished (particularly in the US), due in part to public perception and escalating costs of building commercial nuclear reactors. There was also the increasingly pressing concern for a permanent solution to the problem of the growing volume of highly radioactive nuclear waste worldwide. Because of its remarkable durability as a reactor fuel and the apparent persistence of uraninite in nature, many countries consider direct geologic disposal of spent UO_2 fuel to be a potentially safe and cost-effective means of solving the nuclear-waste problem. Research efforts in U geochemistry began to shift away from U exploration and towards understanding the chemical durability of the UO_2 component of spent nuclear fuel, which houses many radioactive and toxic radionuclides generated during fission reactions towards predicting future geochemical behavior of U in and around a geologic repository for nuclear waste (see Wronkiewicz and Buck, and Janeczek, this volume). Towards this end, the Nuclear Energy Agency (NEA) under the direction of the Organization for Economic Co-operation and Development (OECD) in Europe, published a compilation and critical review of existing thermodynamic data for U (Grenthe et al. 1992).

Published a decade after the papers by Hemingway (1982) and Langmuir (1978), Grenthe et al. (1992) provided a valuable up-to-date resource for research in U geochemistry. Unfortunately, of the approximately 200 U minerals known only four were accepted in the NEA compilation, all of them synthetic analogues: uraninite (synthetic UO_{2+x}, x = 0, 0.25, 0.33), coffinite (synthetic $USiO_4$), metaschoepite (synthetic $UO_3 \cdot 2H_2O$) and rutherfordine (synthetic UO_2CO_3).

Concurrent with the publication of the NEA database, several studies of the thermodynamics of U solids were published. Vochten and van Haverbeke (1990) reported the solubilities of three synthetic uranyl oxyhydroxides: becquerelite, billietite and $PbU_2O_7 \cdot 2H_2O$ (the latter is isostructural with wölsendorfite). Sandino and Bruno (1992) determined the solubility of $(UO_2)_3(PO_4)_2 \cdot 4H_2O$ (a phase unknown in nature) and reported stability constants for several U(VI)-phosphate solution complexes. Nguyen et al. (1992) published experimentally determined Gibbs free energies of formation for four synthetic uranyl silicates, uranophane, soddyite, Na-boltwoodite, and Na-weeskite. Sandino and Grambow (1995) studied the solubility of synthetic becquerelite and compreignacite, reporting a solubility constant for becquerelite quite close to that determined by Vochten and van Haverbeke (1990). A subsequent study of the solubility of a natural becquerelite

crystal determined a solubility constant that is lower than that reported for synthetic becquerelite by approximately 13 orders of magnitude, suggesting that the stability of becquerelite may be greater than previously thought (Casas et al. 1997). Gibbs free energies of formation were reported recently for the synthetic analogues of cliffordite (Mishra et al. 1998) and schmitterite (Mishra et al. 1998; Singh et al. 1999).

The paucity of thermodynamic data for even common U minerals prompted Finch (1994) to estimate the Gibbs free energies of formation for some uranyl oxyhydroxides in order to help explain the paragenesis of uranyl minerals at the Shinkolobwe mine in southern Democratic Republic of Congo. He used a method similar to that developed by Tardy and Garrels (1976, 1977) and used by Van Genderen and Van der Weijden (1984): summing free energy contributions of fictive oxide components to the total Gibbs free energy of formation of the mineral of interest. Activity-activity (mineral stability) diagrams were used to compare predicted and observed mineral relationships, providing an independent check on the reliabilities of estimates. Due to the success of this method, it was expanded to include uranyl silicates and uranyl carbonates (Finch and Ewing 1995). Finch (1997a) published estimated Gibbs free energies of formation for several uranyl oxyhydroxides, uranyl silicates and uranyl carbonates, and used these values to construct mineral stability diagrams for two geochemically important aqueous systems: CaO-CO_2-UO_3-H_2O and CaO-SiO_2-UO_3-H_2O. A brief description of the method reported by Finch (1997a) follows.

Given the ΔGf° values for stoichiometrically simple oxides and hydroxides, one may estimate the contribution of the constituent oxides to the total ΔG_f° value of each mineral; that is, the ΔG_f^* of each oxide *in the mineral structure*. The ΔG_f° value of a mineral is the arithmetic sum of the oxide contributions: $\Delta G_f^\circ = \Sigma \Delta G_f^*{}_i$. Finch (1997a) estimated $\Delta G_f^*{}_i$ values from a small number of synthetic hydrated uranyl minerals. Chen et al. (1999) expanded on this by deriving $\Delta G_f^*{}_i$ values by regression analyses of a large number of uranyl compounds, both hydrated and anhydrous. The large data set used by Chen et al. (1999) appears to be an improvement over the limited set used by Finch (1997a), and Tables 18 and 19 list the data derived by Chen et al. (1999). The values for the hypothetical oxides in Table 18 are used to estimate ΔG_f° for the uranyl minerals in Table 19 by adding $\Delta G_f^*{}_i$ contributions from the constituent oxides in their stoichiometric proportions.

Estimated ΔG°_f values are used to construct activity-activity (stability) diagrams, and the predicted stability fields can be compared with observed mineral occurrences and reaction pathways. With some exceptions, natural occurrences agree well with the mineral stability fields estimated for the systems SiO_2-CaO-UO_3-H_2O and CO_2-CaO-UO_3-H_2O, providing some confidence in the estimated thermodynamic values. Activity-activity diagrams are sensitive to small differences in ΔG°_f values, and mineral compositions must be known accurately, including structurally bound H_2O (Finch 1997a). Estimated ΔG°_f values may not be reliable for a few minerals (e.g. liebigite, zellerite, uranosilite) for two reasons: (1) the structures of the minerals in question are not closely similar to those used to estimate the ΔG_f^* values of the component oxides, or (2) the minerals in question may be exceptionally fine grained, leading to large surface energies that increase effective mineral solubilities (Finch 1997a).

As an illustration of the difficulties encountered when constructing stability diagrams from experimental data, Figure 5 compares two stability diagrams for the SiO_2-CaO-UO_3-H_2O system. The reported solubility constant for synthetic becquerelite (Vochten and Van Haverbeke 1990; Sandino and Grambow 1995): log K_{so} 42, is more than ten orders of magnitude greater than that reported for a natural becquerelite crystal (Casas et al. 1997): log K_{so} 29. The difference this makes to a stability diagram is clearly seen in Figure 5. If

Table 18. Molar contributions of structural components to $\Delta G^0_{f,298}$ and $\Delta H^0_{f,298}$ of U(VI) phases reported by Chen et al. (1999) (kJ.mol^{-1})

Component	UO_3	$Li_2O_{(l)}$	$Na_2O_{(l)}$	$K_2O_{(l)}$	$Rb_2O_{(l)}$	$Cs_2O_{(l)}$	$CaO_{(l)}$
$\Delta G_f^*{}_i$	-1161.05	-692.14	-686.54	-637.45	-639.05	-644.35	-715.77
$\Delta H_f^*{}_i$	-1233.75	-737.75	-736.3	-686.95	-688.95	-694.25	-726.57

Component	$BaO_{(l)}$	$SiO_{2(IV)}$	$SO_{3(IV)}$	$CO_{2(III)}$	$N_2O_{5(III)}$	$P_2O_{5(IV)}$	$H_2O_{(S)}$	$H_2O_{(H)}$
$\Delta G_f^*{}_i$	-725.91	-853.96	-538.87	-400.61	21.95	-1638.25	-237.94	-241.1
$\Delta H_f^*{}_i$	-761.98		-624.17	-455.59	-78.99	-1802.37	-299.93	-295.58

Table 19. $\Delta G^\circ_{f,298}$ and $\Delta H^\circ_{f,298}$ for uranyl minerals indicated in Figs. 5, 6, and 7 (kJ·mol^{-1}).

Mineral	$\Delta G^0_{f,298}$	$\Delta H^0_{f,298}$	*M/C**	*Ref.*
Schoepite	-13299.4	-14908.7	C	1
Metaschoepite	-13092.0	-14608.8	M	2
Becquerelite	-10324.7		C	1
Rutherfordine	-1563.0	1689.6	M	3
Urancalcarite	-6036.7		C	1
Sharpite	-11607.6		C	1
Fontanite	-6524.7		C	1
Zellerite	-3879.9		C	1
Liebigite	-6226.0	-7301.6	M	4
Uranosilite	-7126.1		C	1
Haiweeite	-9367.2		C	1
Ursilite	-20377.4		C	1
Soddyite	-3658.0		M	5
Uranophane	-6210.6		M	5

*M/C designates measured or calculated values. References: 1. Chen et al. (1999); 2. O'Hare et al. (188); 3. Sergeyeva et al. (172); 4. Alwan & Williams (1980); 5 Nguyen et al. (1992). Chen et al. re-evaluated the data of Nguyen et al. (1992) and determined GFE values of -3655.7 and -6192.3 kJ·mol^{-1} for soddyite and uranophane, respectively. The ΔGf° values for dissolved species, calcite and CO_2, used to construct Figs. 5, 6, and 7 are from Grenthe et al. (1992).

we assume that the solubility of synthetic becquerelite best represents the solubility of becquerelite in nature (Fig. 5a), then becquerelite is unstable in all but those groundwaters with vanishingly small dissolved silica concentrations ($<10^{-6}$ mol L^{-1} H_4SiO_4); a conclusion that seems contrary to observation (Finch and Ewing 1992b; Finch 1994; Finch et al. 1995, 1996). On the other hand, the exceptionally large stability field indicated for the natural becquerelite crystal suggests that becquerelite should predominate in most natural waters (Fig. 5b), which also seems contrary to observation (however, note that most other compounds in Fig. 5 are synthetic). Of course, simple comparisons of thermodynamic stabilities with natural occurrences ignore potential kinetic effects on mineral relationships. Nevertheless, because of the apparent discrepancies between observation and the stability diagrams shown in Figure 5, we will use the estimated Gibbs free energy of formation for becquerelite derived by Chen et al. (1999), which corresponds to a solubility product intermediate between the experimental values: log K_{so} 36.

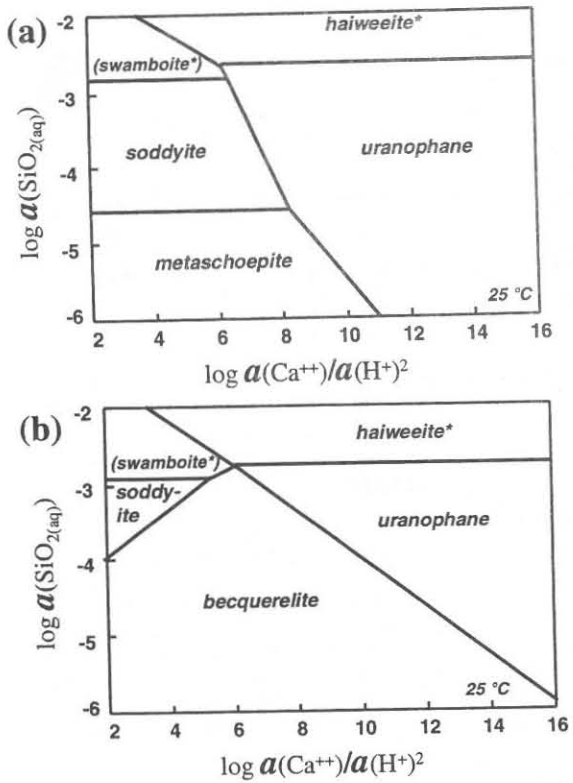

Figure 5. Activity-activity diagrams for the system SiO_2-CaO-UO_3-H_2O, calculated with $\Delta G°_f$ values derived from from solubility studies of (a) synthetic becquerelite powders (Vochten and Van Haverbeke 1990; Sandino and Grambow 1995), and (b) a natural becquerelite crystal (Casas et al. 1997). All data are derived from experimental studies except minerals marked with an asterisk (*), for which stability fields were calculated from estimated $\Delta G°_f$ values in Table 19.

Two systems are analyzed in detail: SiO_2-UO_3-CaO-H_2O and CO_2-UO_3-CaO-H_2O. The SiO_2– and CO_2–bearing system are important in nature, and will help to understand the paragenesis of uranyl minerals. The Ca-con-taining systems are considered because Ca is virtually ubiquitous in near-surface groundwaters, and many Ca-bearing uranyl minerals are known, representing a variety of near-surface environ-ments.

System CO_2-CaO-UO_3-H_2O. Figure 6 illustrates the stability fields for several uranyl carbonate minerals. The concentration of Ca in many groundwaters is controlled by equilibrium with calcite and dissolved $CO_{2(g)}$: $CaCO_3 + 2H+ \Leftrightarrow Ca^{2+} + H_2O + CO_{2(g)}$. This equilibrium is indicated as a diagonal dotted line in Figure 6. The calcite equilibrium line passes through the fields for becquerelite, schoepite and rutherfordine. These are the most common minerals among those represented in Figure 6, and rutherfordine is by far the most common uranyl carbonate (Frondel 1958; Smith 1984). Chen et al. (1999) showed that many natural groundwater compositions plot within the stability field of bec-querelite, consistent with it being the most common uranyl oxyhy-droxide mineral in nature (Frondel 1958; Smith 1984). Sharpite and urancalcarite are rare and occur in deposits where the predominant carbonate mineral in the host rocks is magnesian calcite or dolomite (Deliens et al. 1981); however, if Figure 6 is accurate, sharpite may be more common than currently thought, likely to form in calcite-bearing rocks in high pCO_2 groundwaters, such as saturated soils. Fontanite, which coexists with becquerelite and uranophane, occurs in pelitic silts and shales (Deliens and Piret 1992).

Two uranyl carbonates not shown in Figure 6 are liebigite and zellerite (Table 19). Stability fields calculated for these two minerals replace most of the area shown in Figure 6, contrary to observation. The Gibbs free energy of formation for liebigite was determined by Alwan and Williams (1980) for synthetic material. Liebigite and zellerite are commonly found as efflorescences on mine walls, surface outcrops, and elsewhere that evaporation is high. These minerals also tend to be extremely fine grained, suggesting that high surface free energies may enhance their effective solubilities.

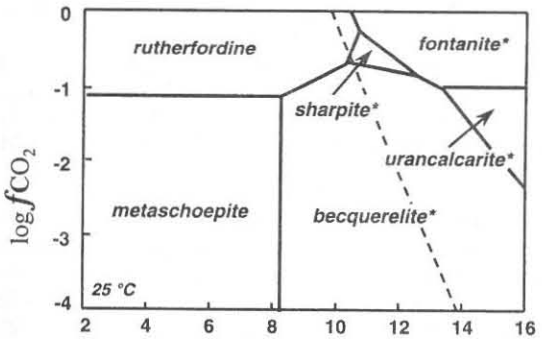

Figure 6. Activity-activity diagram for the system CO_2-CaO-UO_3-H_2O, calcu-lated using measured and estimated $\Delta G°_f$ values in Table 19. Data are derived from experimental studies except minerals marked with an asterisk (*), for which stability fields were calculated from estimated Gibbs free energies of formation (Table 19). Diagonal dotted line represents calcite equilibrium.

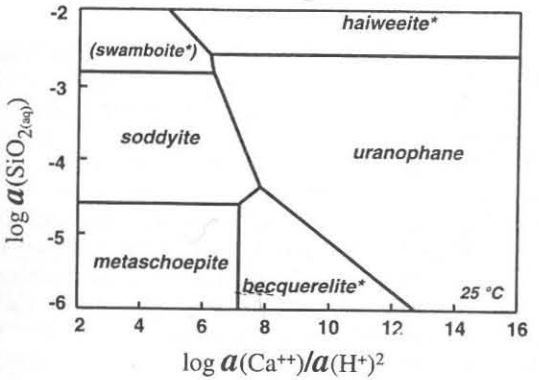

Figure 7. Activity-activity diagram for the system SiO_2-CaO-UO_3-H_2O, calcu-lated using measured and estimated $\Delta G°_f$ values from Table 19. Data are derived from experimental studies except minerals marked with an asterisk (*), for which stability fields were calculated from estimated $\Delta G°_f$ values (Table 19). Swamboite field is approximate only, shown for completeness.

System SiO_2-CaO-UO_3-H_2O. Figure 7 illustrates the stability fields of minerals common in Si-bearing groundwaters. The most common Pb-free U(VI) minerals are schoepite and metaschoepite, becquerelite, soddyite, uranophane and rutherfordine. Schoepite forms early in the alteration paragenesis of uraninite oxidation products (Finch and Ewing 1992b; Finch 1994). Though common, schoepite is not usually abundant at most oxidized U deposits, because it is commonly replaced by uranyl silicates and carbonates, especially uranophane, soddyite and rutherfordine (Frondel 1956; Finch and Ewing 1992a,b; Finch 1994; Pearcy et al. 1994). Although the direct replacement of schoepite by becquerelite is not readily confirmed, this reaction has been reported from several experimental studies (Vochten and Van Haverbeke 1990; Sandino and Grambow 1995; Sowder et al. 1996). Although well-formed crystals are known, schoepite, metaschoepite and "dehydrated schoepite" commonly form fine-grained masses, effectively increasing their solubilities, and schoepite dehydrates spontaneously, becoming polycrystalline (Finch et al. 1998, also see below). The lower hydrates also have higher solubilities in water at ~25°C (O'Hare et al. 1988). Uranophane is the most common U(VI) mineral in nature (Smith 1984) and is the stable uranyl mineral in contact with groundwaters whose compositions are controlled by calcite and silica equilibria (Langmuir 1978). These observations are consistent with the large uranophane stability field in Figure 7. Soddyite is another common mineral in oxidized U deposits, where it replaces schoepite and, less commonly, uranophane (Finch 1994). Haiweeite is relatively rare, and is usually associated with volcaniclastic rocks in arid environments.

The rare mineral swamboite commonly occurs with soddyite and uranophane (Deliens et al. 1984), suggesting a genetic relationship. The swamboite stability field indicated in

Figure 7 is only approximate, and was estimated by assuming that the additional U atom in the swamboite formula (Table 8), presumably in an interlayer site, makes a lower free energy contribution than does U in the structural unit. Swamboite is probably stable near the upper limit for the activity H_4SiO_4 in natural waters. The extremely rare minerals, calciouranoite and metacalciouranoite are not shown in Figure 7, and should only be stabile in very Si-poor waters at high values of pH and dissolved Ca, a conclusion consistent with their occurrence (Rogova et al. 1973, 1974).

Stability fields estimated for two uranyl silicates, uranosilite and "ursilite," are excluded from Figure 7, as they would replace the entire field of uranophane illustrated in Figure 7, contrary to observation. Like the carbonates liebigite and zellerite, uranosilite and "ursilite" always form as fine-grained masses, and surface-free energy must contribute to their solubilities (ursilite also contains Mg and may be synonymous with haiweeite, Smith 1984). The structure of the rare mineral uranosilite is unknown but is probably unique among the uranyl silicates (Table 8).

Structural considerations. A fundamental assumption of this method to estimate Gibbs free energies is that each oxide component occurs in every structure with the same relative "fit." That is, we ignore possible structural distortions that may arise in individual minerals, due to, for example, changing the size of an interstitial cation. An example of such a distortion is evident by comparing the nearly isostructural minerals becquerelite and billietite. The ionic radii of Ca^{2+} (1.12 Å) and Ba^{2+} (1.42) (both for 8-coordination) differ by nearly 25%. This difference has two effects. (1) the structural sheets in becquerelite are more corrugated than those in billietite (Pagoaga et al. 1987), and (2) uranyl coordination in one-half of the structural sheets of billietite differs slightly from that in becquerelite. Corrugated structural sheets in becquerelite are required to accommodate the smaller Ca^{2+} ion, and this may contribute strain energy to the becquerelite structure that is not a factor in billietite. However, $\Delta G°_f$* for UO_3 is the same for both minerals (i.e. an average value). Structural strain may become increasingly severe as the number of interlayer Ca^{2+} ions increase progressively in synthetic $Ca(UO_2)_3O_4{\cdot}5H2O$ ("Ca-protasite") and calciouranoite. In fact, additional cations in calciouranoite may help reduce structural strain and stabilize this mineral in nature (Finch 1994). That the larger Ba^{2+} cation induces less structural strain is evident from the nearly flat structural sheets in protasite, which may explain why protasite occurs as a mineral (albeit rare) but not its Ca analogue.

Dehydration and the role of H_2O

Virtually all minerals that contain the uranyl ion, UO_2^{2+}, also contain substantial amounts of structurally bound H_2O, as well as OH^- ions. Many uranyl minerals are weathering products, formed at low-temperatures in near-surface aqueous environments, and structurally bound molecular H_2O strongly influences the structural and thermodynamic stabilities of these minerals. The hydronium ion, H_3O^+, may occur in some uranyl minerals, but it has never really been verified and is an unusual constituent in mineral structures (Hawthorne 1992). Structurally bound H_2O groups most commonly occur in interstitial (interlayer) sites in mineral structures, where they may be bonded to an interlayer cation, or they may occupy sites in which H_2O groups act as an H-bond "bridge" only. The ease with which H_2O groups may be removed from interstitial sites depends on bonding environments, and H_2O groups that are H-bonded only appear to be lost most readily (Finch et al. 1998). Numerous uranyl minerals display significant structural changes caused by the loss of structurally bound H_2O groups. Such structural changes are the reason that many uranyl minerals dehydrate irreversibly, although a few uranyl sulfates, vanadates, and uranyl phosphates are known to dehydrate reversibly (see Cejka, Chapter 12, this volume). No uranyl oxyhydroxides are known to dehydrate reversibly. This is a

significant fact, since these minerals are commonly the earliest to form during corrosion of uraninite in weathering environments.

Finch (1997b) described the structural role of H_2O in uranyl minerals. The structures of most uranyl minerals are based on sheets of uranyl polyhedra polymerized in the two dimensions perpendicular to the approximately linear uranyl ion. These structural sheets are most commonly bonded to each other through divalent cations and molecular H_2O. The uranyl O atom is strongly bonded to the U^{6+} cation, with a bond valence (b.v.) of ~1.8 valence units (v.u.) and, therefore, contributes only ~0.2 v.u. to interlayer cations. In minerals based on sheet structures, the cations in interlayer sites can bond to no more than six neighboring uranyl O atoms. This contributes a maximum of ~1.2 v.u. to the central cation, leaving a deficit of ~0.8 v.u. This deficit is accommodated in most of these structures through cation-H_2O bonds within the interlayer, each of which contributes ~0.2 v.u. Interlayer divalent cations are commonly coordinated by four H_2O groups, thereby satisfying the cations' valence requirements. Interlayer H_2O groups that are not bonded to a cation are not "excess water" but contribute ~0.2 v.u. from H-bonds to those uranyl O atoms not bonded to an interlayer cation. These interlayer H_2O groups also act as H-bond acceptors for OH groups in the structural sheets. In addition, interlayer H_2O groups may act as bond modifiers by distributing the bond valence from central cations to multiple uranyl O atoms through an array of H-bonds, with each H-bond contributing ~ 0.2 v.u.

The removal of structurally bound H_2O groups from interlayer sites requires significant re-adjustment of local bonding arrangements and commonly results in phase transformations or even complete structural decomposition. For these reasons, most dehydration reactions among the uranyl minerals are irreversible, even at near-ambient temperatures. Furthermore, the relatively low energies required to remove H_2O groups from the interlayer sites in many of these structures results in narrow temperature ranges over which each mineral is stable with respect to other uranyl phases with more or less H_2O.

Perhaps the most dramatic and best understood effect of dehydration is that due to the loss of H_2O from schoepite (Finch et al. 1998). Schoepite, $[(UO_2)_8O_2(OH)_{12}](H_2O)_{12}$, transforms slowly in air at ambient temperature (Fig. 8) to metaschoepite, $[(UO_2)_8O_2(OH)_{12}](H_2O)_{10}$. The transformation is characterized by a two-percent decrease in

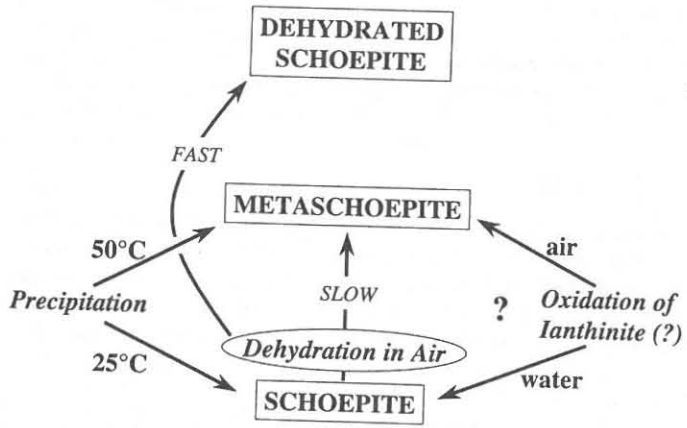

Figure 8. Representation of the phase relationships among schoepite, metaschoepite, and dehydrated schoepite, inferred from natural occurrences and experimental studies (from Finch et al. 1998).

the *a* cell dimension. There may be a slight decrease in the *b* cell dimension, but there is no significant change in the *c* cell dimension. The observed unit-cell changes may be due to the loss of one-sixth of the interlayer H_2O groups in schoepite, and this must result in changes to H-bonding arrangements. Differences in unit cell volumes induce strain to crystals for which the transformation to metaschoepite is incomplete, and stored strain energy may be sufficient to rapidly drive the transformation of schoepite to "dehydrated schoepite" when exposed to an external stress (e.g. heat or mechanical pressure). The complete transformation of schoepite to "dehydrated schoepite" is

$$[(UO_2)_8O_2(OH)_{12}](H_2O)_{12} \Rightarrow 8\,[(UO_2)O_{0.25}(OH)_{1.5}] + 12H_2O$$

"Dehydrated schoepite" is a defect structure-derivative of α-$UO_2(OH)_2$. Crystals that undergo dehydration change from translucent yellow schoepite to opaque yellow, polycrystalline "dehydrated schoepite" ± metaschoepite. The complete transformation occurs in three steps: (1) loss of interlayer H_2O from schoepite, causing collapse of the layers; (2) atomic rearrangement within the sheets from a schoepite-type arrangement to a configuration which may be similar to that of metaschoepite; (3) a second rearrangement to the defect α-$UO_2(OH)_2$-type sheet. Finch et al. (1998) proposed that the formula of "dehydrated schoepite" be written $(UO_2)O_{0.25-x}(OH)_{1.5+2x}$ ($0 \le x \le 0.15$) to reflect the observed non-stoichiometry. Dehydration of schoepite and metaschoepite to "dehydrated schoepite" are irreversible (Christ and Clark 1960). Upon re-exposure to water, "dehydrated schoepite" does not hydrate, but vacancies and O atoms in the structural sheets may be replaced by OH groups (increasing *x*).

Suzuki et al. (1998) examined dehydration behaviors of saleeite and metatorbernite. These two uranyl phosphates each lose H_2O groups two at a time as temperature is increased. This reduces their d_{200} spacings by ~0.1 nm for each pair of H_2O groups lost. Both saleeite and metatorbernite rehydrate at room temperature; however, the d_{200} spacings of the rehydrated minerals differ slightly from their original values (Suzuki et al. 1998).

Some important physical effects of dehydration of uranyl minerals include the expansion of gaps between grain boundaries (due a reduction in molar volume) and reduced grain sizes (due to structural changes). These phenomena can increase available pathways for the penetration of groundwater into corrosion rinds formed on altered uraninite and increase reactive surface areas of exposed minerals. Dehydration of uranyl oxyhydroxides is irreversible, and dehydrated minerals dissolve when recontacted by groundwater, replaced by minerals such as soddyite and uranophane. Dehydrated schoepite may even inhibit the reprecipitation of schoepite (Finch et al. 1992). Although common, schoepite is not normally abundant in weathered uraninite deposits (Frondel 1958). Becquerelite, and the Pb-uranyl oxyhydroxides, vandendriesscheite and curite, tend to be more common.

Groundwater alteration

Precipitated early during uraninite alteration, the uranyl oxyhydroxides themselves alter as they continue to interact with groundwaters. Their alteration may include complete dissolution; e.g. where carbonate or sulfate complexes are available, or replacement; e.g. by uranyl silicates or carbonates (commonly rutherfordine). At uraninite deposits where carbonates are abundant, dissolved carbonate concentrations and pH can increase during interaction with the host rocks. Above a pH of about 8, the dissolution of schoepite in the presence of bicarbonate can release U to solution:

$$[(UO_2)_8O_2(OH)_{12}](H_2O)_{12} + 24\,HCO_3^{2-} \Rightarrow 8\,UO_2(CO_3)_3^{2-} + 32\,H^+ + 14\,H_2O$$

where pH remains relatively low (< 6), schoepite may be replaced by rutherfordine if

groundwater pCO_2 increases due to biological respiration and decomposition (Fig. 6):

$$[(UO_2)_8O_2(OH)_{12}](H_2O)_{12} + 8\,CO_{2\,(g)} \Rightarrow 8\,UO_2CO_3 + 16\,H_2O$$

The alteration of becquerelite and many other uranyl oxyhydroxides is essentially identical to that of schoepite, with UO_2^{2+} being solubilized in carbonate groundwaters, except where pCO_2 exceeds atmospheric levels, under which conditions, rutherfordine or one of several uranyl carbonates illustrated in Figure 6 may become stable. Becquerelite is more stable than schoepite at higher $\{Ca^{2+}\}/\{H^+\}^2$ values (Figs. 6 and 7) and so, perhaps, is more resistant to dissolution. In dilute, low pH, non-complexing waters (e.g. fresh rain water), becquerelite may dissolve incongruently by losing Ca preferentially to U (Casas et al. 1994), possibly to form schoepite:

$$4\,Ca[(UO_2)_6O_4(OH)_6](H_2O)_8 + 8\,H^+ + H_2O \Rightarrow 4\,Ca^{2+} + 3\,[(UO_2)_8O_2(OH)_{12}](H_2O)_{12}$$

If the activity of dissolved silica is sufficient, UO_2^{2+} can complex with silicic acid to precipitate as uranyl silicates. Whether soddyite or uranophane forms depends on the activity ratio, $\{Ca^{2+}\}/\{H^+\}^2$ (Fig. 7). Low pH, Ca-poor waters favor formation of soddyite (Fig. 7); for example, replacing schoepite:

$$[(UO_2)_8O_2(OH)_{12}](H_2O)_{12} + 4\,H_4SiO_4 \Rightarrow 4\,(UO_2)_2SiO_4(H_2O)_2 + 12\,H_2O$$

or becquerelite

$$Ca[(UO_2)_6O_4(OH)_6](H_2O)_8 + 2\,H^+ \Rightarrow 3\,(UO_2)_2SiO_4(H_2O)_2 + Ca^{2+} + 6\,H_2O$$

More alkaline, Ca-bearing waters favor formation of uranophane, assuming carbonate concentrations remain relatively low (Fig. 7):

$$[(UO_2)_8O_2(OH)_{12}](H_2O)_{12} + 4\,Ca^{2+} + 8\,H_4SiO_4 \Rightarrow$$
$$4\,Ca(UO_2)_2(SiO_3OH)_2(H_2O)_5 + 8\,H^+ + 12\,H_2O$$

and

$$Ca[(UO_2)_6O_4(OH)_6](H_2O)_8 + 2\,Ca^{2+} + 6\,H_4SiO_4 \Rightarrow$$
$$3\,Ca(UO_2)_2(SiO_3OH)_2(H_2O)_5 + 8\,H^+ + H_2O$$

The above reactions constitute some of the more important replacement reactions that occur as groundwaters interact with corrosion rinds of uranyl oxyhydroxides. The alteration of the Pb-uranyl oxyhydroxides is slightly different from that of the Pb-free minerals, and we will consider their alteration in the next section.

Comparable reactions are relevant for the replacement of uranyl oxyhydroxides by minerals such as uranyl phosphates, arsenates and vanadates. However, in the presence of these ions, the uranyl oxyhydroxides tend to be rare or non-existent (Garrels and Christ 1959; Langmuir 1978).

The alteration of uranyl silicates is less commonly reported than that of the uranyl oxyhydroxides. Uranyl silicates are less soluble than oxy-hydoxides in most natural waters and tend to be less vulnerable to groundwater attack. However, as for becquerelite, uranophane may dissolve incongruently in fresh waters, releasing Ca^{2+} and silica, and precipitating soddyite. The replacement of uranophane by soddyite has been observed in natural samples from Shinkolobwe (Deliens 1977b; Finch 1994), as well as experimentally (Casas et al. 1994):

$$Ca(UO_2)_2(SiO_3OH)_2(H_2O)_5 + 2\,H^+ \Rightarrow (UO_2)_2SiO_4(H_2O)_2 + Ca^{2+} + H_4SiO_4 + 3\,H_2O$$

To our knowledge, the reverse reaction has not been reported.

The interaction of uranyl silicates with strongly complexing solutions, such as alkaline

bicarbonate waters, might result in the preferential release of U, which would increase the Si:U ratio in the residual solid, and might help explain compositional uncertainties for minerals such as "ursilite."

The following sequence summarizes observed U mineral paragenesis at many oxidized uraninite deposits:

1. Dissolution of uraninite and precipitation of uranyl oxyhydroxides: becquerelite, schoepite, (ianthinite) and vandendriesscheite. These minerals tend to first precipitate within voids and fractures in uraninite as it dissolves. Deliens (1977b) noted that the earliest-formed uranyl oxyhydroxides tend to be very fine grained.
2. Replacement of earlier-formed uranyl oxyhydroxides by uranyl silicates and replacement of Pb-poor minerals by Pb-enriched uranyl minerals. In weakly complexing waters, some U is transported short distances to precipitate on the outer surfaces of corroding uraninite as a coarsely crystalline rind of uranyl oxyhydroxides schoepite and becquerelite (± ianthinite). Monocarbonates such as rutherfordine may also precipitate where pCO_2 values are sufficient.
3. The continued replacement of both coarse and fine grained uranyl oxyhydroxides repeats the alteration sequence. Uranyl phosphates commonly form relatively late.

The dehydration and alteration of uranyl oxyhydroxides notwithstanding, schoepite and becquerelite, may persist for many thousands of years. Uranium-series activity ratios for several uranyl minerals from the Shinkolobwe mine in southern Democratic Republic of Congo indicate that these minerals did not experience significant preferential loss of U since their formation more than 100,000 years ago. The minerals examined included rutherfordine, schoepite, becquerelite, and uranophane. No correlation was found between mineral species and mineral age (Finch et al. 1995, 1996). Finch et al. (1996) concluded that the oxidative dissolution of primary uraninite maintains locally high dissolved U, keeping waters supersaturated with respect to most uranyl minerals and providing an inexhaustible source of dissolved U^{6+} for new mineral precipitation and growth. These results suggest that, as long as uraninite persists in an oxidizing environment, the assemblage of secondary uranyl minerals is determined by local groundwater chemistry (including transitory changes), but not necessarily towards formation of uranyl minerals with lower solubilities.

THE ROLE OF RADIOGENIC Pb IN U MINERAL PARAGENESIS

Because U is radioactive and ultimately decays to Pb, the mineralogy of U is intimately tied to that of Pb. As radiogenic Pb accumulates in a U mineral, U content decreases concomitantly. Because the crystal chemistries of U and Pb are so different, the accumulation of Pb and attrition of U can combine to destabilize structures of U minerals that are old enough to contain substantial radiogenic Pb. What we mean by "substantial" depends, of course, on the mineral, its age, and the amount of U initially present.

Lead is incompatible in the uraninite structure (Berman 1957; Janeczek and Ewing 1995), where it may occupy interstitial sites. X-ray studies indicate that unit-cell volumes of Pb-rich uraninite are larger than those of Pb-poor uraninite (Janeczek and Ewing 1992c, 1995), suggesting that Pb accumulation can induce significant strain. Lead is relatively immobile in most groundwaters (Mann and Deutscher 1980), and under reducing conditions, Pb released from U minerals commonly forms galena, provided the activity of S is sufficient. Recrystallization of uraninite under reducing conditions may proceed according to a reaction such as,

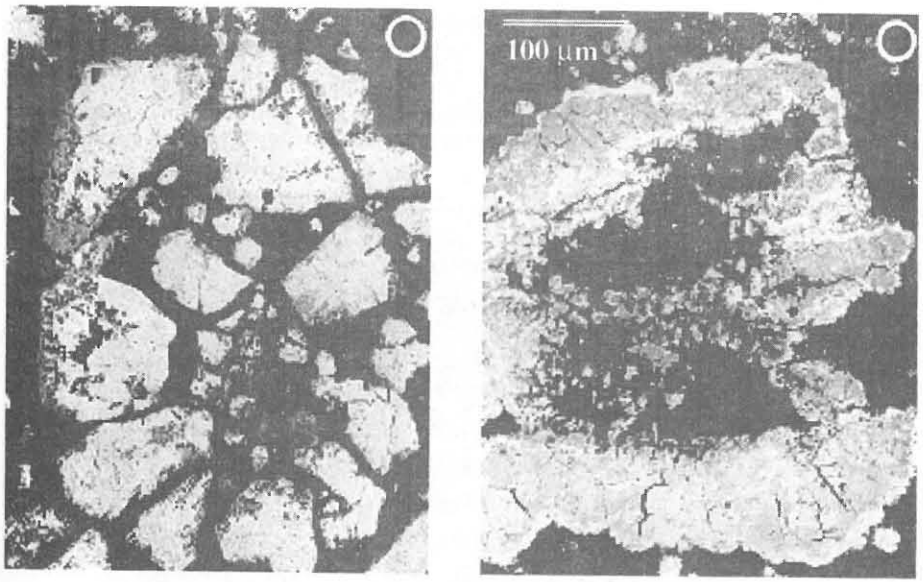

Figure 9. BSE images of fragmented uraninite crystals dissolved at their cores, a texture that may be related to strain caused by accumulation of radiogenic Pb and precipitation of galena. (from Janeczek and Ewing 1995; reprinted by permission of Pergamon Press).

$$(U^{4+}_{1-2y}U^{6+}_{y}Pb^{2+}_{y})O_{2\,(cr)} + yHS^{-} \Rightarrow (1-y)UO_{2\,(cr)} + yPbS_{\,(cr)} + yOH^{-} + {}^{1}/_{2}\,yO_{2\,(aq)}$$

An interesting consequence of this reaction is that the volume of uraninite steadily decreases without any loss of U to groundwater! Galena has a larger molar volume than uraninite (31.490 $cm^3 \cdot mol^{-1}$ and ~24.62 $cm^3 \cdot mol^{-1}$, respectively), and precipitation of galena within uraninite could induce substantial strain, helping to fragment crystals and providing pathways for groundwater infiltration. Brecciation of uraninite and dissolution of their cores may reflect this phenomenon (Janeczek and Ewing 1992c, 1995) (Fig. 9).

Under oxidizing conditions, Pb can combine with UO_2^{2+} to form one or more of the nearly 25 known Pb-uranyl minerals (Table 20). Virtually every chemical group of uranyl minerals is represented by at least one species in which Pb is an essential constituent, with eight or more being oxyhydroxides. The Pb-uranyl oxyhydroxides commonly form directly from precursor uraninite; however, many Pb-uranyl minerals do not, and their genesis is probably related to the accumulation of radiogenic Pd in nominally Pb-free minerals after formation. For example, kasolite formed at depth in the Koongarra U deposit does not replace uraninite, as originally believed (Snelling 1980). Instead, accumulation of radiogenic Pb in sklodowskite causes continual recrystallization of Pb-free sklodowskite (Isobe et al. 1992). Lead lost from the original sklodowskite precipitates as kasolite within sklodowskite veins (Fig. 10). Accumulation of radiogenic Pb and U loss combine to destabilize the structure of clarkeite, which eventually recrystallizes to wölsendorfite or curite (Finch and Ewing 1997). Studtite crystals commonly have Pb-rich cores, which appear as thin "threads" of Pb-uranyl oxyhydroxides, such as fourmarierite, that are evident from XRD data (Deliens and Piret 1983b). Asselbornite is compositionally zoned, with Pb concentrations highest at the cores of crystals (Sarp et al. 1983). Crystals of vandendriesscheite, schoepite, and becquerelite commonly contain inclusions of Pb-uranyl oxyhydroxides such as masuyite and fourmarierite (Finch and Ewing 1992b; Finch 1994)

Table 20. Pb-bearing U minerals

Plumbobetafite	$(Pb,U,Ca)(Ti,Nb)_2O_6(OH,F)$	
Plumbomicrolite	$(Pb,U,Ca)_2Ta_2O_6(OH)$	
Plumbopyrochlore	$(Pb,U,Ca)_{2-x}Nb_2O_6(OH)$	
Uraninite	$(U,Pb)O_2$	To ~20 wt % PbO
Wölsendorfite	xCaO·(6-x)PbO·12UO_3·12H_2O (x = 0 - 1)	
Sayrite	$Pb_2(UO_2)_5O_6(OH)_2(H_2O)_4$	
Curite	$Pb_3(UO_2)_8O_8(OH)_6(H_2O)_2$	
Masuyite	$Pb[(UO_2)_3O_3(OH)_2](H_2O)_3$ also 4PbO·9UO_3·12H_2O and 3PbO·8UO_3·10H_2O	"grooved masuyite" "type masuyite" and a synthetic analogue
Fourmarierite	$Pb(UO_2)_4O_3(OH)_4(H_2O)_4$	
Richetite	$M_xPb_{8.57}[(UO_2)_{18}O_{18}(OH)_{12}]_2(H_2O)_{41}$	
Vandendriesscheite	$Pb_{1.57}(UO_2)_{10}O_6(OH)_{11}(H_2O)_{11}$	
Meta-vandendriesscheite	PbO·7UO_3·(12-x)H_2O	uncertain formula
Calciouranoite	(Ca,Ba,Pb,K,Na)O·UO_3·5H_2O	minor Pb
Meta-calciouranoite	(Ca,Ba,Pb,K,Na)O·UO_3·2H_2O	minor Pb
Kasolite	$Pb(UO_2)(SiO_4)(H_2O)$	
"Pilbarite"	PbO·ThO_2·UO_3·2SiO_2·4H_2O (?)	doubtul species
Widenmannite	$Pb_2(UO_2)(CO_3)_3$	
Demesmaekerite	$Cu_5Pb_2(UO_2)_2(SeO_3)_6(OH)_6(H_2O)_2$	
Parsonsite	$Pb_2(UO_2)(PO_4)_2(H_2O)_2$	
Dewindtite	$Pb_3[(UO_2)_3O(OH)(PO_4)_2]_2(H_2O)_{12}$	
Dumontite	$Pb_2[(UO_2)_3O_2(PO_4)_2](H_2O)_5$	
Przhevaskite	$Pb[(UO_2)(PO_4)]_2(H_2O)_2$	
"Renardite"	$Pb[(UO_2)_4(OH)_4(PO_4)_2](H_2O)_7$	mixture
Kamitugaite	$PbAl(UO_2)_5([P,As]O_4)_2(OH)_9(H_2O)_{9.5}$	
Hügelite	$Pb_2[(UO_2)_3O_2(AsO_4)_2](H_2O)_5$	
Hallimondite	$Pb(UO_2)(AsO_4)_2$	
Asselbornite	$(Pb,Ba)(BiO)_4(UO_2)_6(AsO_4)_2(OH)_{12}(H_2O)_3$	zoned: Pb-rich cores
"Kivuite"	$(Th,Ca,Pb)(UO_2)_4(HPO_4)_2(OH)_8(H_2O)_7$	uncertain species
Curiénite	$Pb(UO_2)_2(V_2O_8)(H_2O)_5$	
Francevillite	$(Ba,Pb)(UO_2)_2(V_2O_8)(H_2O)_5$	minor Pb
Moctezumite	$Pb(UO_2)(TeO_3)_2$	
Uranotungstite	$(Ba,Pb,Fe^{2+})(UO_2)_2(WO_4)(OH)_4(H_2O)_{12}$	minor Pb

(Fig. 11). Schoepite and metaschoepite may contain epitaxial intergrowths of fourmarierite or vandendriesscheite that are evident in X-ray precession photographs of schoepite and metaschoepite single crystals, which could be misinterpreted as being representative of the host mineral, and may explain conflicting unit-cell data for minerals such as paraschoepite, masuyite and vandendriesscheite (Christ and Clark 1960). Confusion about compositions

of Pb-bearing minerals such as calciouranoite and bauranoite (Belova et al. 1993), clarkeite (Finch and Ewing 1997), renardite (Deliens et al. 1990) and masuyite (Deliens and Piret 1996) may also reflect continuous recrystallization of Pb-rich minerals from Pb-poor minerals at a fine scale. Recent detailed analyses (Deliens et al. 1990; Deliens and Piret 1996) and single-crystal structure determinations (Burns 1997, 1998a, 1999e; Burns and Hanchar 1999) have greatly improved our understanding of the structural and paragenetic relationships among Pb-uranyl oxyhydroxides, although many questions still remain.

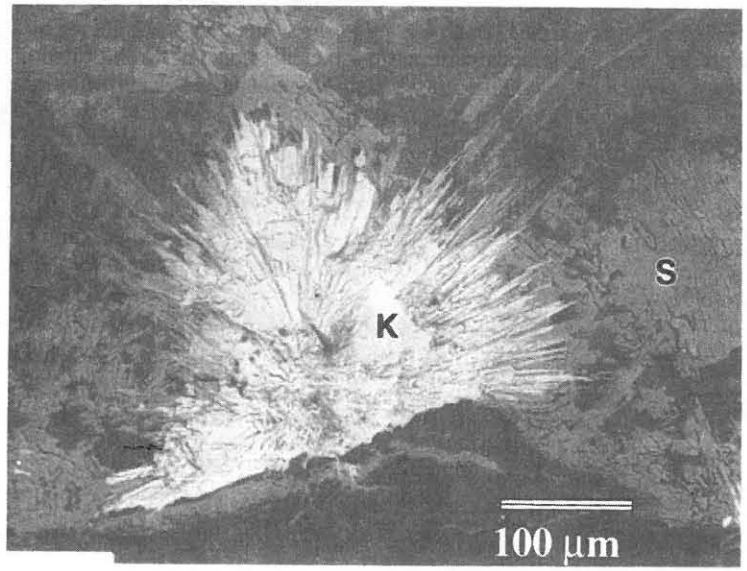

Figure 10. BSE image of acicular kasolite crystals (K) at the margin of a sklodowskite (S) vein in a sample from Koongarra. Kasolite replaces the sklodowskite. Width of vein is approximately 2 mm. (from Isobe et al. 1992; reprinted by permission of North-Holland, Elsevier).

Another factor in the development of the complex (and often confusing) mineralogy of Pb-uranyl minerals is alteration by groundwater. Due to the different mobilities of Pb and U in most groundwaters, Pb-bearing uranyl minerals tend to dissolve incongruently. This is especially notable during alteration of Pb-uranyl oxyhydroxides.

Frondel (1956) first explained the enrichment of Pb in corrosion rinds by the preferential loss of U to groundwater. Vandendriesscheite and fourmarierite are commonly the earliest Pb-uranyl oxyhydroxides to precipitate when Pb-bearing uraninite corrodes, forming more Pb-enriched minerals as they interact with Si- and carbonate-bearing groundwaters (Frondel 1956; Deliens 1977a; Finch and Ewing 1992a,b; Finch 1994). Preferential removal of U increases the residual Pb content within the dissolving vandendriesscheite, and polycrystalline masuyite, sayrite and curite may precipitate as inclusions within vandendriesscheite crystals (Finch and Ewing 1992a,b; Finch 1994). Inclusions of masuyite are common where vandendriesscheite is replaced by uranyl silicates (Fig. 12). Cryptocrystalline corrosion rinds that are veined by uranophane also show increased Pb concentrations adjacent to uranophane veins (Fig. 13); Ca from becquerelite and U from becquerelite and vandendriesscheite are incorporated into uranophane, whereas Pb is not. Because Pb is not removed by groundwater, it accumulates adjacent to uranyl-silicate veins as fine-grained Pb-enriched uranyl oxyhydroxides. Thus,

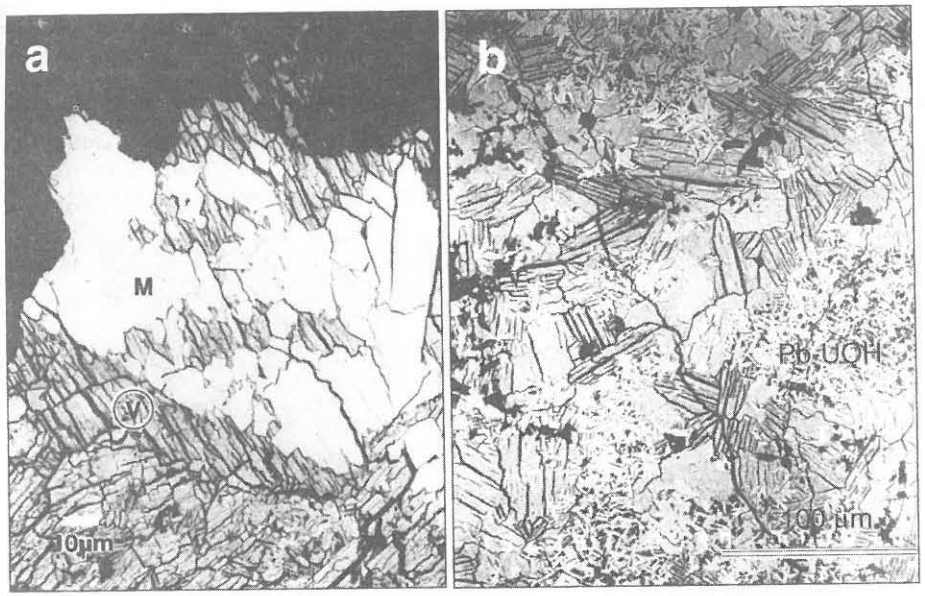

Figure 11. (a) BSE image of a polished section through an altered vandendriesscheite grain showing polycrystalline masuyite inclusion within optically continuous vandendriesscheite. The vandendriesscheite has partially dissolved and been replaced by rutherfordine (black); masuyite has also dissolved at the upper left of the image (from Finch 1994). (b) BSE image of polycrystalline becquerelite with 1-10 μm inclusions of an undetermined Pb-uranyl oxyhydroxide.

the precipitation of Pb-rich uranyl oxyhydroxides does not necessarily require high concentration of dissolved Pb.

Lead is not incorporated into rutherfordine, soddyite or uranophane, minerals that commonly replace early-formed Pb uranyl oxyhydroxides. The only known Pb-uranyl silicate, kasolite, has a Pb:U ratio (1:1), higher than that of any of the Pb-uranyl oxyhydroxides. The same is true for the uranyl carbonate widenmannite (Pb:U = 2:1). Rather than being associated with the alteration of vandendriesscheite, kasolite commonly occurs within fractures inherited from precursor uraninite (Isobe et al. 1992; Finch 1994) where Pb is derived from dissolving galena, or kasolite crystallizes from nominally Pb-free uranyl silicates that have accumulated radiognic Pb (Isobe et al. 1992). Kasolite commonly coexists with curite, a late-stage weathering product of uraninite.

The incongruent dissolution of vandendriesscheite to masuyite by carbonate groundwaters releases some U to groundwater but retains some in the residual solid (Finch and Ewing 1992a,b):

$$Pb_{1.5}(UO_2)_{10}O_6(OH)_{11}(H_2O)_{11(cr)} + 11\,HCO_3^-{}_{(aq)} \Rightarrow$$
$$1.5\,Pb[(UO_2)_3O_3(OH)_2](H_2O)_{3(cr)} + 5.5\,UO_2(CO_3)_2^{2-} + 16.5\,H_2O$$

The replacement of Pb-uranyl oxyhydroxides by uranyl silicates is common (Finch and Ewing 1992a,b). In the presence of sufficient dissolved silica and Ca^{2+}, vandendriesscheite alters incongruously to masuyite plus uranophane (Finch and Ewing 1992a):

$$\text{vandendriesscheite} + Ca^{2+} + H_4SiO_{4\,(aq)} \Rightarrow \text{uranophane} + \text{masuyite} + 4\,H^+ + H_2O$$

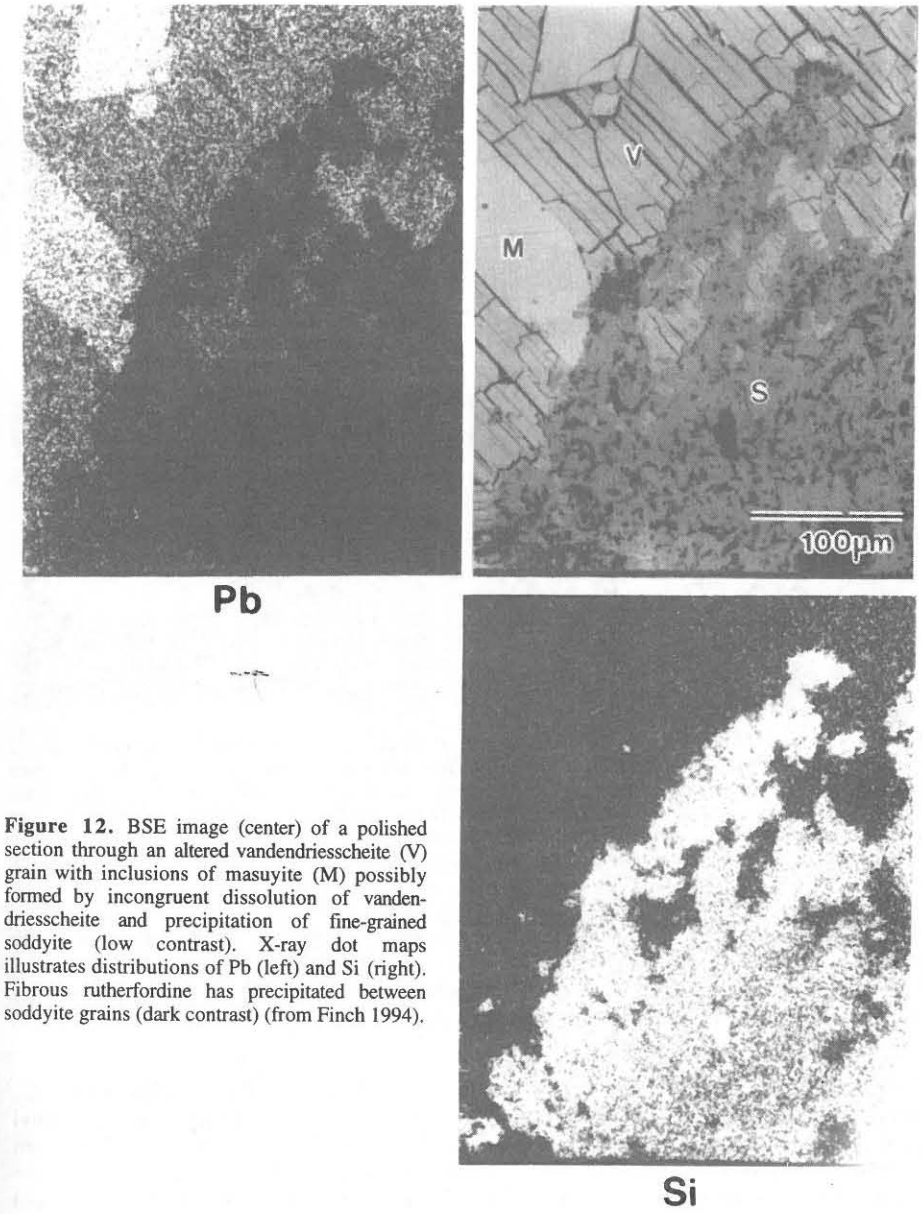

Figure 12. BSE image (center) of a polished section through an altered vandendriesscheite (V) grain with inclusions of masuyite (M) possibly formed by incongruent dissolution of vandendriesscheite and precipitation of fine-grained soddyite (low contrast). X-ray dot maps illustrates distributions of Pb (left) and Si (right). Fibrous rutherfordine has precipitated between soddyite grains (dark contrast) (from Finch 1994).

Or, without sufficient dissolved Ca, soddyite precipitates (Fig. 12):

$$\text{vandendriesscheite} + H_4SiO_{4_{(aq)}} \Rightarrow \text{soddyite} + \text{masuyite} + H_2O$$

These reactions are written with U retained in the solids, which, given the relative insolubility of uranyl silicates (Langmuir 1978; Grenthe et al. 1992), is a reasonable simplification (Both reactions are illustrative and not strictly balanced.). These three reactions demonstrate how Pb helps reduce the mobility of U during the interaction of

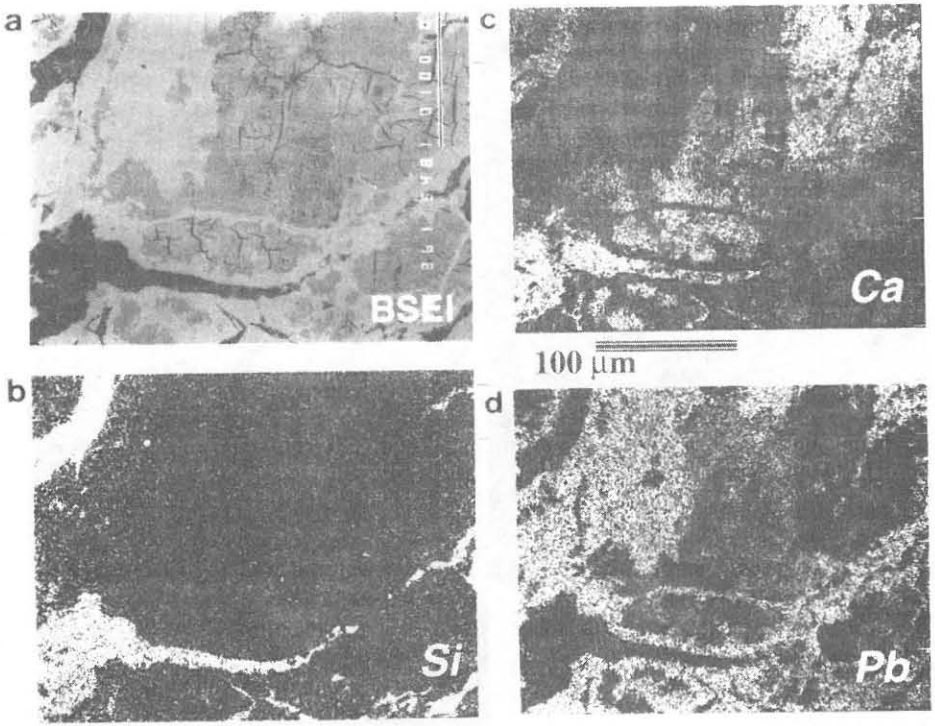

Figure 13. (a) BSE image of a polished section through an altered region of a fine-grained uraninite corrosion rind showing Pb enrichment and Ca depletion associated with alteration by Si-bearing groundwater. Becquerelite dissolves during alteration, with Ca and U incorporated into uranophane. Central area of BSE image (a) (dark gray contrast) is intermixed vandendriesscheite and becquerelite. Darkest contrast veins contain uranophane. Regions of brightest contrast correspond to Pb-rich regions, probably masuyite or fourmarierite. (b) X-ray dot maps illustrating the distribution of Si, (c) Ca, and (d) Pb. (from Finch 1994).

uranyl oxyhydroxides in carbonate- and Si-bearing groundwaters. The earliest minerals to form tend to have relatively low Pb:U ratios (Frondel 1956, Isobe et al. 1992, Finch and Ewing 1992b, Finch 1994). Continued interaction with groundwater forms increasingly enriched Pb-bearing minerals, such as curite or wölsendorfite (Isobe et al. 1992, Finch and Ewing 1992a,b, Finch 1994) (Fig. 14).

Curite is commonly one of the last remaining minerals after the complete oxidation, dissolution and replacement of uraninite (Isobe et al. 1992; Finch 1994). Uranyl phosphates and curite are so commonly associated that a genetic relationship has long been supposed (Frondel 1956; Frondel 1958; Deliens 1977b). The direct replacement of curite by uranyl phosphates has been observed at the Shinkolobwe mine (Fig. 15), and Finch and Ewing (1992b) proposed that curite may serve as a "substrate" for the nucleation of certain phosphates, similar to the role of Fe and Mn oxyhydroxides (Murakami et al. 1997; see below), except that curite contains abundant U required for uranyl phosphate formation.

PARAGENESIS OF THE URANYL PHOSPHATES

Uranyl phosphates help control U concentrations in many natural waters. They generally have solubilities below those of the uranyl silicates and are associated with a wide

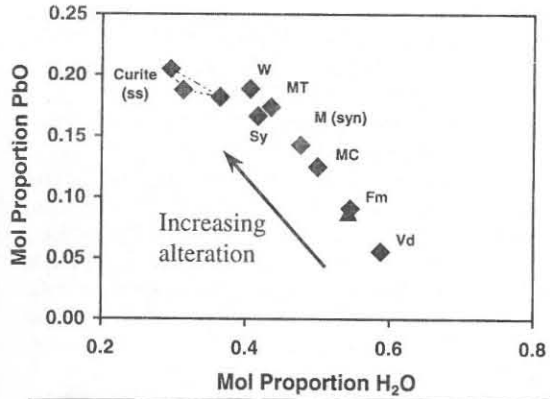

Figure 14. Compositional diagram (as for Fig. 3) illustrating the reaction pathway for increasing alteration of Pb uranyl oxyhydroxides (from Finch and Ewing 1992b).

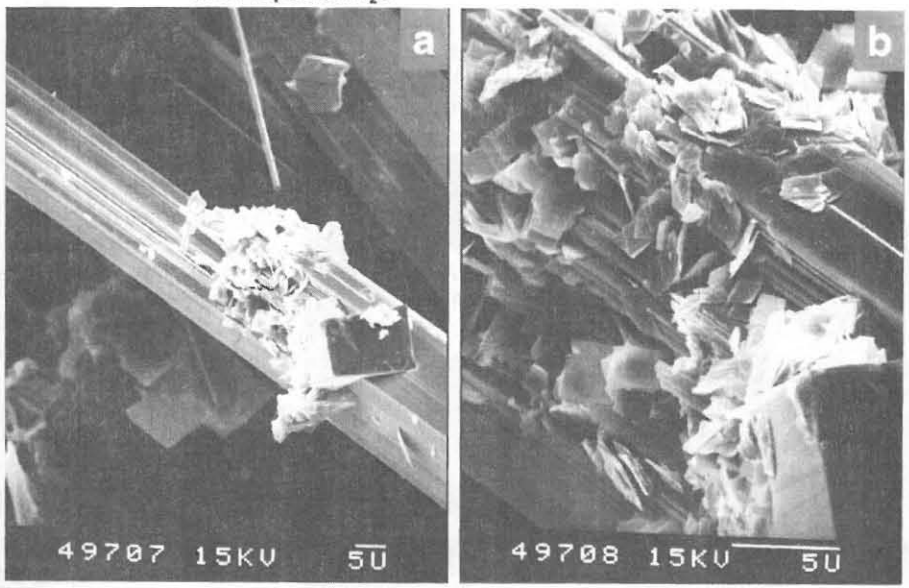

Figure 15. SEM images of curite crystal partly replaced by an unidentified uranyl phosphate, possibly chernikovite. (b) Magnified view of (a) (from Finch 1994).

range of weathered U deposits. Uranyl phosphates are known to precipitate from groundwater with U concentrations in the range 10^{-8} to 10^{-9} mol/kg (Dall'aglio et al. 1974), values that approach the solubility of uraninite in some reducing environments. Uranyl phosphates may occur well removed from any U source (Weeks and Thompson 1954; Frondel 1956). In groundwaters where $\log\{[PO_4^{3-}]_T/[CO_3^{2-}]_T\} > -3.5$, uranyl phosphate complexes predominate over uranyl carbonate complexes (Sandino and Bruno 1992). Apatite controls the phosphate concentrations in many natural waters, keeping phosphate activities below 10^{-7} mol/kg^{-1} above pH = 7 (Stumm and Morgan 1981), but synthesis experiments show that the phosphate concentrations necessary to precipitate uranyl phosphates can be quite high (on the order of 10^{-2} mol/kg) (Markovic and Pavkovic 1983; Sandino 1991). Uranyl phosphates are typically most stable below approximately pH 5, where apatite solubility tends to increase (Stumm and Morgan 1981).

Perhaps one of the most studied occurrences of uranyl phosphates is the Koongarra U

deposit in the Northern Territory, Australia. The alteration of uraninite and the genesis of uranyl phosphates at Koongarra were examined extensively by Snelling (1980, 1992) and Isobe et al. (1992, 1994). A variety of uranyl phosphates has been identified among the Koongarra U minerals, including, saléeite, dewindtite, sabugalite, and torbernite. Saléeite is the predominant uranyl phosphate in the weathered zone at Koongarra. Three mineralogical zones are defined at Koongarra, based on the predominant types of U minerals that occur within them: U oxide zone, uranyl silicate zone, and uranyl phosphate zone (Snelling 1980). Dissolved U is transported roughly from the U oxide zone at depth to the silicate zone, also at depth, then upward to the phosphate zone. The uranyl phosphate zone is in the most oxidized weathered zone near the surface. Macroscopic saléeite crystals can be seen with the unaided eye as yellow-green, platy crystals within millimeter-wide veins, suggesting that saléeite is the thermodynamically stable mineral in contact with the groundwater that flowed through those veins. In addition, microscopic saléeite crystals, tens to hundreds of μm across, commonly replace sklodowskite and apatite (Fig. 16).

Most groundwaters in and around the Koongarra deposit are considered undersaturated with respect to saléeite (Payne et al. 1992, Murakami et al. 1997). Autunite, the Ca analogue of saléeite, is absent even on the surfaces of dissolving uranophane and apatite crystals, both of which should supply abundant Ca to solution. The solubility

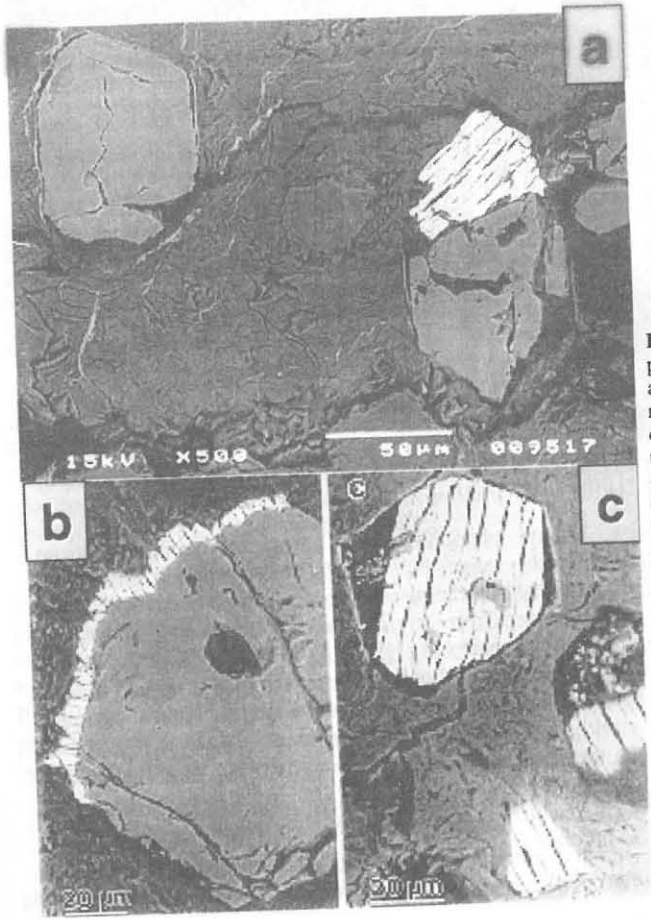

Figure 16. BSE images of polished sections showing (a) apatite crystal on right partly replaced by saléeite (brightest contrast); (b) incipient saléeite on the surface of an apatite crystal; (c) saléeite pseudomorph after apatite with remnant apatite inclusions (gray) (from Murakami et al. 1996a; Murakami et al. 1997).

constant for autunite, log K_{so} = -19.43 (Grenthe et al. 1992), is greater than that of saléeite, log K_{so} = -22.3 (Magelhaes et al. 1985) (both for 25°C), and Murakami et al. (1997) showed from thermodynamic calculations that saléeite should precipitate instead of autunite even at apatite surfaces. Their calculations, combined with observed textural relationships between saléeite and sklodowskite and between saléeite and apatite (Fig. 16), indicate that microscopic saléeite crystals precipitate directly on the surfaces of sklodowskite and apatite due to local saturation, with Mg, U and P derived from dissolving sklodowskite and apatite in addition to the availability of those elements in groundwater. The two types of saléeite occurrences (vein-filling and surface-controlled precipitation) strongly suggest that uranyl phosphate formation at Koongarra not only reflects macroscopic thermodynamic equilibrium with percolating groundwaters, but is also influenced by kinetic factors. This is probably true for uranyl phosphate precipitation in many natural environments, helping to explain the existence of uranyl phosphates in groundwaters with especially low U concentrations (Dall'aglio et al. 1974).

Phosphate is a ubiquitous anion in near-surface environments. Dissolved phosphate concentrations in most river waters are on the order of 20 ppb, and dissolved U concentrations are typically less than 0.3 ppb (Holland 1978), suggesting that most rivers are well below saturation with respect to uranyl phosphates. Sorption of U onto Fe and Mn oxyhydroxides and clay minerals is an important mechanism influencing U migration in natural waters (e.g. Guthrie 1989; Ivanovich et al. 1994; McKinley et al. 1995; Buck et al. 1996, 1999). Groundwater concentrations of Si may also influence U adsorption if dissolved Si competes with U for surface sites on goethite, as demonstrated experimentally by Gabriel et al. (1998). The chemical forms of U adsorbed on various minerals have been examined by several authors. For example, Waite et al. (1994) modeled the adsorption of U as mononuclear uranyl complexes on ferrihydrite surfaces, and extended X-ray-absorption fine-structure spectroscopy (EXAFS) shows that U may be sorbed either as outer-sphere uranyl complexes on smectite (Dent et al. 1992) or as inner-sphere complexes, which may influence subsequent reduction of U (Giblin 1982; Giaquinta et al. 1997). Glinka et al. (1997) found that U is sorbed weakly onto colloidal silica as outer-sphere complexes. Uranium sorption on Fe and Mn oxyhydroxides has long been known to be an important process. A combined experimental and modeling study by Bruno et al. (1995) suggested that U may co-precipitate on Fe(III) oxyhydroxides surfaces as schoepite or "dehydrated schoepite." Murakami et al. (1997) examined a sample from Koongarra by high-resolution transmission electron microscopy (HRTEM) and found microcrystals of saléeite, 10-50 nm across, within a microvein of goethite or hematite a few μm wide. The sample was from a region where the groundwater is far below saturation with respect to saléeite (Mg = 13 ppm, P < 5 ppb, U = 30 ppb). Murakami et al. (1997) explained the crystallization of saléeite microcrystals ("microcrystallization") as follows. Ferrihydrite is formed early during weathering of ferrous minerals (Murakami et al. 1996b). Dissolved P from groundwater is incorporated onto or into ferrihydrite by adsorption, co-precipitation, or both. Phosphorous in ferrihydrite is then released during the transformation of ferrihydrite to goethite and hematite (Ostwald ripening). This localized source of P and locally available U (which can strongly sorb onto fine-grained ferric oxyhydroxides) permits precipitation of saléeite microcrystals directly on the surfaces of goethite and hematite. Buck et al. (1996) identified microcrystals of meta-autunite in U-contaminated soils at Fernald, Ohio, USA, and Sato et al. (1997) reported microcrystals of torbernite on Fe-oxyhydroxide nodules at Koongarra. Microcrystallization is therefore a potentially important mechanism by which U can be immobilized in natural environments for long periods.

ACKNOWLEDGMENTS

We are grateful to Peter Burns for substantial help editing the manuscript and for many informative discussions about U mineralogy. We thank Christopher Cahill, Jennifer Jackson, and Sarah Scott for critically reading the manuscript in record time. Helpful comments and suggestions about Ta-Nb-Ti oxides were provided by Reto Gieré, who also generously provided data on zirconolites. TM is grateful to Toshihiko Ohnuki, Hiroshi Isobe, and Tsutomu Sato for many discussions about U mineralogy and geochemistry. Leslie Finch helped with typing references and several sections. Much of the content here derives from our long and fruitful collaborations with Rodney Ewing, whose guidance, encouragement, and insight provided the seeds from which this chapter grew. Finally, and perhaps most importantly, we thank our wives, Leslie and Emiko, whose support and patience were invaluable to achieving this end. Financial support for this work was provided to RJF by the U.S. Department of Energy, Environmental Management and Sciences Program (DE-FG07-97ER14820), and to TM by the Ministry of Education, Science and Culture [Japan] (11440160).

REFERENCES

Alberman KB, Blakely RC, Anderson JS 1951 The oxides of uranium—Part II, Binary system UO_2-CaO. J Chem Soc 1951:1352-1356

Allen GC 1985 An angle-resolved X-ray photoelectron spectroscopic study of air oxidized UO_2 pellet surfaces. Phil Mag B51:465-473

Allen GC, Tempest PA 1982 Linear ordering of oxygen clusters in hyperstoichiometric uranium dioxide. J Chem Soc, Dalton Trans 1982:2169-2173

Allen GC, Tucker PM, Tyler JW 1982 Oxidation of uranium dioxide at 298 K studied by using X-ray photoelectron spectroscopy. J Phys Chem 86:224-228

Allen GC, Tempest PA, Tyler JW 1987 Oxidation of polycrystalline UO_2 studied by using X-ray photoelectron spectroscopy. J Chem Soc, Faraday Trans 1 83:925-935

Alwan AK, Williams PA 1980) The aqueous chemistry of uranium minerals. Part 2. Minerals of the liebigite group. Mineral Mag 43:665-667

Anderson JS 1953 Recent work on the chemistry of uranium oxides. Bull Soc Chim France. 1953:781-788

Anderson JS, Edgington DN, Roberts LEJ, Wait E 1954 Oxides of uranium. IV. System UO_2-ThO_2-O. J Chem Soc (London) 3:3324-3331

Ansell VE, Chao GY 1987 Thornasite, a new hydrous sodium thorium silicate from Mount St-Hillaire, Quebec. Can Mineral 25:181-183

Atkin D, Basham I, Bowles JFW 1983 Tristramite, a new calcium uranium phosphate of the ekanite group. Mineral Mag 47:393-396

Atencio D 1988 Chernikovite, a new mineral name for $(H_3O)_2(UO_2)_2(PO_4)_2{\cdot}6H_2O$ superceding "hydrogen autunite." Mineral Rec 19:249-252

Atencio D, Newman R, Silva AJGC, Mascarenhas YP 1991) Phurcalite from Perus, São Paulo, Brazil, and redetermination of its crystal structure. Can Mineral 29:95-105

Aurisicchio C, Orlandi P, Pasero M, Perchiazzi N 1993 Uranopolycrase, the uranium-dominant analogue of polycrase-(Y), a new mineral from Elba Island, Italy, and its crystal structure. Eur J Mineral 5:1161-1165

Bachet B, Brassey C, Cousson A 1991) Structure of $Mg[(UO_2)(AsO_4)]_2{\cdot}4H_2O$. Acta Crystalogr C47:2013-2015 (in French)

Bariand P, Bachet B, Brassey C, Medenbach O, Deliens M 1993 Seelite, a new uranium mineral from the Talmessi mine, Iran, and Rabejac, France. Mineral Record 24:463-467

Baturin SV, Sidorenko GA 1985 Crystal structure of weeksite, $(K_{0.62}Na_{0.38})_2(UO_2)_2[Si_5O_{13}]{\cdot}3H_2O$. Doklady Akad Nauk SSSR 282:1132-1136 (in Russian)

Bayliss P, Mazzi F, Munno R, White TJ 1989 Mineral nomenclature: Zirconolite. Mineral Mag 53:565–569

Beddoe-Stephens B, Secher K 1982 Barian wölsendorfite from east Greenland. Mineral Mag 46:130-132

Belbeoch B, Boivineau JC, Perio P 1967 Changements de structure de l'oxyde U_4O_9. J Phys Chem Solids 28:1267

Belova LN, Gorshkov AI, Doinikova OA, Mokhov AV, Trubkin NV, Sivtsov AV 1993 New data on coconinoite. Doklady Akad Nauk 329:772-775

Belova LN, Gorshkov AI, Ivanova, Sivtsov AV 1980 Nature of the so-called phosporous-bearing coffinite. Doklady Akad Nauk SSSR 255:428-430 (English translation in Doklady Earth Sci Sec 255:156-158)

Belova LN, Gorshkov AI, Ivanova, Sivtsov AV, Lizorkina, Boronikhin 1984 Vyacheslavite. Zap Vses Mineral Obshch 113:360 (in Russian)

Belova LN, Ryzhov BI, Federov OV, Lyubomilova GV 1985 Typomorphism and isomorphism of the wölsendorfite group of uranium hydroxides. Izv Akad Nauk SSSR Ser Geol 2:65-72

Berman RM 1957 The role of lead and excess oxygen in uraninite. Am Mineral 42:705-731

Bignand C 1955 Sur les propriétés et les synthèses de quelques minéraux uranifères. Bull Soc fr Minér Crist 78:1-26

Billiet V, de Jong WF 1935 Schoepiet en Becquereliet. Natuur Tijd Ned-Indië 17:157-162

Birch WD, Mumme WG, Segnit ER 1988 Ulrichite-a new copper calcium uranium phosphate from Lake Boga, Victoria, Australia. Australian Mineral 3:125-134

Boatner LA, Sales BC 1988 Monazite. *In* Radioactive Waste Forms for the Future. Lutze W, Ewing RC (Eds) North-Holland, Amsterdam, p 495-564

Bobo JC 1964 Physical and chemical properties in systems between U-O and a metallic element. Rev Chim Minerale 1:3-37

Bowels JFW, Morgan DJ 1984 The composition of rhabdophane. Mineral Mag 48:146-148

Brasseur H 1949) Étude de la billietite. Bull Acad Royale Belg Cl Sci 35:793-804

Bruno J, Casas I, Cera E, Finch RJ, Ewing RC, Werme LO 1995 The assessment of the long-term evolution of the spent nuclear fuel matrix by kinetic, thermodynamic and spectroscopic studies of uranium minerals. Mater Res Soc Symp Proc 353:633-639

Bruno J, Casas I, Puigdoměnech I 1991 The kinetics of dissolution of UO_2 under reducing conditions and the influence of an oxidized surface layer (UO_{2+x}): Application of a continuous flow-through reactor. Geochim Cosmochim Acta 55:647-658

Blanc P-L 1996 Oklo—Natural Analogue for a Radioactive Waste Repository. Vol. 1. Acquirements of the Project. Nuclear Science and Technology Report EUR 16857/1 EN, 123 p

Braithwaite RSW, Paar WH, Chisholm JE 1989 Phurcalite from Dartmoor, Southwest England, and its identity with 'nisaite' from Portugal. Mineral Mag 53:583–589

Brindley GW, Bastanov M 1982 Interaction of uranyl ions with synthetic zeolites of type A and formation of compreignacite-like and becquerelite-like products. Clays Clay Minerals 30:135-142

Brooker EJ Nuffield EW 1952 Studies of radioactive compounds: IV—pitchblende from Lake Athabasca, Canada. Am Mineral 37:363–385

Brugger J, Gieré R, Graeser S, Meisser N 1997 The crystal chemistry of roméite. Contrib Mineral Petrol 127:136-146

Bruno J, Casas I, Cera E, Ewing RC, Finch RJ, Werme LO 1995 The assessment of the long-term evolution of the spent nuclear fuel matrix by kinetic, thermodynamic and spectroscopic studies of uranium minerals. Mater Res Soc Symp Proc 353:633-639

Bruno J, Casas I, Sandino A 1992 Static and dynamic SIMFUEL dissolution studies under oxic conditions. J Nucl Mater 190:61-69

Bruno J, de Pablo J, Duro L, Figeurola E 1995 Experimental study and modeling of the U(VI)-Fe$(OH)_3$ surface precipitation/coprecipitation equilibria. Geochim Cosmochim Acta 59:4113-4123

Buck EC, Bates JK 1999) Microanalysis of colloids and suspended particles from nuclear waste glass alteration, Appl Geochem 14:635-653

Buck EC, Wronkiewicz DJ, Finn PA, Bates JK 1997 A new uranyl oxide hydrates phase derived from spent fuel alteration. J Nucl Mater 249:70-76

Buck EC, Brown NR, Dietz NL 1996 Contaminant uranium phases and leaching at the Fernald site in Ohio. Environ Sci Technol 30:81-88

Buck EC, Finch RJ, Bates JK 1998 Retention of neptunium in uranyl alteration phases formed during spent fuel corrosion. Mater Res Soc Symp Proc 506:83-91

Burns PC 1997 A new uranyl oxide hydrate sheet in vandendriesscheite: Implications for mineral paragenesis and the corrosion of spent nuclear fuel. Am Mineral 82:1176-1186

Burns PC 1998a The structure of richetite, a rare lead uranyl oxide hydrate. Can Mineral 36:187-199

Burns PC 1998b CCD area detectors of X-rays applied to the analysis of mineral structures. Can Mineral 36:847-853

Burns PC 1998c The structure of compreignacite, $K_2[(UO_2)_3O_2(OH)_3]_2(H_2O)_7$. Can Mineral 36:1061-1067
Burns PC 1998d The structure of boltwoodite and implications for the solid-solution with sodium boltwoodite. Can Mineral 36:1069-1075
Burns PC 1999a Cs boltwoodite obtained by ion exchange from single crystals: Implications for radionuclide release in a nuclear repository. J Nucl Mater 265:218-223
Burns PC 1999b A new uranyl silicate sheet in the structure of haiweeite and comparison to other uranyl silicates. Can Mineral (submitted).
Burns PC 1999c A new uranyl phosphate chain in the structure of parsonsite. Am Mineral (submitted).
Burns PC 1999d The crystal chemistry of uranium. *In* Rev Mineral 38 (this volume)
Burns PC 1999e Wölsendorfite: a masterpiece of structural complexity. GAC-MAC Abstracts 24:16
Burns PC 1999f A new uranyl silicate sheet in the structure of haiweeite and comparison to other uranyl silicates. Can Mineral (submitted)
Burns PC, Ewing RC, Miller ML 1997a Incorporation mechanisms of actinide elements into the structures of U^{6+} phases formed during the oxidation of spent nuclear fuel. J Nucl Mater 245:1-9
Burns PC, Finch RJ 1999) Wyartite, crystallographic evidence for the first pentavalent uranium mineral. Am Mineral 84 (in press)
Burns PC, Finch RJ, Hawthorne FC, Miller ML, Ewing RC 1997b The crystal structure of ianthinite, $[U_2^{4+}(UO_2)_4O_6(OH)_4(H_2O)_4](H_2O)_5$: A possible phase for Pu^{4+} incorporation during the oxidation of spent nuclear fuel. J Nucl Mater 249:199-206
Burns PC, Hanchar JM 1999) The structure of masuyite, $Pb[(UO_2)_3O_3(OH)_2](H_2O)_3$. Can Mineral (in press)
Burns PC, Hawthorne FC, Ewing RC 1997c The crystal chemistry of hexavalent uranium: Polyhedral geometries, bond-valence parameters, and polyhedral polymerization. Can Mineral 35:1551-1570
Burns PC, Hill FC 1999a Implications of the synthesis and structure of the Sr analogue of curite. Can Mineral 37 (in press)
Burns PC, Hill FC 1999b A new uranyl sheet in $K_5[(UO_2)_{10}O_8(OH)_9](H_2O)$. Implications for understanding sheet anion-topologies. Can Mineral (submitted)
Burns PC, Miller ML, Ewing RC 1996 U^{6+} minerals and inorganic phases: A comparison and hierarchy of crystal structures. Can Mineral 34:845-880
Burns PC, Olson RA, Finch RJ, Hanchar JM, Thibault Y. 1999) $KNa_3(UO_2)_2(Si_4O_{10})_2(H_2O)_4$, a new compound formed during vapor hydration of an actinide-bearing borosilicate waste glass. J Nucl Mater (submitted)
Cahill CL, Burns PC 1999) The structure of agrinierite: a K-Ca-Sr uranyl oxide hydrate sheet of the alpha-U_3O_8 type. Geol Soc America Annual Meeting, Abstracts
Calos NJ, Kennard CHL 1996 Crystal structure of copper bis(uranyl phosphate) octahydrate (metatorbernite), $Cu(UO_2PO_4)_2{\cdot}8(H_2O)$. Z Zristallogr 211:701-702
Casas I, Bruno J, Cera E, Finch RJ, Ewing RC 1994 Kinetic and thermodynamic studies of uranium minerals. Assessment of the long-term evolution of spent nuclear fuel. SKB Technical Report 94-16, Stockholm, 73 p
Casas I, Bruno J, Cera E, Finch RJ, Ewing RC 1997 Characterization and dissolution kinetics of becquerelite from Shinkolobwe, Zaire. Geochim Cosmochim Acta 61:3879-3884
Casas I, de Pablo J, Giménez J, Torrero ME, Bruno J, Cera E, Finch RJ, Ewing RC 1998 The role of pe, pH, and carbonate on the solubility of UO_2 and uraninite under nominally reducing conditions. Geochim Cosmochim Acta 62:2223-2231
Cejka J 1994 Vandenbrandeite, $CuUO_2(OH)_4$: Thermal analysis and infrared spectrum. N Jb Mineral Mh 1994:112-120
Cejka J, Cejka J, Skála R, Sejkora J, Muck A 1998 New data on curite from Shinkolobwe, Zaire. N Jb Miner Mh 1998:385-402
Cejka J, Mrázek Z, Urbanec Z 1984 New data on sharpite, a calcium uranyl carbonate. N Jb Miner Mh, H3:109-117
Cejka J, Sejkora J, Deliens M 1996a New data on studtite, $UO_4{\cdot}4H_2O$ from Shinkolobwe, Shaba, Zaire. N Jb Miner Mh 3:125-134
Cejka J, Sejkora J, Deliens M 1999 To the infrared spectrum of haynesite, a hydrated uranyl selenite, and its comparison with other uranyl selenites. Neues Jb Miner Mh H6:241-252
Cejka J, Sejkora J, Mrázek Z, Urbanec Z, Jarchovsky T 1996b Jáchymovite, $(UO_2)_8(SO_4)(OH)_{14}{\cdot}13H_2O$, a new uranyl mineral from Jáchymov, the Krusné Hory Mts., Czech Republic, and its comparison with uranopilite. N Jb Mineral Abh 170:155-170
Cejka J, Sejkora J, Skála R, Cejka J, Novotná M, Ederová J 1998 Contribution to the crystal chemistry of synthetic becquerelite, billietite and protasite. N Jb Miner Abh 174:159-180
Cejka J, Urbanec Z 1988 Contribution to the hydrothermal origin of rutherfordine, UO_2CO_3. Casopis Národního Muzea 157:1-10
Cejka J, Urbanec Z 1990 Secondary uranium minerals. Trans Czechoslovak Academy of Sciences, Math Natur History Series 100, Academia, Prague. 93 p

Cejka J, Urbanec Z, Cejka J Jr 1987 Contribution to the crystal chemistry of andersonite. N Jb Mineral Mh 11:488-501
Cesbron F 1970 La roubaultite, $Cu_2(UO_2)_3(CO_3)_2O_2(OH)_2(H_2O)_4$, une nouvelle espèce minérale. Bull Soc fr Minér Crist 93:550-554
Cesbron F, Ildefonse P, Sichere M-C 1993 New mineralogical data on uranophane and β-uranophane; synthesis of uranophane. Mineral Mag 57:301-308
Chakoumakos BC 1984 Systematics of the pyrochlore structure type, ideal $A_2B_2X_6Y$. J Solid State Chem 53:120-129
Chakoumakos BC 1986 Pyrochlore. *In* McGraw-Hill Yearbook of Science and Technology 1987. Parker SP (Ed) McGraw-Hill, New York, p 393-395
Chen C-H 1975 A method of estimation of standard free energies of formation of silicate minerals at 298.15 K. Am J Sci 275:801-817
Chen F, Ewing RC, Clark SB 1999 The Gibbs free energies and enthalpies of formation of U^{6+} phases: An empirical method of prediction. Am Mineral 84:650-664
Chen Z, Luo K, Tan F, Zhang Y, Gu X 1986 Tengchongite, a new mineral of hydrated calcuim uranyl molybdate. Kexue Tongbao 31:396-401
Chen Z, Huang Z, Gu X 1990 A new uranium mineral-Yingjiangite. Acta Mineral Sinica 10:102-105
Chernikov AA, Krutetskaya OV, Sidelnikova VD 1957 Ursilite—a new silicate of uranium. Atomnaya Energ, Voprosy Geol Urana (Suppl) 6:73-77 (English translation *In* The Geology of Uranium. Consultants Bureau, Inc., New York, 1958)
Chernorukov N, Korshunov E, and Voenova L 1985 New uranium compound. Uranium(IV) hydrogen-arsenate tetrahydrate. Radiokhimiya 5:676-679 (in Russian)
Chevalier R, Gasperin M 1970 Crystal structure of UVO_5. Bull Soc fr Minér Crist 93:18-22
Chiappero P-J, Sarp H 1993 New data and the second occurrence of znucalite. Archs Sci Genève 46:291-301 (in French, English abstract)
Christ CL 1965 Phase transformations and crystal chemistry of schoepite. Am Mineral 50:235-239
Christ CL, Clark JR 1960 Crystal chemical studies of some uranyl oxide hydrates. Am Mineral 45:1026-1061
Christ CL, Clark JR, Evans HT Jr 1955 Crystal structure of rutherfordine, UO_2CO_3. Science 121:472-473
Clark DL, Hobart DE, Neu MP 1995 Actinide cabonate complexes and their importance in actinide environmental chemistry. Chem Rev 95:25-48
Clark JR 1960 X-ray study of alteration in the uranium mineral wyartite. Am Mineral 45, 200-208
Contamin P, Backmann JJ, Marin JF 1972 Autodiffusion de l'oxygene dans le 'dioxide d'uranium surstochiometrique. J Nucl Mater 42:54-64
Cooper MA, Hawthorne FC 1995 The crystal structure of guilleminite, a hydrated Ba-U-Se sheet structure. Can Mineral 33:1103-1109
Dall'aglio M, Gragnani R, Locardi E 1974 Geochemical factors controlling the formation of the secondary minerals of uranium. *In* Formation of Uranium Ore Deposits. Int'l Atomic Energy Agency, Vienna, p 33-48
Debets PC 1963 X-ray diffraction data on hydrated uranium peroxide. J Inorg Nucl Chem 25:727-730
Debets PC, Loopstra BO 1963 On the uranates of ammonium—II. X-ray investigation of the compounds in the system NH_3-UO_3-H_2O. J Inorg Nucl Chem 25:945-953
Deliens M 1977a Review of the hydrated oxides of U and Pb, with new X-ray powder data. Mineral Mag 41:51-57
Deliens M 1977b Associations de minéraux secondaires d'uranium à Shinkolobwe (région du Shaba, Zaïre). Bull Soc fr Minér Crist 100:32-38
Deliens M, Piret P 1980 New aluminum and uranyl phosphates from Kobokobo, Kivu, Zaire. Rocks Minerals 55:169-171
Deliens M, Piret P 1981a La swamboite, nouveau silicate d'uranium hydraté du Shaba, Zaïre. Can Mineral 19:553-557
Deliens M, Piret P 1981b Les phosphates d'uranyl et d'aluminum de Kobokobo; V, la mundite, nouveau minéral. Bull Minéral 104:669-671
Deliens M, Piret P 1982a Bijvoetite et lepersonnite, carbonates hydratés d'uranyle et de terres rares de Shinkolobwe, Zaïre. Can Mineral 20:231-238
Deliens M, Piret P 1982b Les phosphates d'uranyl et d'aluminum de Kobokobo; VI, la triangulite, $Al_3(OH)_5[(UO_2)(PO_4)]_4(H_2O)_5$, nouveau minéral. Bull Minér 105:611-614
Deliens M, Piret P 1983a L'oursinite, $(Co_{0.86}Mg_{0.10}Ni_{0.04})O{\cdot}2UO_3{\cdot}2SiO_2{\cdot}6H_2O$, nouveau minéral de Shinkolobwe, Zaïre. Bull Minér 106:305-308
Deliens M, Piret P 1983b Metastudtite, $UO_4{\cdot}2H_2O$, a new mineral from Shinkolobwe, Shaba, Zaire. Am Mineral 68:456-458

Deliens M, Piret P 1984a Kamitugaite, $PbAl(UO_2)_5[(P,As)O_4]_2(OH)_9{\cdot}9.5H_2O$, a new mineral from Kobokobo, Kivu, Zaire. Bull Minéral 107:15-19 (in French)
Deliens M, Piret P 1984b L'urancalcarite, $Ca(UO_2)_3CO_3(OH)_6{\cdot}3H_2O$, nouveau minéral de Shinkolobwe, Zaïre. Bull Minéral 107:21-24
Deliens M, Piret P 1985a Les phosphates d'uranyle et d'aluminium de Kobokobo VII. La moreauite, $Al_3UO_2(PO_4)_3(OH)_2{\cdot}13H_2O$, nouveau minéral. Bull Minéral 108:9-13
Deliens M, Piret P 1985b Les phosphates d'uranyl et d'aluminium de Kobokobo. VIII. La furongite. Ann Soc Geol Gelg 108:365-368
Deliens M, Piret P 1990a La shabaite-(Nd), $CaREE_2(UO_2)(CO_3)_4(OH)_6{\cdot}6H_2O$, nouveau espèce minérale de Kamoto, Shaba, Zaïre. Eur J Mineral 1:85-88
Deliens M, Piret P 1990b L'astrocyanite-(Ce), $Cu_2(TR)_2(UO_2)(CO_3)_5(OH)_2{\cdot}1.5H_2O$, nouvelle espèce minérale de Kamoto, Shaba, Zaïre. Eur J Mineral 2:407-411
Deliens M, Piret P 1991 La haynesite, sélénite hydraté d'uranyl, nouvelle espèce minérale de la mine Repete, comté de San Juan, Utah. Can Mineral 29:561-564
Deliens M, Piret P 1992 La fontanite, carbonate hydraté d'uranyle et de calcium, nouvelle espèce minérale de Rabejac, Hérault, France. Eur J Mineral 4:1271-1274.
Deliens M, Piret P 1993 Rabejacite, $Ca(UO_2)_4(SO_4)_2(OH)_6{\cdot}6H_2O$, a new uranyl and calcium sulfate from Lodève, Hérault, France. Eur J Mineral 5:873-877
Deliens M, Piret P 1996 Les masuyites de Shinkolobwe (Shaba, Zaïre) constituent un group formé de deux variétés distinct par leur composition chimique et leuras propriétés radiocristallographiques. Bull Mus Royal Central Africa, Tervuren, Belgium, Sci Terres 66:187-192
Deliens M, Piret P, Comblain G 1981 Les minéraux secondaires du Zaïre. Editions du Musée royal de l'Afrique centrale, Tervuren, Belgium, 113 p
Deliens M, Piret P, Comblain G 1984 Les minéraux secondaires du Zaïre. Complement. Institute Editions du Musée royal de l' Afrique centrale, Tervuren, Belgium, 37 p
Deliens M, Piret P, van der Meersche E 1990 Les minéraux secondaires du Zaïre. Deuxième complement. Editions du Musée royal de l' Afrique centrale, Tervuren, Belgium, 39 p
Demartin F, Diella V, Donzelli S, Gramaccioli CM, Pilati T 1991 The importance of accurate crystal structure determination of uranium minerals. I. Phosphuranylite $KCa(H_3O)_3(UO_2)_7(PO_4)_4O_4{\cdot}8H_2O$. Acta Crystallogr B47:439-446
Demartin F, Diella V, Donzelli S, Gramaccioli CM, Pilati T 1992 The importance of accurate crystal structure determination of uranium minerals. II. Soddyite $(UO_2)_2(SiO_4){\cdot}2H_2O$. Acta Crystallogr C48:1-4
Dent AJ, Ramsay JDF, Swanton SW 1992 An EXAFS study of uranyl ion in solution and sorbed onto silica and montmorillonite clay colloids. J Colloid Interface Sci 150:45-60
Dent Glasser LS, Lachowski EE 1980 Silicate species in solution. Part 1. Experimental Observations. J Chem Soc (London) Dalton Trans 1980:393-398
Diaz Arocas P, Grambow B 1998 Solid-liquid phase equilibria of U(VI) in NaCl solutions. Geochim Cosmochim Acta 62:245-263
Diella V, Mannucci G 1986 A uranium-rich ekanite, $(Th_{0.75},U_{0.21})(Ca_{2.01},Fe_{0.04}Mn_{0.01})Si_{7.99}O_{20}$, from Pitigliano, Italy. Rend Soc Ital Mineral Petrol 41:3-6
Dickens PG, Stuttard GP, Ball RGJ, Powell AV, Hull S, Patat S 1992 Powder neutron-diffraction study of the mixed uranium vanadium oxides, $Cs_2(UO_2)_2(V_2O_8$ and UVO_5. J Mater Chem 2(2):161-166
Douglass RM 1956 Tetrasodium uranyl tricarbonate, $Na_4(UO_2)(CO_3)_3$. Anal Chem 28:1635
Dubessy J, Pagel M, Beny JM, Christensen, H, Hickel B, Kosztolanyi C, Poty B 1988 Radiolysis evidenced by H_2-O_2 and H_2-bearing fluid inclusions in three uranium deposits. Geochim Cosmochim Acta 52:1155-1167
D'yachenko OGD, Taachenko VV, Tali R, Kovba LM, Marinder B-O, Sudberg M 1996 Structure of $UMoO_5$ studied by single-crystal X-ray diffraction and high-resolution transmission miocroscopy. Acta Crystallogr B52:961-965
Einziger RE, Thomas LE, Buchanan HC, Stout RB 1992 Oxidation of spent fuel in air at 175 to 195°C. J Nucl Mater 190:53-60
Elton NJ, Hooper, JJ 1992 Andersonite and schröckingerite from Geevor mine, Cornwall: two species new to Britain. Mineral Mag 56:124-125
Elton NJ, Hooper JJ 1995 Supergene U-Pb-Cu mineralization at Loe Warren, St Just, Cornwall, England. J Russel Soc 6:17-26
Evans HT Jr 1963 Uranyl ion coordination. Science 141:154-158.
Ewing RC 1975 Alteration of metamict, rare earth, AB_2O_6-type Nb-Ta-Ti oxides. Geochim Cosmochim Acta 39:521-530
Ewing RC 1993 The long-term performance of nuclear waste forms: natural materials—three case studies. Mater Res Soc Symp Proc 294:559-568
Fareeduddin JAS 1990 Significance of the occurrence of detrital pyrite and uraninite on the Kalasapura

conglomerate, Karnataka. Indian Minerals 44:335-340
Fayek M, Janeczek J, Ewing RC 1997 Mineral chemistry and oxygen isotopic analyses of uraninite, pitchblende and uranium alteration minerals from the Cigar Lake deposit, Saskatchewan, Canada. Appl Geochem 12:549-565
Fayek M, Kyser TK 1997 Characterization of multiple fluid-flow events and rare-earth-element mobility associated with formation of unconformity-type uranium deposits in the Athabasca basin, Saskatchewan. Can Mineral 35:627-658
Finch RJ 1994 Paragenesis and crystal chemistry of the uranyl oxide hydrates. Ph.D. Thesis, University of New Mexico, 257 p
Finch RJ 1997a Thermodynamic stabilities of U(VI) minerals: Estimated and observed relationships. Mater Res Soc Symp Proc 465:1185-1192
Finch RJ 1997b The role of H_2O in minerals containing the uranyl ion. Eos 78:S328
Finch RJ, Cooper MA, Hawthorne FC, Ewing RC 1996 The crystal structure of schoepite, $[(UO_2)_8O_2(OH)_{12}](H_2O)_{12}$. Can Mineral 34:1071-1088
Finch RJ, Cooper MA, Hawthorne FC, Ewing RC 1999a Refinement of the crystal structure of rutherfordine. Can Mineral 37 (in press)
Finch RJ, Ewing RC 1991 Uraninite alteration in an oxidizing environment and its relevance to the disposal of spent nuclear fuel. SKB Technical Report 91-15, SKB, Stockholm, 107 p
Finch RJ, Ewing RC, 1992a Alteration of uranyl oxide hydrates in Si-rich groundwaters: Implications for uranium solubility. Mater Res Soc Symp Proc 257:465-472
Finch RJ, Ewing RC 1992b The corrosion of uraninite under oxidizing conditions. J Nucl Mater 190:133-156
Finch RJ, Ewing RC 1994 Formation, oxidation and alteration of ianthinite. Mater Res Soc Symp Proc 333:625-630
Finch RJ, Ewing RC 1995 Estimating the Gibbs free energies of some uranium(VI) minerals: calculated and observed mineral relationships. Joint Ann Meeting Geol Assoc Canada, Mineral Assoc Canada, Victoria BC, Canada, May, 1995, Abstracts Vol 20
Finch RJ, Ewing RC 1997 Clarkeite: New chemical and structural data. Am Mineral 82:607-619
Finch RJ, Finn PA, Buck EC, Bates JK 1999b Oxidative corrosion of spent UO_2 fuel in vapor and dripping groundwater at 90°C. Mater Res Soc Symp Proc 556 (in press)
Finch RJ, Hanchar JM, Hoskin PWO, Burns PC 1999c Rare-earth elements in zircon. 2. Single crystal X-ray study of xenotime substitution. Am Mineral (submitted)
Finch RJ, Hawthorne FC, Ewing RC 1998 Crystallographic relations among schoepite, metaschoepite and dehydrated schoepite. Can Mineral 36:831-845
Finch RJ, Hawthorne FC, Miller ML, Ewing RC 1997 Distinguishing among schoepite, $[(UO_2)_8O_2(OH)_{12}](H_2O)_{12}$, and related minerals by X-ray powder diffraction. Powder Diff 12:230-238
Finch RJ, Miller ML, Ewing RC 1992 Weathering of natural uranyl oxide hydrates: schoepite polytypes and dehydration effects. Radiochim Acta 58/59:433-443
Finch RJ, Suksi J, Rasilainen K, Ewing RC 1995 The long-term stability of becquerelite. Mater Res Soc Symp Proc 353:647-652
Finch RJ, Suksi J, Rasilainen K, Ewing RC 1996 Uranium series ages of secondary uranium minerals with applications to the long-term storage of spent nuclear fuel. Mater Res Soc Symp Proc 412:823-830
Finch WI 1996 Uranium Provinces of North Amrerica—Their definition, Distribution, and Models. U S Geol Surv Bull 2141, 18 p
Finn PA, Finch RJ, Buck EC, Bates JK 1998 Corrosion mechanisms of spent fuel under oxidizing conditions. Mater Res Soc Symp Proc 506:123-131
Finn PA, Hoh JC, Wolf SF, Surchik MT, Buck EC, Bates JK 1997 Spent fuel reaction: The behavior of the ε-phase over 3.1 years. Mater Res Soc Symp Proc 465:527-534
Foord EE, Korzeb SL, Lichte FE, Fitpatrick JJ 1997 Additional studies on mixed uranyl oxide-hydroxide hydrate alteration products of uraninite from Palermo and Ruggles granitic pegmatities, Grafton County, New Hampshire. Can Mineral 35:145-151
Förster H-J 1998a The chemical composition of REE-Y-Th-U-rich accessory minerals in peraluminous granites of the Erzgebirge-Fichtelgebirge region, Germany. Part I: The monazite-(Ce)-brabantite solid solution series. Am Mineral 83:259-272
Förster H-J 1998b The chemical composition of REE-Y-Th-U-rich accessory minerals in peraluminous granites of the Erzgebirge-Fichtelgebirge region, Germany. Part II: Xenotime. Am Mineral 83:1302-1315
Förster, H-J 1999 The chemical composition of uraninite in Variscan granites of the Erzgebirge, Germany. Mineral Mag 63:239-252
Forsyth RS, Werme LO 1992 Spent fuel corrosion and dissolution. J Nucl Mater 190:3-19
Frondel C 1956 The mineralogical composition of gummite. Am Mineral 41:539-568

Frondel C 1958 Systematic Mineralogy of Uranium and Thorium. US Geol Surv Bull 1064, 400 p
Frondel C, Ito J, Honca RM, Weeks AM 1976 Mineralogy of the zippeite group. Can Mineral 14:429-436
Frondel C, Meyrowitz R 1956 Studies of uranium minerals (XIX) rutherfordine, diderichite and clarkeite. Am Mineral 41:127-133
Gabriel U, Gaudet J-P, Spadini L, Charlet L 1998 Reactive transport of uranyl in a goethite column: an experimental and modelling study. Chem Geol 151:107-128
Gaines RV, Skinner HCW, Foord EE, Mason B, Rosenzweig A, King VT, Dowty E 1997 Dana's New Mineralogy. 8th Edition. Wiley & Sons, New York, 1819 p
Gaines RV 1965 Moctezumite, a new lead uranyl tellurate. Am Mineral 50:1158-1163
Garrels RM, Christ CL 1959 Behavior of uranium minerals during oxidation. *In* Geochemistry and Mineralogy of the Colorado Plateau Uranium Ores. Garrels RM, Larsen ES (Eds) US Geol Surv Prof Paper 320:81-89
Gasperin M 1960 Contribution à l'étude de quelques oxydes doubles que forme le tantale avec l'uranium et la calcium. Bull Soc fr Minéral Cristallogr 83:1-21
Gauthier JP, Fumey P 1988 Un gemme metamict; l'ekanite. Rev Gemmol Assoc France Gemmol 94:3-7
Giaquinta DM, Soderholm L, Yuchs SE, Waserman SR 1997 The speciation of uranium in a smectite clay: evidence for catalysed uranyl reduction. Radiochim Acta 76:113-121
Giblin AM 1982 The role of clay adsorption in genesis of uranium ores. *In* Uranium in the Pine Creek Geosyncline. Ferguson J, Goleby AB (Eds) Int'l Atomic Energy Agency, Vienna, p. 521-529
Giblin AM, Appleyard EC 1987 Uranium mobility in non-oxidizing brines: field and experimental evidence. Appl Geochem 2:285-295
Gieré R, Williams CT, Lumpkin GR 1998 Chemical characteristic of zirconolite. Schweiz mineral petrogr Mitt 78:443-459
Ginderow D 1988 Structure de l'uranophane alpha, $Ca(UO_2)_2(SiO_3OH)_2{\cdot}5H_2O$. Acta Crystallogr C44:421-424
Ginderow D, Cesbron F 1983a Structure de demesmaekerite. Acta Crystallogr C39:824-827
Ginderow D, Cesbron F 1983b Structure de derriksite. Acta Crystallogr C39:1605-1607
Ginderow D, Cesbron F 1985 Structure de la roubaultite, $Cu_2(UO_2)_3(CO_3)_2O_2(OH)_2.4H_2O$. Acta Crystallogr C41:654-657
Glinka YD, Jaroniec M, Rozenbaum VM 1997 Adsorption energy evaluation from luminescence spectra of uranyl ions UO_2^{2+} adsorbed on disperse silica surfaces. J Colloid Interface Sci 194:455-469.
Gong W 1991a A study on high-temperature phase transition of metamict fergusonite group minerals. Acta Mineral Sinica 11:1-8 (in Chinese with English abstract)
Gong W 1991b Chemistry and evolution of fergusonite group minerals, Bayan, Obo, Inner Mongolia. Acta Mineral Sinica 11:200-208 (English translation in: Chinese J Geochem 10:266-276
Graham J, Thornber MR 1974 The crystal chemistry of complex niobium and tantalum oxides. I. Structural classification of MO_2 phases. Am Mineral 59:1026-1039
Grambow B 1989 Spent fuel dissolution and oxidation: an evaluation of literature data. SKB Technical Report 89-13, SKB, Stockholm, 42 p
Grandstaff DE 1976 A kinetic study of the dissolution of uraninite. Econ Geol 71:1493
Gray WJ, Thomas LE, Einziger RE 1993 Effects of air oxidation on the dissolution rate of LWR spent fuel. Mater Res Soc Symp Proc 294:47-54
Grenthe I, Fuger J, Konings RJM, Lemire RJ, Muller AB, Nguyen Trung C, Wanner H 1992 Chemical Thermodynamics. North-Holland, Amsterdam, 656 p
Guesdon A, Raveau B 1998 A new uranium(VI) monophosphate with a layered structure: $Ba_3[UO_2(PO_4)(PO_3(OH))]_2{\cdot}xH_2O$ (x 0.4). Chem Mater 10:3471-3474
Guillemin C, Protas J 1959 Ianthinite et wyartite. Bull Soc fr Minér Crist 82:80-86
Guthrie VA 1989 Fission-track analysis of uranium distribution in granitic rocks. Chem Geol 77:87–103
Hanchar JM, Finch RJ, Watson EB, Hoskin PWO, Cherniak D, Mariano A 1999 Rare-earth elements in zircon. 1. Synthesis and rare-earth element and phosphorous doping. Am Mineral (submitted)
Hansley PL, Fitzpatrick JJ 1989 Compositional and crystallographic data on REE-bearing coffinite from the Grants Uranium region, northwestern New Mexico. Am Mineral 74:263-270
Hanson SL, Simmons WB, Falster AU, Foord EE, Lichte FE 1999 Proposed nomenclature for samarskite-group minerals: New data on ishikawaite and calciosamarskite. Mineral Mag 63:27-36
Hart KP, Lumpkin GR, Gieré R, Williams CT, McGlinn PJ, Payne TE 1996 Naturally-occurring zirconolites analogues for the long-term encapsulation of actinides in Synroc. Radiochim Acta 74:309-312.
Hawthorne FC 1992 The role of OH and H_2O in oxide and oxysalt minerals. Z Kristallogr 201:183-206
Hemingway BS 1982 Thermodynamic properties of selected uranium compounds and aqueous species at 298.15 K and 1 bar and at higher temperatures—Preliminary models for the origin of coffinite deposits. U S Geol Surv Open-file Report 82-619, 89 p

Hikichi Y, Murayama K, Ohsato H, Nomura T 1989 Thermal changes of rare earth phosphate minerals. J Mineral Soc Japan 19:117-126 (Japanese with English abstract)
Hodgeson NA, Le Bas MJ 1992 The geochemistry and cryptic zonation of pyrochlore from San Vincente, Cape Verde Islands. Mineral Mag 56:201-214
Hoekstra HR, Siegel S 1973 The uranium trioxide-water system. J Inorg. Nucl. Chem. 35:761-779
Holland HD 1978 The Chemistry and the Atmosphere and Oceans. Wiley-Interscience, NY, 351 p
Holland HD 1984 The Chemical Evolution of the Atmosphere and Oceans. Princeton Univ Press, Princeton, New Jersey, 582 p
Holland HD 1994 Early Proterozoic atmospheric change. *In* Begtson S (Ed) Early Life on Earth: Nobel Symposium 84, New York. Columbia Univ Press, New York, p 237-380
Hostetler PB, Garrels RM 1962 Transportation and precipitation of uranium and vanadium at low temperatures, with special reference to sandstone-type uranium deposits. Econ Geol 57:137 p
Hunan 230 Laboratory 1976 Furongite—a new uranium mineral found in China. Acta Geologica Sinica 22:203-204 (in Chinese, abstracted in Am Mineral 63:198, 1978)
Isobe H, Murakami T, Ewing RC 1992 Alteration of uranium minerals in the Koongarra deposit, Australia: Unweathered zone. J Nucl Mater 190:174-187
Isobe H, Ewing RC, Murakami T 1994 Formation of secondary uranium minerals in the Koongarra deposit, Australia. Mater Res Soc Symp Proc 333:653-660
Jackson J, Burns PC 1999 The structure of weeksite: a potassium uranyl silicate hydrate. Geol Soc America Annual Meeting. Abstracts
Janeczek J 1991 Composition and origin of coffinite from Jachymov, Czechoslovakia. N Jb Miner Mh 9:385-395
Janeczek J 1999 Natural fission reactors. *In* Rev Mineral 38 (this volume)
Janeczek J, Ewing RC 1991 X-ray powder diffraction study of annealed uraninite. J Nucl Mater 185:66-77
Janeczek J, Ewing RC 1992a Coffinitization—a mechanism for the alteration of UO_2 under reducing conditions. Mater Res Soc Symp Proc 257:497-504
Janeczek J, Ewing RC 1992b Structural formula of uraninite. J Nucl Mater 190:128-132
Janeczek J, Ewing RC 1992c Dissolution and alteration of uraninite under reducing conditions. J Nucl Mater 190:157-173
Janeczek J, Ewing RC 1995 Mechanisms of lead release from uraninite in the natural fission reactors in Gabon. Geochim Cosmochim Acta 59:1917-1931
Janeczek J, Ewing RC 1996 Phosphatian coffinite with rare earth elements and Ce-rich françoisite-(Nd) from sandstone beneath a natural fission reactor at Bangombé, Gabon. Mineral Mag 60:665-669
Janeczek J, Ewing RC, Oversby VM, Werme LO 1996 Uraninite and UO_2 in spent nuclear fuel: a comparison. J Nucl Mater 238:121-130
Janeczek J, Ewing RC, Thomas LE 1993 Oxidation of uraninite: Does tetragonal U_3O_7 occur in nature? J Nucl Mater 207:177-191
Jamtveit B, Dahlgren S, Austrheim H 1997 High-grade metamorphism of calcareous rocks from the Oslo Rift, southern Norway. Am Mineral 82:1241-1254
Jensen KA, Ewing RC, Gauthier-Lafaye F 1997 Uraninite: A 2 Ga spent nuclear fuel from the natural fission reactor at Bangombé in Gabon, West Africa. Mater Res Soc Symp Proc 465:1209-1218
Johnsen O, Stahl K, Petersen OV, Micheelsen HI 1999 Structure refinement of natural non-metamict polycrase-(Y) from Zomba-Malosa complex, Malawi. N Jb Mineral Mh 1999:1-10
Johnson LH, Shoesmith, DW 1988 Spent fuel. *In* Radioactive Wasteforms for the Future. Lutze W, Ewing RC (Eds) Elsevier, Amsterdam, p 635-698
Johnson LH, Werme LO 1994 Materials characteristic and dissolution behavior of spent nuclear fuel. Mater Res Soc Bull XIX(12):24-27
Kaufman A, Ku T-L 1989 The U-series ages of carnotites and implications regarding their formation. Geochim Cosmochim Acta 53:2675-2681
Keller L, Wagner CNJ 1983 Diffraction analysis of metamict samarskite. Am Mineral 68:459-465
Keppler H, Wyllie PJ 1990 Role of fluids in transport and fractionation of uranium and thorium in magmatic provinces. Nature 348:531-533
Kolitschn U 1997 Uranosphärite und weitere neue Mineralien von der Grube Clara im Schwarzwald. Mineralien Welt 8:18-26
Korzeb SL, Foord EE, Lichte FE 1997 The chemical evolution and paragenesis of uranium minerals from Ruggles and Palermo granitic pegmatites, New Hampshire. Can Mineral 35:135-144
Kotzer TG, Kyser TK 1993 O, U, and Pb isotopic and chemical variations in uraninite: Implications for determining the temporal and fluid history of ancient terranes. Am Mineral 78:1262-1274
Krause W, Effenberger H, Brandstätter F 1995 Orthowalpurgite, $(UO_2)Bi_4O_4(AsO_4)_2{\cdot}2H_2O$, a new mineral from the Black Forest, Germany. Eur J Mineral 7:1313-1324
Lambor 1994 New mineral names. Am Mineral 79:1012

Langmuir D 1978 Uranium solution-minerals equilibria at low temperatures with applications to sedimentary ore deposits. Geochim Cosmochim Acta 42:547-569
Lazebnik KA et al. 1985 Typomorphism and Geochemical Features of Endogenic Minerals of Yakutia. Yakutsk 132-142
Lazebnik KA, Kayakina NV, Mathotko VF 1994 A new thorium silicate from carbonates of the Syrenevyi Kamen' deposit. Doklady Akad Nauk 334:735-738
Li Y, Burns PC 1999a A single-crystal diffraction study of the crystal chemistry of curite. GAC-MAC Abstracts 24:71
Li Y, Burns PC 1999b A new REE-bearing uranyl carbonate sheet in the structure of bijvoetite. Geol Soc Am Annual Mtg. Abstracts (in press)
Livingstone A, Atkin D, Hutchison D, Al-Hermezi HM 1976 Iraqite, a new rare earth mineral of the ekanite group. Mineral Mag 40:441-445
Loopstra BO, Rietveld HM 1969 The structures of some alkaline-earth metal uranates. Acta Crystallogr B25:787-791
Lumpkin GR, Chakoumakos BC 1988 Chemistry and radiation effects of thorite-group minerals from the Harding pegmatite, Taos County, New Mexico. Am Mineral 73:1405-1419
Lumpkin GR, Ewing RC 1988 Alpha-decay damage in minerals of the pyrochlore group. Phys Chem Mineral 16:2-20
Lumpkin GR, Ewing RC 1992a Geochemical alteration of pyrochlore group minerals: Microlite subgroup. Am Mineral 77:179-188
Lumpkin GR, Ewing RC 1992b Chemistry and radiation effects of thorite-group minerals of the Harding pegmatite, Taos County, New Mexico. Am Mineral 73:1405-1419.
Lumpkin GR, Ewing RC 1995 Geochemical alteration of pyrochlore group minerals: Pyrochlore subgroup. Am Mineral 80:732-743
Lumpkin GR, Ewing RC 1996 Geochemical alteration of pyrochlore group minerals: Betafite subgroup. Am Mineral 81:1237-1248
Lumpkin GR, Hart KP, McGlinn PJ, Payne TE, Gieré R, Williams CT 1994 Retention of actinides in natural pyrochlores and zirconolites. Radiochim Acta 66/67:469-474
Magalhaes MCF, Pedrosa de Jesus JD, Williams PA 1985 The chemistry of uranium dispersion in groundwaters at the Pinhal do Souto mine, Portugal. Inorg Chim Acta 109:71-78
Mandarino J 1999 Fleischer's Glossary of Mineral Species. Mineralogical Record, Tucson, Arizona
Mann AW, Deutscher RL 1980 Solution chemistry of lead and zinc in water containing carbonate, sulfate and chloride ions. Chem Geol 29:293-311
Markovic M, Pavkovic N 1983 Solubility and equilibrium constants of uranyl(2+) in phosphate solutions. Inorg Chem 22:978–982
Marshall RH, Hoekstra HR 1965 Preparation and properties of $TiUO_5$. J Inorg Nucl Chem 27:1947-1950
Martin M, Massanek A 1995 Asselbornite aus Schneeberg/Sachsen. Lapis 20:34-35
Matzke Hj 1992 Radiation damage-enhanced dissolution of UO_2 in water. J Nucl Mater 190:101-106
Mazzi F, Munno R 1983 Calciobetafite (new mineral of the pyrochlore group) and related minerals from Campi Flegrei, Italy; crystal structures of polymignyte and zirkelite: cmparison with pyrochlore and zirconolite. Am Mineral 68:262-276
McCready AJ, Pernell J 1997 Uraniferous bitumens from the Orcadian basin, Scotland: analogues for Witwatersrand uranium mineralization. *In* Mineral Deposits. Papunen H (Ed). Blakema, Rotterdam. p 83-86
McCready AJ, Pernell J 1998 A Phanerozoic analogue for Witwatersrand-type uranium mineralization: uranium-titanium-bitumen nodules in Devonian conglomerate/sandstone, Orkney, Scotland. Trans Inst Min Metall B, Appl Earth Sci 107:B89-B97
McEachern RJ, Dorn DC, Wood DD 1998 The effect of rare-earth fission products on the rate of U_3O_8 formation on UO_2. J Nucl Mater 252:145-149
McEachern RJ, Taylor P 1998 A review of the oxidation of uranium dioxide at temperatures below 400°C. J Nucl Mater 254:87-121
McKinley JP, Zachara JM, Smith SC, Turner GD 1995 The influence of uranyl hydrolysis and multiple site-binding reactions on absorption of U(VI) to montmorillonite. Clays Clay Mineral 43:586-598
McMillan RH 1978 Genetic aspects and classification of important Canadian uranium deposits. In Uranium Deposits: Their Mineralogy and Origin. Kimberly MM (Ed) Mineral Soc Canada Short Course Handbook 3:187-204
Meere PA, Banks DA 1997 The effects of water radiolysis on local redox conditions in the Oklo, Gabon, natural fission reactors 10 and 16. Geochim Cosmochim Acta 61:4479-4494
Mereiter K 1979 The crystal structure of curite, $[Pb_{6.56}(H_2O,OH)_4][(UO_2)_8O_6(OH)_8]_2$. Tschermaks mineral petrogr Mitt 26:279-292
Mereiter K 1982 The crystal structure of walpurgite. Tschermaks mineral petro Mitt 30:129-139

Mereiter K 1984 The crystal structure of albrechtschaufite, $MgCa_4F_2(UO_2)(CO_3)_3{\cdot}17(H_2O)$. Acta Crystallogr A40, Supplement C-247 (abstract)
Mereiter K 1986 Crystal structure and crystallographic properties of schröckingerite from Joachimsthal. Tschermaks mineral petrogr Mitt 35:1-18
Miller LJ 1958 The chemical environment of pitchblende. Econ Geol 53:521-544
Miller ML, Finch RJ, Burns PC, Ewing RC 1996 Description and classification of uranium oxide hydrate sheet topologies. J Mater Res 11:3048-3056
Mishra R, Namboodiri PN, Tripathi SN, Bharadwaj SR, Dharwadkar SR 1998 Vaporization behaviour and Gibbs' energy of formation of $UTeO_5$ and UTe_3O_9 by transpiration. J Nucl Mater 256:139-144
Miyake C, Sugiyama D, Mizuno M 1994 Oxidation states of U and Ti in U-Ti-O ternary mixed oxides. J Alloys Compounds 213/214:516-519
Moll H, Matz W, Schuster G, Brendler E, Bernhard G, Nitsche H 1995 Synthesis and characterization of uranyl orthosilicate, $(UO_2)_2SiO_4{\cdot}2H_2O$. J Nucl Mater 227:40-49
Molon J 1990 Through the 'scope: minerals of the Clara mine, Wolfach, Germany—an update. Rocks and Minerals 65:448-454
Moroni LP, Glasser FP 1995 Reactions between cement components and U(VI) oxide. Waste Management 15:243:254
Morris DE, Allen PG, Berg JM, Chisolm-Brause CJ, Conradson SD, Hess NJ, Musgrave JA, Tait CD 1996 Speciation of uranium in Fernald soils by molecular spectroscopic methods: Characterization of untreated soils. Environ Sci Technol 30:2322–2331
Mücke A 1988 Lehnerite, $Mn[UO_2/PO_4]_2{\cdot}8H_2O$, a new mineral from the Hagendorf pegmatite, Oberpfalz. Aufschluss 39:209-217 (in German; abstract in Am Mineral 75:221
Mücke A, Strunz H 1978 Petscheckite and liandratite, two new pegmatite minerals from Madagascar. Am Mineral 63:941
Murakami T, Isobe H, Ohnuki T, Sato T, Yanase N, Kiyoshige J 1996a Mechanism of saléeite formation at the Koongarra secondary uranium deposit. Mater Res Soc Symp Proc 412:809-816
Murakami T, Isobe H, Sato T, Ohnuki T 1996b Weathering of chlorite in a quartz-chlorite schist: I. Mineralogical and chemical changes. Clays Clay Minerals 44:244-256
Murakami T, Ohnuki T, Isobe H, Sato T 1997 Mobility of uranium during weathering. Am Mineral 82:888-899
Murphy WM 1995 Natural analogs for Yucca Mountain. Radwaste Mag 2:44-50
Murphy WM, Shock EL 1999 Environmental aqueous geochemistry of actinides. Rev Mineral 38 (this volume)
Naito K 1974 Phase transitions of U_4O_9. J Nucl Mater 51-126
Nguyen SN, Silva RJ, Weed HC, Andrews JE Jr 1992 Standard Gibbs free energies of formation at the temperature 303.15 K of four uranyl silicates: soddyite, uranophane, sodium boltwoodite and sodium weeksite. J Chem Therm 24:359-376
Nickel EH, Nichols MC 1992 Mineral Reference Manual. Van Norstrand-Reinhold, New York, 250 p
Noe-Spirlet MR, Sobry R 1974 Les uranates hydratés de forment pas une série continue. Bull Soc Royale Sci Liège 43:164-171
Oliver NHS, Pearson PJ, Holcombe RJ, Ord A 1999 Mary Kathleen metamorphic-hydrothermal uranium—rare-earth element deposit: ore genesis and numerical model of coupled deformation and fluid flow. Australian J Earth Sci 46:467-483
O'Hare PAG, Lewis BM, Nguyen SN 1988 Thermochemistry of uranium compounds XVII. Standard molar enthalpy of formation at 298.15 K of dehydrated schoepite $UO_3{\cdot}0.9H_2O$. Thermodynamics of (schoepite + dehydrated schoepite + water). J Chem Therm 20:1287-1296
Ondrus P, Veselovsky, F, Hlousek J 1997a A review of mineral associations and paragenetic groups of secondary minerals of the Jáchymov (Joachimsthal) ore district. J Czech Geol Soc 42:109-114
Ondrus Minerals of the Jáchymov (Joachimsthal) ore district. J Czech Geol Soc 42:3-76
Ondrus O, Veslovsky F, Rybka R 1990 Znucalite, $Zn_{12}(UO_2)Ca(CO_3)_3(OH)_{22}{\cdot}4H_2O$, a new mineral from Pribram, Czecholslovakia. N Jb Mineral Mh 1990:393-400
Ondrus P, Veselovsky F, Skála R, Císarová I, Hlousek J, Fryda J, Vavrín I, Cejka J, Gabasová A 1997c New naturally occurring phases of secondary origin from Jáchymov (Joachimsthal). J Czech Geol Soc 42:77-108
Pagel M, Pinte G, Rotach-Toulhoat N 1987 The rare earth elements in natural uranium oxides. *In* Monograph Series on Mineral Deposits 27. Gebruder Bortraeger, Berlin-Stuttgart. p 81-85.
Pagoaga MK, Appleman DE, Stewart JM 1986 A new barium uranyl oxide hydrate mineral, protasite. Mineral Mag 50:125-128
Pagoaga MK, Appleman DE, Stewart JM 1987 Crystal structure and crystal chemistry of the uranyl oxide hydrates becquerelite, billietite, and protasite. Am Mineral 72:1230-1238
Palenzona A, Selmi P 1998 Uranophane-beta ed altri minerali del ghiacciaio della Brenva. Rivista

Mineralogica Italiana 22:58-60
Paulis P 1992 Curiénite from Abertamy near Jáchymov. Casopis Mineral Geol 37:55-56 (in Czech)
Parks, GA Pohl DC 1988 Hydrothermal solubility of uraninite. Geochim Cosmochim Acta 52:863-875
Pearcy EC, Prikryl JD, Murphy WM, Leslie BW 1994 Alteration of uraninite from the Nopal I deposi Peña Blanca District, Chihuahua, Mexico, compared to degradation of spent nuclear fuel in th proposed US high-level nuclear waste repository at Yucca Mountain, Nevada. Appl Geochem 9:71 732
Pialoux A, Touzelin B 1998 Étude du système U-Ca-O par diffractométrie de rayons X à haute température J Nucl Mater 255:14-25
Piret P 1984 Structure cristalline de la fourmariérite, $Pb(UO_2)_4O_3(OH)_4{\cdot}4(H_2O)$. Bull Minéral 108:659-665
Piret P, Deliens M 1979 New crystal data for Ca-Cu-UO_2-hydrate carbonate: voglite. J Appl Crystallo 12:616
Piret P, Deliens M 1982 Vanmeersscheite and metavanmeersscheite. Bull Minéral 105:125-128
Piret P, Deliens M. 1984 New data for richetite $PbO{\cdot}4UO_3{\cdot}4H_2O$. Bull Minéral 107:581-585
Piret P, Deliens M 1986 La kamotoïte-(Y), un nouveau carbonate d'uranyl et de terres rares de Kamot Shaba, Zaïre. Bull Minér 109:643-647
Piret P, Deliens M 1987 Les phosphates d'uranyl et d'aluminium de Kobokobo. L'althupit $AlTh(UO_2)[UO_2)_3O_2(OH)(PO_4)_2]_2(OH)_3{\cdot}15H_2O$, nouveau minéral. Propriétés et structure cristalline. Bu Minéral 110:65-72
Piret P, Deliens M 1990 L'astrocyanite, $Cu_2(REE)_2(UO_2)(CO_3)_5(OH)_2(H_2O)_{1.5}$, nouvelle espèce minérale Kamoto, Shaba, Zaïre. Eur J Miner 2:407-411
Piret P, Deliens M, Piret-Meunier J 1988 La françoisite-(Nd), nouveau phosphate d'uranyl et terres rare propriétés et structure cristalline. Bull Minéral 111:443-449
Piret P, Deliens M, Piret-Meunier J, Germain G 1983 La sayrite, $Pb_2[(UO_2)_5O_6(OH)_2]{\cdot}4H_2O$, nouve minéral; propriétés et structure cristalline. Bull Minéral 106, 299-304
Piret P, Piret-Meunier J 1988 Nouvelle détermination de la structure de la dumonti $Pb_2[(UO_2)_3O_2(PO_4)_2]{\cdot}5H2O$. Bull Minéral 111:439-442
Piret P, Piret-Meunier J 1991 Composition chimique et structure cristalline de la phosphuranyli $Ca(UO_2)(UO_2)_3(OH)_2(PO_4)_2.12H_2O$. Eur J Mineral 3:69-77
Piret P, Piret-Meunier J, Deliens M 1990 Composition chimique et structure cristalline de la dewindt $Pb_3[H(UO_2)_3O_2(PO_4)_2]{\cdot}12H_2O$. Eur J Mineral 2:399-405
Plesko EP, Scheetz BE, White WB 1992 Infrared vibrational characterization and synthesis of a family hydrous alkali uranyl silicates and hydrous uranyl silicate minerals. Am Mineral 77:431-437
Podor R, Cuney M, Nguyen Trung C 1995 Experimental study of the solid solution between monazite-(L and $(Ca_{0.5}U_{0.5})PO_4$ at 780°C and 200 MPa. Am Mineral 80:1261-1268
Posey-Dowty J, Axtmann E, Crerar D, Borcsik M, Ronk A, Woods W 1987 Dissolution rate of uranini and uranium role-front ores. Econ Geol 82:184-194
Pourcelot L, Gauthier-Lafaye F 1998 Mineralogical, chemical and O-isotopic data on uraninites fro natural fission reactors (Gabon): effects of weathering conditions. CR Acad Sci Paris, Sci terre planét 326:485-492
Protas J 1959 Contribution à l'étude des oxydes d'uranium hydratés. Bull Soc franç Minéral Cristallo 82:239-272
Pu Congjian 1990 Boltwoodite discovered for the first time in China. Acta Mineral Sinica 10:157-160 Chinese)
Putnam RL, Navrotsky A, Woodfield BF, Boerio-Goates J, Shapiro JL 1999 Thermodynamics of formati for zirconolite ($CaZrTi_2O_7$). J Chem Thermodynamics 31:229-243
Rasmussen B, Buick R 1999 Redox state of the Archean Atmosphere: evidence from detrital heavy miner in ca. 3250-2750 Ma sandstones from the Pilbara Craton, Australia. Geology 27:115-118
Rastsvetaeva RK, Arakcheeva AV, Pushcharovsky DY, Atencio D, Menezes Filho LAD 1997 New silic band in the haiweeite structure. Crystallogr Reports 42:927-933
Ringwood AE, Kesson SE Reeve KD, Levins DM Ramm EJ 1988 Synroc. *In* Radioactive Waste For for the Future. Lutze W, Ewing RC (Eds) p 233-334
Robie RA, Hemingway BS, Fisher JR 1979 Thermodynamic properties of minerals and related substanc at 298.15 K and 1 bar (10^5 Pascals) pressure and at higher temperatures. US Geol. Surv. Bulletin 14 456 p
Rogova VP, Belova LN, Kiziyarov GP, Kuznetsova NN 1973 Bauranoite and metacalciouranoite—n minerals of the group of hydrous uranium oxides. Zap Vses Mineral Obshch 102:75-81 (in Russian)
Rogova VP, Belova LN, Kiziyrov GP, Kuznetsova NN 1974 Calciouranoite, a new hydroxide of uraniu Zap Vses Mineral Obshch 103:103-109 (In Russian; abstract in Am Mineral 60:161, 1975)
Sandino A, Bruno J 1992 The solubility of $(UO_2)_3(PO_4)_2.4H_2O$(s) and the formation of U(VI) phosph complexes: Their influence in uranium speciation in natural waters. Geochim Cosmochim A

56:4135-4145
Sandino MCA, Grambow B 1995 Solubility equilibria in the U(VI)-Ca-K-Cl-H_2O system: Transformation of schoepite into becquerelite and compreignacite. Radiochim Acta 66/67:37-43
Sarp H, Bertrand J, Deferne J 1983 Asselbornite, $(Pb,Ba)(BiO)_4(UO_2)_6(AsO_4)_2(OH)_{12}(H_2O)_3$, a uranium, bismuth and barium arsenate. N Jb Mineral Mh 1983:417-423
Sarp H, Chiappero PJ 1992 Deloryite, $Cu_4(UO_2)(MoO_4)_2(OH)_6$, a new mineral from the Cap Garonne mine near Le Pradet, Var, France. N Jb Miner Mh 1992:58-64
Sato T, Murakami T, Yanase N, Isobe H, Payne TE, Airey PL 1997 Iron nodules scavenging uranium from groundwater. Environ Sci Technol 31:2854-2858
Savary V, Pagel M 1997 The effects of water radiolysis on local redox conditions in the Oklo, Gabon, natural fission reactors 10 and 16. Geochim Cosmochim Acta 61:4479-4494
Schoep A 1930 Les minéraux du gîte uranifère du Katanga. Musée Congo Belge Ann Ser 1, Tome 1, Fasc 2, 43 p
Serezhkin VN, Tshubaev VF, Kovba LM, Trnov VK 1973 The structure of synthetic iriginite. Doklady Akad Nauk SSSR Ser Chem 210:873-876 (in Russian)
Sergeyeva EI, Nikitin AA. Khodakovkiy IL, Naumov GB 1972 Experimental investigation of equilibria in the system UO_3-CO_2-H_2O in 25-200°C temperature interval. Geokhimiya 11:1340 (in Russian) [English translation in Geochem Int'l 9:900]
Sharmová M, Scharm B 1994 Rabdophane-group minerals in the uranium ore district of northern Bohemia (Czech Republic). 39:267-280
Shen J, Peng Z 1981 The crystal structure of furongite. Acta Crystallogr A37 supplement C-186
Shoesmith DW, Sunder S 1991 An electrochemistry-based miodel for the dissolution of UO_2. AECL-10488, Atomic Energy of Canada, Whiteshell Laboratories, 97 p
Shoesmith DW, Sunder S, Tait JC 1998 Validation of an electrochemical model for the oxidative dissolution of used CANDU fuel. J Nucl Mater 257:89-98
Singh Z, Dash S, Krishnan K, Prasad R, Venugopal V 1999 Standard Gibbs energy of formation of $UTeO_5$(s) by the electrochemical method. J Chem Thermodynamics 31:197-204
Singh KDP, Bhargava LR, Ali MA, Swarnkar BM 1990 An unusual brannerite from Tai, Arunachal Pradesh, India. Explor Res Atomic Minerals [India] 1:117-122
Singh Y 1999 Phurcalite: a rare secondary calcium uranium phosphate mineral from Putholi, Chittaurgarh district, Rajasthan. J Geol Soc India 53:355-357.
Skakle JMS, Moroni LP, Glasser FP 1997 X-ray diffraction data for two new calcium uranium(VI) hydrates. Powd Diff 12:81-86
Smith DK Jr 1984 Uranium mineralogy. *In* Uranium Geochemistry, Mineralogy, Geology, Exploration and Resources. DeVivo B, Ippolito F, Capaldi G, Simpson PR (Eds) Institute of Mining and Metallurgy, London, p 43-88
Smith DK Jr, Scheetz BE, Anderson CAF, Smith KL 1982 Phase relations in the uranium-oxygen-water system and its significance on the stability of nuclear waste forms. Uranium 1:79-111
Smits G 1989 (U,Th)-bearing silicates in reefs of the Witwatersrand, South Africa. Can Mineral 27:643-656
Snelling AA 1980 Uraninite and its alteration products, Koongarra uranium deposit. *In* Uranium in the Pine Creek Geosyncline. Ferguson J, Goleby AB (Eds) Int'l Atomic Energy Agency, Vienna, p 487-498
Snelling AA 1992 Geologic setting, Alligator Rivers Analogue Project Final Report 2, ISBN 0-642-59928-9. Australian Nuclear Science and Technology Organisation, Sydney, 118 p
Speer A 1982 Actinide orthosilicates. Rev Mineral 5:113-135
St A Hubbard HV, Griffiths TR 1987 An investigation of defect structures in single-crystal UO_{2+x} by optical absorption spectroscopy. J Chem Soc, Faraday Trans 2 83:1215-1227
Stalbauer E, Wichmann V, Lott V, Keller C 1974 Relationships of the ternary La-U-O system. J Solid State Chem 10:341-350
Steen H 1998 Ein kleines Vorkommen von Uran- und Bleimineralien im Schweizergrund bie Sulzburg, Südschwarzwald. Der Erzgräber 7:1-3
Stieff LR, Stern TW, Sherwood AM 1956 Coffinite, a uranous silicate with hydroxyl substitution—a new mineral. Am Mineral 41:675-688
Stergiou AC, Rentzeperis PJ, Sklavounos S 1993 Refinement of the crystal structure of metatorbernite. Z Kristallogr 205:1-7
Stohl FV, Smith DK Jr 1981 The crystal chemistry of the uranyl silicate minerals. Am Mineral 66:610-625
Stout PJ, Lumpkin GR, Ewing RC, Eyal Y 1988 An annealing study of alpha-decay damage in natural UO_2 and ThO_2. Mater Res Soc Symp Proc 112:495-504
Stumm W, Morgan JJ 1981 Aquatic Chemistry, 2nd Edn. Wiley-Interscience, New York, 780 p
Sugitani Y, Suzuki Y, Nagashima K 1984 Recovery of the original samarskite structure by heating in a

reducing atmosphere. Am Mineral 69:377-379
Sunder S, Cramer JJ, Miller NH 1996 Geochemistry of the Cigar Lake deposit: XPS studies. Radiochim Acta 74:303-307
Sunder S, Miller NH Duclos AM 1994 XPS and XRD studies of samples from the natural fission reactors in the Oklo uranium deposits. Mater Res Soc Symp Proc 333:631-638
Sunder S, Shoesmith DW, Christensen H, Miller NH 1992 Oxidation of UO_2 fuel by the products of gamma radiolysis of water. J Nucl Mater 190:78–86
Suzuki Y, Murakami T, Kogure T, Isobe H, Sato T 1998 Crystal chemistry and microstructures of uranyl phosphates. Mater Res Soc Symp Proc 506:839-846
Swihart GH, Sen Gupta PK, Schlemperer EO, Back ME, Gaines RV 1993 The crystal structure of moctezumite $[PbUO_2](TeO_3)_2$. Am Mineral 18:835-839
Szymanski JT, Scott JD 1982 A crystal structure refinement of synthetic brannerite UTi_2O_6 and its bearing on rate of alkaline-carbonate leaching of brannerite in ore. Can Mineral 20:271-280
Tardy Y, Garrels RM 1976 Prediction of Gibbs free energies of formation: I. Relationship between Gibbs energies of formation of hydroxides, oxides and aqueous ions. Geochim Cosmochim Acta 40:1051-1056
Tardy Y, Garrels RM 1977 Prediction of Gibbs free energies of formation: II. Monovalent and divalent metal silicates. Geochim Cosmochim Acta 41:87-92
Taylor JC 1971 The structure of the α form of uranyl hydroxide. Acta Crystallogr B27:1088-1091
Taylor JC, Stuart WI, Mumme IA 1981 The crystal structure of curite. J Inorg Nucl Chem 43:2419-2423
Thomas LE, Einziger RE, Woodley RE 1989 Microstructural examination of oxidized spent PWR fuel by transmission electron microscopy. J Nucl Mater 166:243-251
Thomas LE, Einziger RE, Buchanan HC 1993 Effects of fission products on air oxidation of LWR spent fuel. J Nucl Mater 201:310-319
Threadgold IM 1960 The mineral composition of some uranium ores from the south Alligator River area, Northern Territory. Mineralog Invest CSIRO Technical Paper 2
Tschernikov AA, Organova NI 1994 Sodium autunite and sodium meta-autunite. Doklady Akad Nauk 338:368-371
Trocellier P, Cachoir C, Guilbert S 1998 A simple thermodynamic model to describe the control of the dissolution of uranium dioxide in granite groundwater by secondary phase formation. J Nucl Mater 256:197-206
van Genderen LCG, van der Weijden CH 1984 Prediction of Gibbs free energies of formation and stability constants of some secondary uranium minerals containing the uranyl group. Uranium 1:249-256
Vance ER, Ball CJ, Day RA, Smith KL, Blackford MG, Begg BD, Angel P 1994 Actinide and rare earth incorporation into zirconolite. J Alloys Comp 213/214:406-409
Vdovina OL, Serezhkina LB, Serezhkin VN, Boiko NV 1984 Interaction of magnesium and uranyl chromates in aqueous solution. Radiokhimiya 25:345-349
Vishnev AI, Gorshkov AI, Federov OV 1991 Iriginite according to the data of electron microscopy and electronography. Izvestia Akad Nauk SSSR Ser Geol 1991:143-149
Viswanathan K, Harnett O 1986 Refined crystal structure of beta-uranophane, $Ca(UO_2)_2(SiO_3OH)_2{\cdot}5H_2O$. Am Mineral 71:1489-1493
Vochten R, Blaton N 1999 Synthesis of rutherfordine and its stability in water and alkaline solutions. N Jb Miner Mh 1999:372-384
Vochten R, Blaton N, Peeters O 1997a Synthesis of sodium weeksite and its transformation into weeksite. N Jb Miner Mh 1997:569-576
Vochten R, Blaton N, Peeters O 1997b Deliensite, $Fe(UO_2)_2(SO_4)_2(OH)_2{\cdot}3\ H_2O$, a new ferrous uranyl sulfate hydroxyl hydrate from Mas d'Alary, Lodève, Hérault, France. Can Mineral 35:1021-1025
Vochten R, Blaton N, Peeters O, Deliens M 1996 Piretite, $Ca(UO_2)_3(SeO_3)_2(OH)_2{\cdot}4H_2O$, a new calcium uranyl selenite from Shinkolobwe, Shaba, Zaire. Can Mineral 34:1317-1322
Vochten R, Blaton N, Peeters O, van Springel K, van Haverbeke L 1997c A new method of synthesis of boltwoodite and of formation of sodium boltwoodite, uranophane, sklodowskite and kasolite from boltwoodite. Can Mineral 35:735-741
Vochten R, de Grave E, Pelsmaekers J 1984 Mineralogical study of bassetite in relation to its oxidation. Am Mineral 69:967-978
Vochten R, Deliens M 1998 Blatonite, $UO_2CO_3{\cdot}H_2O$, a new uranyl carbonate monohydrate from San Juan County Utah. Can Mineral 36:1077-1081
Vochten R, van Haverbeke L 1990 Transformation of schoepite into the uranyl oxide hydrates: becquerelite, billietite and wölsendorfite. Mineral Petrol 43:65-72
Vochten R, van Haverbeke L, Sobry R 1991 Transformation of schoepite into the uranyl oxide hydrates: of the bivalent cations Mg^{2+}, Mn^{2+} and Ni^{2+}. J Mater Chem 1:637-642
Vochten R, van Haverbeke L, van Springel K 1995 Soddyite: Synthesis under elevated temperature and

pressure, and study of some physicochemical characteristics. N Jb Miner Mh H 10:470-480
Vochten R, van Haverbeke L, van Springel K, Blaton N, Peeters OM 1994 The structure and physicochemical characteristics of a synthetic phase compositionally intermediate between liebigite and andersonite. Can Mineral 32:553-561
Vochten R, van Haverbeke K, van Springel K, Blaton N, Peeters OM 1995 The structure and physicochemical characteristics of synthetic zippeite. Can Mineral 33:1091-1101
Vochten R, van Springel K 1996 A natural ferrous substituted saléeite from Arcu su Linnarbu, Capoterra, Cagliari, Sardinia. Mineral Mag 60:647-651
Von Weitzel H, Schröcke H 1980 Kristallstrukturfeinerungen von Euxenit, $T(Nb_{0.5}Ti_{0.5})_2O_6$, und M-Fergusonit, $YNbO_4$. Z Kristallogr 152:69-82
Voultsidis V, Clasen D 1978 Probleme und grenzbereiche der uranmineralogie. Erzmetall 31:8-13
Waber N, Schorscher HD, Peters T 1990 Mineralogy, petrology and geochemistry of the Poços de Caldas analogue study sites, Minas Gerais, Brazil. I: Osamu Utsumi uranium mine. SKB Technical Report 90-11, SKB, Stockholm, 514 p
Waite TD, Davis JA, Payne TE, Waychunas GA, Xu N 1994 Uranium(VI) adsorption to ferrihydrite: Application of a surface complexation model. Geochim Cosmochim Acta 58:5465-5478
Walenta K 1974 On studtite and its composition. Am Mineral 59:166-171
Walenta K 1976 Widenmannit und Joliotite, zwei neue Uranylcarbonatmineralien aus den Schwartzwald. Schweiz mineral petrogr Mitt 56:167-185
Walenta K 1983 Uranosilite, a new mineral from the uranium deposit at Menzenschwand (southern Black Forest). N Jb Mineral Mh 1983:259-269
Walenta K 1985 Uranotungstite, a new secondary uranium mineral from the Black Forest, West Germany. Tschermaks mineral petrol Mitt 25-34 (in German)
Walenta K 1993a Phurcalit von Wittichen. Der Erzgräber 7:1-3
Walenta K 1993b Gesicherte und fragliche Mineralfunde von Vorkommen im Schwarzwald. Der Erzgräber 7:54-64
Warner JK, Ewing RC 1993 Crystal chemistry of samarskite. Am Mineral 78:419-424
Weeks AD, Thompson ME 1954 Identification and occurrence of uranium and vanadium minerals from the Colorado plateaus. U S Geol Surv Bull 1009-B, 62 p
Williams CT, Gieré R 1996 Zirconolite: a review of localities worldwide, and a compilation of its chemical compositions. Bull Nat Hist Museum Geol Ser 52:1-24
Willis BTM 1963 Positions of the oxygen atoms in $UO_{2.13}$. Nature 197:755-756
Willis BTM 1978 The defect structure of hyperstoichiometric uranium dioxide. Acta Crystallogr A34:88
Willis BTM 1987 Crystallographic studies of anion-excess uranium oxides. J Chem Soc Faraday Trans 2:1073-1081
Weijun S, Fengjun M, Shijie Z 1983 Fergusonite-beta-Nd. Sci Geol Sinica 78-81 (in Chinese)
Wolf SF, Bates JK, Buck EC, Dietz NL, Fortner JA, Brown NR 1997 Physical and chemical characterization of actinides in soil from Johnston Atoll. Environ Sci Technol 31:467–471
Woodfield BF, Boerio-Goates J, Shapiro JL, Putnam RL, Navrotsky A 1999 Molar heat capacity and thermodynamic functions of zirconolite $CaZrTi_2O_7$. J Chem Thermodynamics 31:245-253
Wronkiewicz DJ, Bates JK, Gerding TJ, Veleckis E, Tani BS 1992 Uranium release and secondary phase formation during unsaturated testing of UO_2 at 90°C. J Nucl Mater 190:107-127
Wronkiewicz DJ, Bates JK, Wolf SF, Buck EC 1996 Ten-year results from unsaturated drip tests with UO_2 at 90°C: Implications for the corrosion of spent nuclear fuel. J Nucl Mater 238:78-95
Wronkiewicz DJ, Buck EC 1999 Uranium mineralogy and the geologic disposal of spent nuclear fuel. Rev Mineral 38 (this volume)
Xu HF, Wang YF 1999 Electron energy-loss spectroscopy (EELS) study of oxidation states of Ce and U in pyrochlore and uraninite—natural analogues for Pu- and U-bearing waste forms. J Nucl Mater 265:117-123
Young EJ, Weeks AD, Meyrowitz R 1966 Coconinoite, a new uranium mineral from Utah and Arizona. Am Mineral 51:651-663
Zhang J, Wan A, Gong W 1992 New data on yingjiangnite. Acta Petrol Mineral 11:178-184 (in Chinese)
Zhangru C, Keding L, Falan T, Yi Z, Xiaofa G 1986 Tengchongite, a new mineral of hydrated calcium uranyl molybdate. Kexue Tongbao 31:396-401
Zwaan PC, Arps CES, de Grave E 1989 Vochtenite, $(Fe^{2+},Mg)Fe^{3+}[UO_2/PO_4]_4(OH){\cdot}12\text{-}13H_2O$, a new uranyl phosphate mineral from Wheal Basset, Redruth, Cornwall, England. Mineral Mag 53:473-478